Journal of Function Spaces and Applications

Some Recent Developments in Applied Functional Analysis

Guest Editors: Manuel Ruiz Galán, María Isabel Berenguer, Gabriel N. Gatica, and Davide La Torre

Some Recent Developments in Applied Functional Analysis

Journal of Function Spaces and Applications

Some Recent Developments in Applied Functional Analysis

Guest Editors: Manuel Ruiz Galán, María Isabel Berenguer, Gabriel N. Gatica, and Davide La Torre

Editorial Board

Contents

Some Recent Developments in Applied Functional Analysis, Manuel Ruiz Galán, María Isabel Berenguer, Gabriel N. Gatica, and Davide La Torre
Volume 2013, Article ID 407425, 1 page

Accurate Numerical Method for Pricing Two-Asset American Put Options, Xianbin Wu
Volume 2013, Article ID 189235, 7 pages

Recent Developments on Hybrid Time-Frequency Numerical Simulation Techniques for RF and Microwave Applications, Jorge F. Oliveira and José C. Pedro
Volume 2013, Article ID 578326, 11 pages

A Finite Difference Scheme for Pricing American Put Options under Kou's Jump-Diffusion Model, Jian Huang, Zhongdi Cen, and Anbo Le
Volume 2013, Article ID 651573, 11 pages

Analysis of the Error in a Numerical Method Used to Solve Nonlinear Mixed Fredholm-Volterra-Hammerstein Integral Equations, D. Gámez
Volume 2012, Article ID 242870, 12 pages

Explicit Solution of Telegraph Equation Based on Reproducing Kernel Method, Mustafa Inc, Ali Akgül, and Adem Kiliçman
Volume 2012, Article ID 984682, 23 pages

Note on Boehmians for Class of Optical Fresnel Wavelet Transforms, S. K. Q. Al-Omari and A. Kılıçman
Volume 2012, Article ID 405368, 14 pages

Positive Periodic Solutions for Second-Order Ordinary Differential Equations with Derivative Terms and Singularity in Nonlinearities, Yongxiang Li and Xiaoyu Jiang
Volume 2012, Article ID 945467, 15 pages

On the Frame Properties of Degenerate System of Sines, Bilal Bilalov and Fatima Guliyeva
Volume 2012, Article ID 184186, 12 pages

Hindawi Publishing Corporation
Journal of Function Spaces and Applications
Volume 2013, Article ID 407425, 1 page
http://dx.doi.org/10.1155/2013/407425

Editorial

Some Recent Developments in Applied Functional Analysis

Manuel Ruiz Galán,[1] María Isabel Berenguer,[1] Gabriel N. Gatica,[2] and Davide La Torre[3]

[1] *Departamento de Matemática Aplicada, E.T.S. Ingeniería de Edificación, Universidad de Granada, 18071 Granada, Spain*
[2] *Departamento de Ingeniería Matemática, Universidad de Concepción, Casilla 160-C, Concepción, Chile*
[3] *Department of Economics, Business and Statistics, University of Milan, 20122 Milan, Italy*

Correspondence should be addressed to Manuel Ruiz Galán; mruizg@ugr.es

Received 21 February 2013; Accepted 21 February 2013

From its early stages, the intensive development of functional analysis and the remarkable advances of its methods cannot be explained without its link with other areas of mathematics and, above all, its role as an essential framework for numerical analysis and computer simulation, PDEs, modeling real-world phenomena, variational inequalities, or optimization, just to name a few.

In this special issue we highlight some aspects of functional analysis which are used in connection with other branches of mathematics or science, either as a direct application or as a theoretical result which is essential for such an application.

Although it is not possible to collect here the huge production of the research activity on this vast field of modern mathematics, the selected works gather together a range of topics which reflect some of the current research on applied functional analysis: bases in Banach spaces, wavelet transforms, fixed point theory, and applications to ODEs, electronic circuit simulation, or numerical solution of PDEs, integral equations, or problems on option pricing in mathematical finance. In this way, we have achieved one of our purposes, which is the exchange of ideas among researchers working both in abstract and applied functional analysis.

Acknowledgments

We would like to express our sincere thanks to the authors for contributing to this issue, as well as to the anonymous reviewers for their generous and accurate refereeing process and their valuable comments and suggestions. Without their evident support this special issue would not have come out. We want also acknowledge with gratitude the assistance and help provided by the editorial board members of this Journal during the preparation of this special issue.

Manuel Ruiz Galán
María Isabel Berenguer
Gabriel N. Gatica
Davide La Torre

Hindawi Publishing Corporation
Journal of Function Spaces and Applications
Volume 2013, Article ID 189235, 7 pages
http://dx.doi.org/10.1155/2013/189235

Research Article

Accurate Numerical Method for Pricing Two-Asset American Put Options

Xianbin Wu

Junior College, Zhejiang Wanli University, Ningbo 315100, China

Correspondence should be addressed to Xianbin Wu; wxb3210@zwu.edu.cn

Received 12 October 2012; Accepted 27 November 2012

Academic Editor: Manuel Ruiz Galan

We develop an accurate finite difference scheme for pricing two-asset American put options. We use the central difference method for space derivatives and the implicit Euler method for the time derivative. Under certain mesh step size limitations, the matrix associated with the discrete operator is an M-matrix, which ensures that the solutions are oscillation-free. We apply the maximum principle to the discrete linear complementarity problem in two mesh sets and derive the error estimates. It is shown that the scheme is second-order convergent with respect to the spatial variables. Numerical results support the theoretical results.

1. Introduction

An option is a financial instrument that gives the holder the right, but not the obligation, to buy (call option) or to sell (put option) an agreed quantity of a specified asset at a fixed price (exercise or strike price) on (European option) or before (American option) a given date (expiry date). It was shown by Black-Scholes [1] that the value of a European option is governed by a second-order parabolic partial differential equation with respect to the time and the underlying asset price. The value of an American option is determined by a linear complementarity problem involving the Black-Scholes operator [2, 3]. Since this complementarity problem is, in general, not analytically solvable, numerical approximation to the solution is normally sought in practice.

Various numerical methods have been proposed for the valuation of single-factor American options. Among them, the lattice method [4], the Monte Carlo method [5], the finite difference method [6–8], the finite element method [9, 10], and the finite volume method [11–13] are the most popular ones in both practice and research.

Finite difference methods applied to the multifactor American option valuation have also been developed. S. O'Sullivan and C. O'Sullivan [14] presented explicit finite difference methods with an acceleration technique for option pricing. Clarke and Parrott [15] and Oosterlee [16] used finite difference schemes along with a projected full approximation scheme (PFAS) multigrid for pricing American options under stochastic volatility. Ikonen and Toivanen [17–19] proposed finite difference methods with componentwise splitting methods on nonuniform grids for pricing American options under stochastic volatility. Hout and Foulon [20] and Zhu and Chen [21] applied finite difference schemes based on the ADI method to price American options under stochastic volatility. Le et al. [22] presented an upwind difference scheme for the valuation of perpetual American put options under stochastic volatility. Yousuf [23] developed an exponential time differencing scheme with a splitting technique for pricing American options under stochastic volatility. Nielsen et al. [24] and Zhang et al. [25] analyzed finite difference schemes with penalty methods for pricing American two-asset options, but their difference methods are first-order convergent.

In part of the domain, the differential operator of the two-asset American option pricing model becomes a convection-dominated operator. The differential operator also contains a second-order mixed derivative term. The classical finite difference methods lead to some off-diagonal elements in the coefficient matrix of the discrete operator due to the dominating first-order derivatives and the mixed derivative. These elements can lead to nonphysical oscillations in the computed solution [17, 18]. In this paper, we present an accurate finite difference scheme for pricing two-asset American options. We use the central difference method for space derivatives and the implicit Euler method for the time derivative. Under certain mesh step size limitations, we obtain a coefficient matrix with an M-matrix property, which ensures that the solutions are oscillation-free. We apply the maximum principle to the discrete linear complementarity problem in two mesh sets and derive the error estimates. We will show that the scheme is second-order convergent with respect to the spatial variables.

The rest of the paper is organized as follows. In the next section, we describe some theoretical results on the continuous complementarity problem for the two-asset American put option pricing model. In Section 3, the discretization method is described. In Section 4, we present a stability and error analysis for the finite difference scheme. In Section 5, numerical experiments are provided to support these theoretical results.

2. The Continuous Problem

We consider the following two-asset American put option pricing model [24, 25]:

$$\begin{aligned}
&\ell P(S_1,S_2,t) \geq 0, \quad S_1,S_2 > 0,\ t \in [0,T),\\
&\ell P(S_1,S_2,t)\cdot[P(S_1,S_2,t)-\phi(S_1,S_2)] = 0,\\
&\qquad S_1,S_2>0,\ t\in[0,T),\\
&P(S_1,S_2,t)-\phi(S_1,S_2)\geq 0, \quad S_1,S_2\geq 0,\ t\in[0,T],\\
&P(S_1,S_2,T)=\phi(S_1,S_2), \quad S_1,S_2\geq 0,\\
&P(0,S_2,t)=g_2(S_2,t), \quad S_2\geq 0,\ t\in[0,T],\\
&P(S_1,0,t)=g_1(S_1,t), \quad S_1\geq 0,\ t\in[0,T],\\
&\lim_{S_1\to\infty}P(S_1,S_2,t)=0, \quad S_2\geq 0,\ t\in[0,T],\\
&\lim_{S_2\to\infty}P(S_1,S_2,t)=0, \quad S_1\geq 0,\ t\in[0,T],
\end{aligned} \tag{1}$$

where ℓ denotes the two-dimensional Black-Scholes operator defined by

$$\begin{aligned}
\ell P(S_1,S_2,t) \equiv\ & -\frac{\partial P}{\partial t}-\frac{1}{2}\sigma_1^2S_1^2\frac{\partial^2 P}{\partial S_1^2}\\
&-\rho\sigma_1\sigma_2S_1S_2\frac{\partial^2 P}{\partial S_1\partial y}-\frac{1}{2}\sigma_2^2S_2^2\frac{\partial^2 P}{\partial S_2^2}\\
&-rS_1\frac{\partial P}{\partial S_1}-rS_2\frac{\partial P}{\partial S_2}+rP,
\end{aligned} \tag{2}$$

and $\phi(S_1,S_2)$ is the final (payoff) condition defined by

$$\phi(S_1,S_2)=\max\{E-(\alpha_1S_1+\alpha_2S_2),0\}. \tag{3}$$

Here, P is the value of the option, S_i is the value of the ith underlying asset, $\rho\in[-1,0)\cup(0,1]$ is the correlation of two underlying assets, r is the risk-free interest rate, and $g_i(\cdot,\cdot)$ is a given function providing suitable boundary conditions. Typically, $g_i(\cdot,\cdot)$ is determined by solving the associated one-dimensional American put option problem

$$\begin{aligned}
&\bar{\ell}_i g_i(S_i,t)\geq 0, \quad S_i>0,\ t\in[0,T),\\
&\bar{\ell}_i g_i(S_i,t)\cdot[g_i(S_i,t)-\max(E-\alpha_iS_i,0)]=0,\\
&\qquad S_i>0,\ t\in[0,T),\\
&g_i(S_i,t)-\max(E-\alpha_iS_i,0)\geq 0, \quad S_i\geq 0,\ t\in[0,T],\\
&g_i(S_i,T)=\max(E-\alpha_iS_i,0), \quad S_i\geq 0,\\
&g_i(0,t)=E, \quad \lim_{S_i\to\infty}g_i(S_i,t)=0, \quad t\in[0,T],
\end{aligned} \tag{4}$$

where $\bar{\ell}_i$ denotes the one-dimensional Black-Scholes operator defined by

$$\bar{\ell}_i g_i(S_i,t)\equiv-\frac{\partial g_i}{\partial t}-\frac{1}{2}\sigma_i^2S_i^2\frac{\partial^2 g_i}{\partial S_i^2}-rS_i\frac{\partial g_i}{\partial S_i}+rg_i, \quad i=1,2. \tag{5}$$

Introducing the logarithmic prices $x=\ln S_1$ and $y=\ln S_2$, the linear complementarity problem (1) is transformed as

$$\begin{aligned}
&Lu(x,y,t)\geq 0, \quad (x,y,t)\in\mathbb{R}\times\mathbb{R}\times[0,T),\\
&Lu(x,y,t)\cdot[u(x,y,t)-\varphi(x,y)]=0,\\
&\qquad (x,y,t)\in\mathbb{R}\times\mathbb{R}\times[0,T),\\
&u(x,y,t)-\varphi(x,y)\geq 0, \quad (x,y,t)\in\mathbb{R}\times\mathbb{R}\times[0,T],\\
&u(x,y,T)=\varphi(x,y), \quad (x,y)\in\mathbb{R}\times\mathbb{R},\\
&u(0,y,t)=g_2(e^y,t), \quad (y,t)\in\mathbb{R}\times[0,T],\\
&u(x,0,t)=g_1(e^x,t), \quad (x,t)\in\mathbb{R}\times[0,T],\\
&\lim_{x\to\infty}u(x,y,t)=0, \quad (y,t)\in\mathbb{R}\times[0,T],\\
&\lim_{y\to\infty}u(x,y,t)=0, \quad (x,t)\in\mathbb{R}\times[0,T],
\end{aligned} \tag{6}$$

where

$$\begin{aligned}
Lu(x,y,t)\equiv\ & -\frac{\partial u}{\partial t}-\frac{1}{2}\sigma_1^2\frac{\partial^2 u}{\partial x^2}-\rho\sigma_1\sigma_2\frac{\partial^2 u}{\partial x\partial y}-\frac{1}{2}\sigma_2^2\frac{\partial^2 u}{\partial y^2}\\
&-\left(r-\frac{1}{2}\sigma_1^2\right)\frac{\partial u}{\partial x}-\left(r-\frac{1}{2}\sigma_2^2\right)\frac{\partial u}{\partial y}+ru,\\
\varphi(x,y)=\ &\max\{E-(\alpha_1e^x+\alpha_2e^y),0\}.
\end{aligned} \tag{7}$$

For applying the numerical method, we truncate the infinite domain into $\Omega\equiv(x_{\min},x_{\max})\times(y_{\min},y_{\max})$, where the boundaries $x_{\min},x_{\max},y_{\min}$, and $y_{\max}$ are chosen so as not to introduce huge errors in the value of the option [26]. Based on Willmott et al.'s estimate [3] that the upper bound of the asset price is typically three or four times the strike price, it is reasonable for us to set $x_{\max} = \ln(4E)$ and $y_{\max} = \ln(4E)$. The artificial boundary conditions at $x = x_{\min}$ and $x = x_{\max}$ are chosen to be $u(x_{\min}, y, t) = g_2(e^y, t), u(x_{\max}, y, t) = 0$. The artificial boundary conditions at $y = y_{\min}$ and $y = y_{\max}$ are chosen to be $u(x, y_{\min}, t) = g_1(e^x, t), u(x, y_{\max}, t) = 0$. Therefore, in the rest of this paper, we will consider the following linear complementary problem:

$$\begin{aligned}
&Lu(x, y, t) \geq 0, \quad (x, y, t) \in \Omega \times [0, T), \\
&Lu(x, y, t) \cdot [u(x, y, t) - \varphi(x, y)] = 0, \\
&\qquad (x, y, t) \in \Omega \times [0, T), \\
&u(x, y, t) - \varphi(x, y) \geq 0, \quad (x, y, t) \in \Omega \times [0, T], \\
&u(x, y, T) = \varphi(x, y), \quad (x, y) \in \Omega, \\
&u(x_{\min}, y, t) = g_2(e^y, t), \quad (y, t) \in [y_{\min}, y_{\max}] \times [0, T], \\
&u(x_{\max}, y, t) = 0, \quad (y, t) \in [y_{\min}, y_{\max}] \times [0, T], \\
&u(x, y_{\min}, t) = g_1(e^x, t), \quad (x, t) \in [x_{\min}, x_{\max}] \times [0, T], \\
&u(x, y_{\max}, t) = 0, \quad (x, t) \in [x_{\min}, x_{\max}] \times [0, T].
\end{aligned} \tag{8}$$

3. Discretization

The operator L contains a second-order mixed derivative term. Usual finite difference approximations lead to some positive off-diagonal elements in the matrix associated with the discrete operator due to the mixed derivative, which may lead to nonphysical oscillations in the computed solution. Hence, it is not easy to construct a discretization with good properties and accuracy for problems with mixed derivatives. There are some works dealing with stable difference approximations of mixed derivatives [27, 28]. In this paper, we present an accurate finite difference scheme to discretize the operator L. We use the technique of [22] to give the mesh step size limitation, which guarantees that the coefficient matrix corresponding to the discrete operator is an M-matrix.

The discretization is performed using a uniform mesh $\Omega^{N,M,K}$ for the computational domain $\Omega \times [0, T]$. The mesh steps to the x direction, y direction, and t direction are denoted by $\Delta x = (x_{\max} - x_{\min})/N$, $\Delta y = (y_{\max} - y_{\min})/M$, and $\Delta t = T/K$. The mesh point values of the finite difference approximation are denoted by

$$U_{i,j}^k \approx u(x_i, y_j, t_k) \quad \text{for } i = 0, 1, \ldots, N; \quad j = 0, 1, \ldots, M; \ k = 0, 1, \ldots, K. \tag{9}$$

We discretize the differential operator L using the central difference scheme on the previous uniform mesh. We set

$$\begin{aligned}
&L^{N,M,K} U_{i,j}^k \\
&\quad \equiv -D_t^+ U_{i,j}^k - \frac{1}{2}\sigma_1^2 \delta_x^2 U_{i,j}^k \\
&\qquad - \sigma_1 \sigma_2 \left(\tilde{\rho}^+ \delta_{xy}^+ U_{i,j}^k + \tilde{\rho}^- \delta_{xy}^- U_{i,j}^k\right) - \frac{1}{2}\sigma_2^2 \delta_y^2 U_{i,j}^k \\
&\qquad - \left(r - \frac{1}{2}\sigma_1^2\right) D_x U_{i,j}^k - \left(r - \frac{1}{2}\sigma_2^2\right) D_y U_{i,j}^k + r U_{i,j}^k,
\end{aligned} \tag{10}$$

where

$$\begin{aligned}
&\delta_x^2 U_{i,j}^k = \frac{D_x^+ - D_x^-}{\Delta x} U_{i,j}^k, \qquad \delta_y^2 U_{i,j}^k = \frac{D_y^+ - D_y^-}{\Delta y} U_{i,j}^k, \\
&\delta_{xy}^+ U_{i,j}^k = \frac{D_x^+ D_y^+ + D_x^- D_y^-}{2} U_{i,j}^k, \\
&\delta_{xy}^- U_{i,j}^k = \frac{D_x^+ D_y^- + D_x^- D_y^+}{2} U_{i,j}^k, \\
&D_x^+ U_{i,j}^k = \frac{U_{i+1,j}^k - U_{i,j}^k}{\Delta x}, \qquad D_y^+ U_{i,j}^k = \frac{U_{i,j+1}^k - U_{i,j}^k}{\Delta y}, \\
&D_x^- U_{i,j}^k = \frac{U_{i,j}^k - U_{i-1,j}^k}{\Delta x}, \qquad D_y^- U_{i,j}^k = \frac{U_{i,j}^k - U_{i,j-1}^k}{\Delta y}, \\
&D_x U_{i,j}^k = \frac{U_{i+1,j}^k - U_{i-1,j}^k}{2\Delta x}, \qquad D_y U_{i,j}^k = \frac{U_{i,j+1}^k - U_{i,j-1}^k}{2\Delta y}, \\
&D_t^+ U_{i,j}^k = \frac{U_{i,j}^{k+1} - U_{i,j}^k}{\Delta t}, \qquad \tilde{\rho}^{\pm} = \frac{1}{2}[\rho \pm |\rho|].
\end{aligned} \tag{11}$$

Denote

$$\begin{aligned}
&\overline{\Omega}_h = \{(i, j, k) \mid 0 \leq i \leq N, \ 0 \leq j \leq M, \ 0 \leq k \leq K\}, \\
&\widetilde{\Omega}_h = \{(i, j, k) \mid 1 \leq i \leq N - 1, \ 1 \leq j \leq M - 1, \\
&\qquad 1 \leq k \leq K - 1\}, \\
&\partial\Omega_h = \overline{\Omega}_h \setminus \widetilde{\Omega}_h.
\end{aligned} \tag{12}$$

Thus, we apply the central difference scheme on the uniform mesh to approximate the parabolic complementarity problem (8) as follows:

$$\begin{aligned}
&L^{N,M,K} U_{i,j}^k \geq 0, \quad (i, j, k) \in \widetilde{\Omega}_h, \\
&U_{i,j}^k - \varphi_{i,j} \geq 0, \quad (i, j, k) \in \widetilde{\Omega}_h, \\
&L^{N,M,K} U_{i,j}^k \cdot \left[U_{i,j}^k - \varphi_{i,j}\right] = 0, \quad (i, j, k) \in \widetilde{\Omega}_h, \\
&U_{i,j}^K = \varphi_{i,j}, \quad 0 \leq i \leq N, \ 0 \leq j \leq M, \\
&U_{0,j}^k = (g_2)_j^k, \quad U_{N,j}^k = 0, \quad 0 \leq j \leq M, \ 0 \leq k < K, \\
&U_{i,0}^k = (g_1)_i^k, \quad U_{i,M}^k = 0, \quad 0 < i < N, \ 0 \leq k < K.
\end{aligned} \tag{13}$$

Here, $(g_1)_i^k$ and $(g_2)_j^k$ are discrete approximates of $g_1(e^x, t)$ and $g_2(e^y, t)$, respectively. Hence, $(g_1)_i^k$ and $(g_2)_j^k$ can be obtained by solving the corresponding one-dimensional Black-Scholes equations [29]. In the next section, we will prove that the system matrix corresponding to the discrete operator $L^{N,M,K}$ is an M-matrix. Hence, from the uniqueness theorem of Goeleven [30], we can obtain that there exists a unique solution U for the previous linear complementarity problem (13).

4. Analysis of the Method

First, we give the stability analysis for the difference scheme (13).

Lemma 1. *If mesh steps satisfy the inequalities*

$$\Delta x \le \frac{\sigma_1^2}{|2r-\sigma_1^2|}, \qquad \Delta y \le \frac{\sigma_2^2}{|2r-\sigma_2^2|}, \tag{14}$$

$$\frac{2|\rho|\sigma_1}{\sigma_2} \le \frac{\Delta x}{\Delta y} \le \frac{2\sigma_1}{|\rho|\sigma_2}, \tag{15}$$

then the system matrix corresponding to the discrete operator $L^{N,M,K}$ is an M-matrix.

Proof. The difference operator $L^{N,M,K}$ can be written as follows:

$$\begin{aligned}
L^{N,M,K}U_{i,j}^k
&= -\frac{\tilde{\rho}^+\sigma_1\sigma_2}{2\Delta x\Delta y}U_{i-1,j-1}^k \\
&\quad + \left[\sigma_1\sigma_2\frac{\tilde{\rho}^+-\tilde{\rho}^-}{2\Delta x\Delta y} - \frac{\sigma_2^2}{2(\Delta y)^2} + \frac{r-(1/2)\sigma_2^2}{2\Delta y}\right]U_{i,j-1}^k \\
&\quad + \frac{\tilde{\rho}^-\sigma_1\sigma_2}{2\Delta x\Delta y}U_{i+1,j-1}^k \\
&\quad + \left[\sigma_1\sigma_2\frac{\tilde{\rho}^+-\tilde{\rho}^-}{2\Delta x\Delta y} - \frac{\sigma_1^2}{2(\Delta x)^2} + \frac{r-(1/2)\sigma_1^2}{2\Delta x}\right]U_{i-1,j}^k \\
&\quad + \left[\frac{1}{\Delta t} + \frac{\sigma_1^2}{(\Delta x)^2} - \sigma_1\sigma_2\frac{\tilde{\rho}^+-\tilde{\rho}^-}{\Delta x\Delta y} + \frac{\sigma_2^2}{(\Delta y)^2} + r\right]U_{i,j}^k \\
&\quad + \left[-\frac{\sigma_1^2}{2(\Delta x)^2} + \sigma_1\sigma_2\frac{\tilde{\rho}^+-\tilde{\rho}^-}{2\Delta x\Delta y} - \frac{r-(1/2)\sigma_1^2}{2\Delta x}\right]U_{i+1,j}^k \\
&\quad + \frac{\tilde{\rho}^-\sigma_1\sigma_2}{2\Delta x\Delta y}U_{i-1,j+1}^k \\
&\quad + \left[\sigma_1\sigma_2\frac{\tilde{\rho}^+-\tilde{\rho}^-}{2\Delta x\Delta y} - \frac{\sigma_2^2}{2(\Delta y)^2} - \frac{r-(1/2)\sigma_2^2}{2\Delta y}\right]U_{i,j+1}^k \\
&\quad - \frac{\tilde{\rho}^+\sigma_1\sigma_2}{2\Delta x\Delta y}U_{i+1,j+1}^k - \frac{1}{\Delta t}U_{i,j}^{k+1}.
\end{aligned} \tag{16}$$

The coefficient of $U_{i,j}$ in the previous expression (which corresponds to the diagonal of the system matrix) is positive since

$$\frac{\sigma_1^2}{(\Delta x)^2} - \sigma_1\sigma_2\frac{\tilde{\rho}^+-\tilde{\rho}^-}{\Delta x\Delta y} + \frac{\sigma_2^2}{(\Delta y)^2} \ge 0. \tag{17}$$

All the coefficients of the other U in the previous expression (which correspond to off-diagonal elements in the system matrix) will be nonpositive once the following inequalities are satisfied:

$$\begin{aligned}
&\frac{\sigma_1^2}{4(\Delta x)^2} - \frac{|r-(1/2)\sigma_1^2|}{2\Delta x} \ge 0, \qquad \frac{\sigma_2^2}{4(\Delta y)^2} - \frac{|r-(1/2)\sigma_2^2|}{2\Delta y} \ge 0, \\
&\sigma_1\sigma_2\frac{\tilde{\rho}^+-\tilde{\rho}^-}{2\Delta x\Delta y} - \frac{\sigma_2^2}{4(\Delta y)^2} \le 0, \qquad \sigma_1\sigma_2\frac{\tilde{\rho}^+-\tilde{\rho}^-}{2\Delta x\Delta y} - \frac{\sigma_1^2}{4(\Delta x)^2} \le 0.
\end{aligned} \tag{18}$$

Together, they require that the following inequalities hold:

$$\begin{aligned}
&\Delta x \le \frac{\sigma_1^2}{|2r-\sigma_1^2|}, \qquad \Delta y \le \frac{\sigma_2^2}{|2r-\sigma_2^2|}, \\
&\frac{2\sigma_1(\tilde{\rho}^+-\tilde{\rho}^-)}{\sigma_2} \le \frac{\Delta x}{\Delta y} \le \frac{2\sigma_1}{\sigma_2(\tilde{\rho}^+-\tilde{\rho}^-)},
\end{aligned} \tag{19}$$

which are (14) and (15), respectively. Thus, we have shown that the system matrix, corresponding to the discrete operator $L^{N,M,K}$ is an M-matrix and the result follows. □

There are only few error estimates for the direct application of finite difference method to linear complementarity problems. Here, we apply the maximum principle to the linear complementarity problem (13) in two mesh sets and derive the error estimates [29, 31].

By using Taylor's formula, we can easily obtain the following truncation error estimate.

Lemma 2. *Let $u(x, y, t)$ be a smooth function defined on $\Omega^{N,M,K}$. Then the truncation error of the difference scheme* (10) *satisfies*

$$\left|L^{N,M,K}u_{i,j}^k - Lu_{i,j}^k\right| = O\left((\Delta x)^2 + (\Delta y)^2 + \Delta x\Delta y + \Delta t\right), \tag{20}$$

for all $(i, j, k) \in \widetilde{\Omega}_h$.

Now we can derive our main result for the difference scheme.

Theorem 3. *Let $u(x, y, t)$ be the solution of the problem* (8) *and let $U_{i,j}^k$ be the solution of the problem* (13). *If mesh steps satisfy conditions* (14) *and* (15), *the difference scheme* (13) *satisfies the following error estimate:*

$$\max_{(i,j,k)\in\overline{\Omega}_h}\left|u(x_i, y_j, t_k) - U_{i,j}^k\right| \le C\left[(\Delta x)^2 + (\Delta y)^2 + \Delta x\Delta y + \Delta t\right], \tag{21}$$

where C is a constant independent of Δx, Δy, and Δt.

Proof. Denote

$$\Omega^{(1)} = \left\{(i,j,k) \in \widetilde{\Omega}_h \mid u\left(x_i, y_j, t_k\right) = \varphi\left(x_i, y_j\right)\right\}, \quad \Omega^{(2)} = \widetilde{\Omega}_h \setminus \Omega^{(1)}. \tag{22}$$

From (8), we have the result

$$Lu\left(x_i, y_j, t_k\right) \geq 0, \quad (i,j,k) \in \Omega^{(1)}, \qquad Lu\left(x_i, y_j, t_k\right) = 0, \quad (i,j,k) \in \Omega^{(2)}. \tag{23}$$

Denote

$$\Omega_h^{(1)} = \left\{(i,j) \in \widetilde{\Omega}_h \mid U_{i,j}^k = \varphi\left(x_i, y_j\right)\right\}, \quad \Omega_h^{(2)} = \widetilde{\Omega}_h \setminus \Omega_h^{(1)}. \tag{24}$$

Obviously,

$$L^{N,M,K} U_{i,j}^k = 0, \quad (i,j,k) \in \Omega_h^{(2)}. \tag{25}$$

Define the function on $\widetilde{\Omega}_h$ by

$$W_{i,j}^k = C\left[(\Delta x)^2 + (\Delta y)^2 + \Delta x \Delta y + \Delta t\right] > 0, \tag{26}$$

where C is a sufficiently large constant.

For $(i,j,k) \in \Omega_h^{(2)}$, by the fact that $Lu(x_i, y_j, t_k) \geq 0$, (25), (26), and Lemma 2, we obtain

$$\begin{aligned} L^{N,M,K} & \left(u\left(x_i, y_j, t_k\right) - U_{i,j}^k + W_{i,j}^k\right) \\ &= L^{N,M,K} u\left(x_i, y_j, t_k\right) + L^{N,M,K} W_{i,j}^k \\ &= \left[L^{N,M,K} u\left(x_i, y_j, t_k\right) - Lu\left(x_i, y_j, t_k\right) + L^{N,M,K} W_{i,j}^k\right] \\ &\quad + Lu\left(x_i, y_j, t_k\right) \geq 0. \end{aligned} \tag{27}$$

On the "boundary" of $\Omega_h^{(2)}$, the nodes $(i,j,k) \in \Omega_h^{(1)}$, so $U_{i,j}^k = \varphi(x_i, y_j)$, but $u(x_i, y_j, t_k) \geq \varphi(x_i, y_j)$, therefore

$$u\left(x_i, y_j, t_k\right) - U_{i,j}^k + W_{i,j}^k = u\left(x_i, y_j, t_k\right) - \varphi\left(x_i, y_j\right) + W_{i,j}^k \geq 0, \tag{28}$$

and the nodes $(i,j,k) \in \partial\Omega_h$,

$$u\left(x_i, y_j, t_k\right) - U_{i,j}^k + W_{i,j}^k = W_{i,j}^k \geq 0. \tag{29}$$

Applying the maximum principle to $\Omega_h^{(2)}$, we get

$$u\left(x_i, y_j, t_k\right) - U_{i,j}^k + W_{i,j}^k \geq 0, \quad (i,j,k) \in \Omega_h^{(2)}. \tag{30}$$

Thus,

$$u\left(x_i, y_j, t_k\right) - U_{i,j}^k + W_{i,j}^k \geq 0, \quad (i,j,k) \in \overline{\Omega}_h. \tag{31}$$

For $(i,j,k) \in \Omega^{(2)}$, $Lu(x_i, y_j, t_k) = 0$, but $L^{N,M,K} U_{i,j}^k \geq 0$, thus,

$$\begin{aligned} L^{N,M,K} & \left(u\left(x_i, y_j, t_k\right) - U_{i,j}^k - W_{i,j}^k\right) \\ &= \left[L^{N,M,K} u\left(x_i, y_j, t_k\right) - Lu\left(x_i, y_j, t_k\right) - L^{N,M,K} W_{i,j}^k\right] \\ &\quad - L^{N,M,K} U_{i,j}^k \leq 0. \end{aligned} \tag{32}$$

On the "boundary" of $\Omega^{(2)}$, the nodes $(i,j,k) \in \Omega^{(1)}$, so $u(x_i, y_j, t_k) = \varphi(x_i, y_j)$, but $U_{i,j}^k \geq \varphi(x_i, y_j)$, therefore

$$u\left(x_i, y_j, t_k\right) - U_{i,j}^k - W_{i,j}^k = \varphi\left(x_i, y_j\right) - U_{i,j}^k - W_{i,j}^k \leq 0, \tag{33}$$

and the nodes $(i,j,k) \in \partial\Omega_h$,

$$u\left(x_i, y_j, t_k\right) - U_{i,j}^k - W_{i,j}^k = -W_{i,j}^k \leq 0. \tag{34}$$

Applying the maximum principle to $\Omega^{(2)}$, we get

$$u\left(x_i, y_j, t_k\right) - U_{i,j}^k - W_{i,j}^k \leq 0, \quad (i,j,k) \in \Omega^{(2)}. \tag{35}$$

Thus,

$$u\left(x_i, y_j, t_k\right) - U_{i,j}^k - W_{i,j}^k \leq 0, \quad (i,j,k) \in \overline{\Omega}_h. \tag{36}$$

From (31) and (36), we obtain

$$\begin{aligned} \max_{(i,j,k)\in\overline{\Omega}_h} & \left|u\left(x_i, y_j, t_k\right) - U_{i,j}^k\right| \\ &\leq \max_{(i,j,k)\in\overline{\Omega}_h} W_{i,j}^k \leq C\left[(\Delta x)^2 + (\Delta y)^2 + \Delta x \Delta y + \Delta t\right], \end{aligned} \tag{37}$$

where C is a sufficiently large constant. From this we complete the proof. □

5. Numerical Experiments

In this section, we verify experimentally the theoretical results obtained in the preceding section. Errors and convergence rates for the second-order finite difference scheme are presented for two test problems.

Test 1. American put option with parameters: $T = 1$, $r = 0.1$, $\sigma_1 = 0.4$, $\sigma_2 = 0.5$, $\rho = 0.5$, $x_{\min} = -\ln(30)$, $x_{\max} = \ln(30)$, $y_{\min} = -\ln(40)$, $y_{\max} = \ln(40)$, $\alpha_1 = 0.3$, $\alpha_2 = 0.7$, and $E = 10$.

Test 2. American put option with parameters: $T = 1$, $r = 0.08$, $\sigma_1 = 0.3$, $\sigma_2 = 0.4$, $\rho = -0.6$, $x_{\min} = -\ln(30)$, $x_{\max} = \ln(30)$, $y_{\min} = -\ln(40)$, $y_{\max} = \ln(40)$, $\alpha_1 = 0.3$, $\alpha_2 = 0.7$, and $E = 10$.

To solve the linear inequality system (13), we use the projection scheme used in [32, page 433]. Since mesh steps need to satisfy conditions (14) and (15), we choose the number of mesh steps in the y direction

$$M = \left[\frac{\left(2\left|\rho\right|\sigma_1/\sigma_2 + 2\sigma_1/\left|\rho\right|\sigma_2\right)N}{2\left(x_{\max} - x_{\min}\right)}\right], \tag{38}$$

Table 1: Numerical results for Test 1.

K	N	Error	Rate
128	6	$1.8124e-1$	—
	12	$5.1852e-2$	1.805
	24	$1.4761e-2$	1.813
	48	$4.1312e-3$	1.837

Table 2: Numerical results for Test 2.

K	N	Error	Rate
128	6	$1.2256e-1$	—
	12	$3.3776e-2$	1.859
	24	$9.2571e-3$	1.867
	48	$2.5124e-3$	1.882

where N is the number of mesh steps in the x direction. The exact solutions of the test problems are not available. Therefore, we use the double mesh principle to estimate the errors and compute the experiment convergence rates in our computed solution. We measure the accuracy in the discrete maximum norm

$$e^{N,M,K} = \max_{i,j,k} \left| U_{i,j,k}^{N,M,K} - U_{i,j,k}^{2N,2M,K} \right|, \tag{39}$$

and the convergence rate

$$R^{N,M,K} = \log_2 \left(\frac{e^{N,M,K}}{e^{2N,2M,K}} \right). \tag{40}$$

The error estimates and convergence rates in our computed solutions of Tests 1 and 2 are listed in Tables 1 and 2, respectively. From Tables 1 and 2, we see that $e^{N,M,K}/e^{2N,2M,K}$ is close to 4 for sufficiently large K, which supports the convergence estimate of Theorem 3. However, the numerical results of Nielsen et al. [24] and Zhang et al. [25] verify that their schemes are only first-order convergent. Hence, our scheme is more accurate.

Acknowledgments

The authors would like to thank the anonymous referees for several suggestions for the improvement of this paper. The work was supported by Zhejiang Province Natural Science Foundation of China (Grant no. Y2111160).

References

[1] F. Black and M. Scholes, "The pricing of options and corporate liabilities," *Journal of Political Economy*, vol. 81, no. 3, pp. 637–654, 1973.

[2] J. Huang and J. S. Pang, "Option pricing and linear complementarity," *Journal of Computational Finance*, vol. 2, no. 3, pp. 31–60, 1998.

[3] P. Wilmott, J. Dewynne, and S. Howison, *Option Pricing: Mathematical Models and Computation*, Oxford Financial Press, Oxford, UK, 1993.

[4] J. C. Cox, S. A. Ross, and M. Rubinstein, "Option pricing: a simplified approach," *Journal of Financial Economics*, vol. 7, no. 3, pp. 229–263, 1979.

[5] A. Ibáñez and F. Zapatero, "Monte Carlo valuation of American options through computation of the optimal exercise frontier," *Journal of Financial and Quantitative Analysis*, vol. 39, no. 2, pp. 253–275, 2004.

[6] C. Vázquez, "An upwind numerical approach for an American and European option pricing model," *Applied Mathematics and Computation*, vol. 97, no. 2-3, pp. 273–286, 1998.

[7] L. Wu and Y. K. Kwok, "A front-xing nite dierence method for the valuation of American options," *Journal of Financial Engineering*, vol. 6, no. 2, pp. 83–97, 1997.

[8] J. Zhao, M. Davison, and R. M. Corless, "Compact finite difference method for American option pricing," *Journal of Computational and Applied Mathematics*, vol. 206, no. 1, pp. 306–321, 2007.

[9] P. A. Forsyth, K. R. Vetzal, and R. Zvan, "A nite element approach to the pricing of discrete lookbacks with stochastic volatility," *Applied Mathematical Finance*, vol. 6, no. 2, pp. 87–106, 1999.

[10] R. Zvan, P. A. Forsyth, and K. R. Vetzal, "A general nite element approach for PDE option pricing models," University of Waterloo, Canada, 1998.

[11] L. Angermann and S. Wang, "Convergence of a fitted finite volume method for the penalized Black-Scholes equation governing European and American option pricing," *Numerische Mathematik*, vol. 106, no. 1, pp. 1–40, 2007.

[12] S. Wang, X. Q. Yang, and K. L. Teo, "Power penalty method for a linear complementarity problem arising from American option valuation," *Journal of Optimization Theory and Applications*, vol. 129, no. 2, pp. 227–254, 2006.

[13] R. Zvan, P. A. Forsyth, and K. R. Vetzal, "A finite volume approach for contingent claims valuation," *IMA Journal of Numerical Analysis*, vol. 21, no. 3, pp. 703–731, 2001.

[14] S. O'Sullivan and C. O'Sullivan, "On the acceleration of explicit finite difference methods for option pricing," *Quantitative Finance*, vol. 11, no. 8, pp. 1177–1191, 2011.

[15] N. Clarke and K. Parrott, "Multigrid for American option pricing with stochastic volatility," *Applied Mathematics Finance*, vol. 6, no. 3, pp. 177–195, 1999.

[16] C. W. Oosterlee, "On multigrid for linear complementarity problems with application to American-style options," *Electronic Transactions on Numerical Analysis*, vol. 15, pp. 165–185, 2003.

[17] S. Ikonen and J. Toivanen, "Componentwise splitting methods for pricing American options under stochastic volatility," *International Journal of Theoretical and Applied Finance*, vol. 10, no. 2, pp. 331–361, 2007.

[18] S. Ikonen and J. Toivanen, "Efficient numerical methods for pricing American options under stochastic volatility," *Numerical Methods for Partial Differential Equations*, vol. 24, no. 1, pp. 104–126, 2008.

[19] S. Ikonen and J. Toivanen, "Operator splitting methods for pricing American options under stochastic volatility," *Numerische Mathematik*, vol. 113, no. 2, pp. 299–324, 2009.

[20] K. J. I. Hout and S. Foulon, "ADI finite difference schemes for option pricing in the Heston model with correlation," *International Journal of Numerical Analysis and Modeling*, vol. 7, no. 2, pp. 303–320, 2010.

[21] S.-P. Zhu and W.-T. Chen, "A predictor-corrector scheme based on the ADI method for pricing American puts with stochastic volatility," *Computers & Mathematics with Applications*, vol. 62, no. 1, pp. 1–26, 2011.

[22] A. Le, Z. Cen, and A. Xu, "A robust upwind difference scheme for pricing perpetual American put options under stochastic volatility," *International Journal of Computer Mathematics*, vol. 89, no. 9, pp. 1135–1144, 2012.

[23] M. Yousuf, "Efficient L-stable method for parabolic problems with application to pricing American options under stochastic volatility," *Applied Mathematics and Computation*, vol. 213, no. 1, pp. 121–136, 2009.

[24] B. F. Nielsen, O. Skavhaug, and A. Tveito, "Penalty methods for the numerical solution of American multi-asset option problems," *Journal of Computational and Applied Mathematics*, vol. 222, no. 1, pp. 3–16, 2008.

[25] K. Zhang, S. Wang, X. Q. Yang, and K. L. Teo, "A power penalty approach to numerical solutions of two-asset American options," *Numerical Mathematics. Theory, Methods and Applications*, vol. 2, no. 2, pp. 202–223, 2009.

[26] R. Kangro and R. Nicolaides, "Far field boundary conditions for Black-Scholes equations," *SIAM Journal on Numerical Analysis*, vol. 38, no. 4, pp. 1357–1368, 2000.

[27] P. Matus and I. Rybak, "Difference schemes for elliptic equations with mixed derivatives," *Computational Methods in Applied Mathematics*, vol. 4, no. 4, pp. 494–505, 2004.

[28] I. V. Rybak, "Monotone and conservative difference schemes for elliptic equations with mixed derivatives," *Mathematical Modelling and Analysis*, vol. 9, no. 2, pp. 169–178, 2004.

[29] Z. Cen and A. Le, "A robust finite difference scheme for pricing American put options with singularity-separating method," *Numerical Algorithms*, vol. 53, no. 4, pp. 497–510, 2010.

[30] D. Goeleven, "A uniqueness theorem for the generalized-order linear complementary problem associated with M-matrices," *Linear Algebra and Its Applications*, vol. 235, pp. 221–227, 1996.

[31] X. Cheng and L. Xue, "On the error estimate of finite difference method for the obstacle problem," *Applied Mathematics and Computation*, vol. 183, no. 1, pp. 416–422, 2006.

[32] R. Glowinski, J. L. Lions, and T. Trémolières, *Numerical Analysis of Variational Inequality*, North-Holland, Amsterdam, The Netherlands, 1984.

Hindawi Publishing Corporation
Journal of Function Spaces and Applications
Volume 2013, Article ID 578326, 11 pages
http://dx.doi.org/10.1155/2013/578326

Review Article

Recent Developments on Hybrid Time-Frequency Numerical Simulation Techniques for RF and Microwave Applications

Jorge F. Oliveira[1,2] and José C. Pedro[2]

[1] *School of Technology and Management, Polytechnic Institute of Leiria, Morro do Lena, Alto Vieiro, Apartado 4163, 2411-901 Leiria, Portugal*
[2] *Institute of Telecommunications, University of Aveiro, Campus Universitário de Santiago, 3810-193 Aveiro, Portugal*

Correspondence should be addressed to Jorge F. Oliveira; jorge.oliveira@ipleiria.pt

Received 11 October 2012; Accepted 11 December 2012

Academic Editor: Davide La Torre

This paper reviews some of the promising doors that functional analysis techniques have recently opened in the field of electronic circuit simulation. Because of the modulated nature of radio frequency (RF) signals, the corresponding electronic circuits seem to operate in a slow time scale for the aperiodic information and another, much faster, time scale for the periodic carrier. This apparent multirate behavior can be appropriately described using partial differential equations (PDEs) within a bivariate framework, which can be solved in an efficient way using hybrid time-frequency techniques. With these techniques, the aperiodic information dimension is treated in the discrete time domain, while the periodic carrier dimension is processed in the frequency domain, in which the solution is evaluated within a space of harmonically related sinusoidal functions. The objective of this paper is thus to provide a general overview on the most important hybrid time-frequency techniques, as the ones found in commercial tools or the ones recently published in the literature.

1. Introduction

Numerical simulation plays an important role in electronics, helping engineers to verify correctness and debug circuits during their design, and so avoiding breadboarding and physical prototyping. The advantages of numerical simulation are especially significant in integrated circuits design, where manufacturing is expensive and probing internal nodes is difficult or prohibitive.

Circuit simulation has emerged in the early 1970's, and many numerical techniques have been developed and improved along the years. Radio frequency (RF) and microwave system design is a field that was an important driver for numerical simulation development, and continues to be so nowadays. Indeed, computing the solution of some current electronic circuits, as is the case of modern wireless communication systems, is still today a hot topic. In effect, serious difficulties arise when these nonlinear systems are highly heterogeneous circuits operating in multiple time scales. Current examples of these are wireless RF integrated circuits (RFICs), or systems-on-a-chip (SoC), combining RF, baseband analog, and digital blocks in the same the circuit.

Signals handed by wireless communication systems can usually be described by a high frequency RF carrier modulated by some kind of slowly varying baseband information signal. Hence, the analysis of any statistically relevant information time frame requires the processing of thousands or millions of time points of the composite modulated signal, turning any conventional numerical integration of the circuit's system of ordinary differential equations (ODEs) highly inefficient, or even impractical. However, if the waveforms produced by the circuit are not excessively demanding on the number of harmonics for a convenient frequency-domain representation, this class of problems can be efficiently simulated with hybrid time-frequency techniques. Handling the response to the slowly varying baseband information signal in the conventional time step by time-step basis, but representing the reaction to the periodic RF carrier as a small set of Fourier components (a harmonic balance algorithm for computing the steady-state response to the carrier) new circuit simulators are taking an enormous profit from functional analysis techniques. But, beyond overcoming the signals' time-scale disparity, one of the recently proposed hybrid time-frequency techniques is also able to deal with highly heterogeneous RF circuits in an efficient way, by applying different numerical strategies to state variables in different parts (blocks) of the circuits.

2. Theoretical Background Material

2.1. Mathematical Model of an Electronic Circuit. The behavior of an electronic circuit can be described with a system of equations involving voltages, currents, charges, and fluxes. This system of equations can be constructed from a circuit description using, for example, nodal analysis, which involves applying the Kirchhoff current law to each node in the circuit, and applying the constitutive or branch equations to each circuit element. Systems generated this way have, in general, the following form

$$\mathbf{p}(\mathbf{y}(t)) + \frac{d\mathbf{q}(\mathbf{y}(t))}{dt} = \mathbf{x}(t), \tag{1}$$

where $\mathbf{x}(t) \in \mathbf{R}^n$ and $\mathbf{y}(t) \in \mathbf{R}^n$ stand for the excitation (independent voltage or current sources) and state variable (node voltages and branch currents) vectors, respectively. $\mathbf{p} : \mathbb{R}^n \rightarrow \mathbb{R}^n$ stands for all linear or nonlinear elements, as resistors, nonlinear voltage-controlled current sources, and so forth, while $\mathbf{q} : \mathbb{R}^n \rightarrow \mathbb{R}^n$ models dynamic linear or nonlinear elements, as capacitors (represented as linear or nonlinear voltage-dependent electric charges), or inductors (represented as linear or nonlinear current-dependent magnetic fluxes).

The system of (1) is, in general, a *differential algebraic equations*' (DAE) system, which represents the general mathematical formulation of lumped problems. However, as reviewed in [1], this DAE circuit model formulation could even be extended to include linear distributed elements. For that, these are substituted, one-by-one, by their lumped-element equivalent circuit models or are replaced, as whole sub-circuits, by reduced order models derived from their frequency-domain characteristics whenever larger distributed linear networks are dealt with.

The substitution of distributed devices by lumped-equivalent models is especially reasonable when the size of the circuit elements is small in comparison to the wavelengths, as is the case of most emerging RF technologies (e.g., new systems on chip (SoCs), or systems in package (SiPs), integrating digital high-speed CMOS baseband processing and RFCMOS hardware).

2.2. Steady-State Simulation. The most natural way of simulating an electronic circuit is to numerically time-step integrate, in time domain, the ordinary differential system describing its operation. This straightforward technique was used in the first digital computer programs of circuit analysis and is still widely used nowadays. It is the core of all SPICE (which means simulation program with integrated circuit emphasis) [2] or SPICE-like computer programs. The dilemma is that these tools focus on transient analysis, and sometimes electronics designers, as is the case of RF and microwave designers, are not interested in the circuits' transient response, but, instead, in their steady-state regimes. This is because certain aspects of circuits' performance are better characterized, or simply only defined, in steady-state (e.g., distortion, noise, power, gain, impedance, etc.). Time-step integration engines, as linear multistep methods, or Runge-Kutta methods, which were tailored for finding the circuit's transient response, are not adequate for computing the steady-state because they have to pass through the lengthy process of integrating all transients and expecting them to vanish. In circuits presenting extremely different time constants, or high Q resonances, as is typically the case of RF and microwave circuits, time-step integration can be very inefficient. Indeed, in such cases, frequencies in steady-state response are much higher than the rate at which the circuit approaches steady-state or the ratio between the highest and the lowest frequency is very large. Thus, the number of discretization time steps used by the numerical integration scheme will be enormous because the time interval over which the differential equations must be numerically integrated is set by the lowest frequency or by how long the circuit takes to achieve steady-state, while the size of the time steps is constrained by the highest frequency component.

It must be noted that there are several different kinds of steady-state behavior that may be of interest. The first one is DC steady-state. Here, the solution does not vary with time. Stable linear circuits driven by sinusoidal sources may exhibit a sinusoidal steady-state regime, which is characterized as being purely sinusoidal except, possibly, for some DC offset. If the steady-state response of a circuit consists of generic waveforms presenting a common period, then the circuit is said to be in a periodic steady-state. Directly computing the periodic steady-state response of an electronic circuit, without having to first integrate its transient response, involves finding the initial condition, $\mathbf{y}(t_0)$, for the differential system that describe the circuit's operation, such that the solution at the end of one period matches the initial condition, that is, $\mathbf{y}(t_0) = \mathbf{y}(t_0 + T)$, where T is the period. Problems of this form, those of finding the solution to a system of ordinary differential equations that satisfies constraints at two or more distinct points in time, are referred to as *boundary value problems*. In this particular case, we have a *periodic boundary value problem* that can be formulated as

$$\begin{gathered} \mathbf{p}(\mathbf{y}(t)) + \frac{d\mathbf{q}(\mathbf{y}(t))}{dt} = \mathbf{x}(t), \qquad \mathbf{y}(t_0) = \mathbf{y}(t_0 + T), \\ t_0 \le t \le t_0 + T, \quad \mathbf{y}(t) \in \mathbb{R}^n, \end{gathered} \tag{2}$$

where the condition $\mathbf{y}(t_0) = \mathbf{y}(t_0 + T)$ is known as the *periodic boundary condition*.

In the following, we will focus our attention to the most widely used technique for computing the periodic steady-state solution of RF and microwave electronic circuits: the harmonic balance method [3–5].

2.3. Harmonic Balance. Harmonic balance (HB) is a mature computer steady-state simulation tool that operates in the frequency domain [3]. Frequency-domain methods differ from time-domain steady-state techniques in the way that, instead of representing waveforms as a collection of time samples, they represent them using coefficients of sinusoids in trigonometric series. The main advantage of the trigonometric series approach is that the steady-state solution can often be represented accurately with a small number of terms. For example, if the circuit is linear and its inputs are all sinusoidal of the same frequency, only two terms (magnitude and phase) of the trigonometric series will represent the solution exactly, whereas an approximate time-domain solution would require a much larger number of sample points.

Another advantage of operating directly in the frequency-domain is that linear dynamic operations, like differentiation or integration, are converted into simple algebraic operations, such as multiplying or dividing by frequency, respectively. For example, when analyzing linear time-invariant circuit devices, the coefficients of the response are easily evaluated by exploiting superposition within phasor analysis [6]. Computing the response of nonlinear devices is obviously more difficult than for linear devices, in part because superposition no longer applies, and also because, in general, the coefficients of the response cannot be computed directly from the coefficients of the stimulus. Nevertheless, in the case of moderate nonlinearities, the steady-state solution is typically achieved much more easily in frequency-domain than in time-domain simulators.

HB handles the circuit, its excitation and its state variables in the frequency domain, which is the format normally adopted by RF designers. Because of that, it also benefits from allowing the direct inclusion of distributed devices (like dispersive transmission lines) or other circuit elements described by frequency-domain measurement data, for which we cannot find an exact time-domain representation.

In order to provide a brief and illustrative explanation of the conventional HB theory, let us start by considering again the boundary value problem of (2), describing the periodic steady-state regime of an electronic circuit. For simplicity, let us momentarily suppose that we are dealing with a scalar problem, that is, that we have a simple circuit described with a unique state variable $y(t)$, and that this circuit is driven by a single source $x(t)$, verifying the periodic condition $x(t) = x(t+T)$. Since the steady-state response of the circuit will be also periodic with period T, both the excitation and the steady-state solution can be expressed as the Fourier series

$$x(t) = \sum_{k=-\infty}^{+\infty} X_k e^{jk\omega_0 t}, \qquad y(t) = \sum_{k=-\infty}^{+\infty} Y_k e^{jk\omega_0 t}, \tag{3}$$

where $\omega_0 = 2\pi/T$ is the fundamental frequency. By substituting (3) into (2), and adopting a convenient harmonic truncation at some order $k = K$, we will obtain

$$p\left(\sum_{k=-K}^{+K} Y_k e^{jk\omega_0 t}\right) + \frac{d}{dt}\left[q\left(\sum_{k=-K}^{+K} Y_k e^{jk\omega_0 t}\right)\right] = \sum_{k=-K}^{+K} X_k e^{jk\omega_0 t}. \tag{4}$$

The HB method consists in converting this differential system into the frequency domain, in way to obtain an algebraic system of $2K+1$ equations, in which the unknowns are the Fourier coefficients Y_k. It must be noted that since p and q are, in general, nonlinear functions, it is not possible to directly compute the Fourier coefficients Y_k in this system. In fact, we only know a priori the trivial solution $y(t) = 0$ for $x(t) = 0$. So, we can possibly guess an initial estimate to $y(t)$ and then adopt an iterative procedure to compute the steady-state response of the circuit. For that, we use a first-order Taylor-series expansion, in which each initial expansion point corresponds to the previous iterated solution. Indeed, we expand the left hand side of the DAE system in (2) to obtain

$$\begin{aligned} & p\left(y^{[r]}(t)\right) + \frac{dq\left(y^{[r]}(t)\right)}{dt} \\ & \quad + \underbrace{\left.\frac{dp(y)}{dy}\right|_{y=y^{[r]}}}_{g(y^{[r]})} \left[y^{[r+1]}(t) - y^{[r]}(t)\right] \\ & \quad + \frac{d}{dt} \underbrace{\left.\frac{dq(y)}{dy}\right|_{y=y^{[r]}}}_{c(y^{[r]})} \left[y^{[r+1]}(t) - y^{[r]}(t)\right] = x(t), \end{aligned} \tag{5}$$

which results in

$$\begin{aligned} & p\left(\sum_{k=-K}^{K} Y_k^{[r]} e^{jk\omega_0 t}\right) + \frac{d}{dt}\left[q\left(\sum_{k=-K}^{K} Y_k^{[r]} e^{jk\omega_0 t}\right)\right] \\ & \quad + g\left(\sum_{k=-K}^{K} Y_k^{[r]} e^{jk\omega_0 t}\right)\left[\sum_{k=-K}^{K}\left(Y_k^{[r+1]} - Y_k^{[r]}\right) e^{jk\omega_0 t}\right] \\ & \quad + \frac{d}{dt}\left[c\left(\sum_{k=-K}^{K} Y_k^{[r]} e^{jk\omega_0 t}\right)\left[\sum_{k=-K}^{K}\left(Y_k^{[r+1]} - Y_k^{[r]}\right) e^{jk\omega_0 t}\right]\right] \\ & \quad = \sum_{k=-K}^{K} X_k e^{jk\omega_0 t}. \end{aligned} \tag{6}$$

The difficulty now arising in solving (6) is that we want to transform this system entirely into the frequency domain, but we do not know how to compute the Fourier coefficients of $p(\cdot)$, $q(\cdot)$, $g(\cdot)$, and $c(\cdot)$ at each iteration r. So, one possible way to do that consists of computing each of these nonlinear functions in the time domain and then calculate their Fourier coefficients. Therefore, according to the properties of the Fourier transform, the time-domain products $g(y^{[r]}) \cdot [y^{[r+1]}(t) - y^{[r]}(t)]$ and $c(y^{[r]}) \cdot [y^{[r+1]}(t) - y^{[r]}(t)]$ will become spectral convolutions, which can be represented as matrix-vector products using the *conversion matrix* formulation [5, 7]. This way, and because of the orthogonality of the Fourier series, (6) can be expressed in the form

$$\begin{aligned} & \mathbf{P}^{[r]} + j\Omega\mathbf{Q}^{[r]} + \mathbf{G}^{[r]}\left[\mathbf{Y}^{[r+1]} - \mathbf{Y}^{[r]}\right] \\ & \quad + j\Omega\mathbf{C}^{[r]}\left[\mathbf{Y}^{[r+1]} - \mathbf{Y}^{[r]}\right] = \mathbf{X}, \end{aligned} \tag{7}$$

where

$$\mathbf{Y}=\begin{bmatrix} Y_{-K} \\ \vdots \\ Y_0 \\ \vdots \\ Y_K \end{bmatrix}, \qquad \mathbf{X}=\begin{bmatrix} X_{-K} \\ \vdots \\ X_0 \\ \vdots \\ X_K \end{bmatrix}, \tag{8}$$

$$j\Omega = \operatorname{diag}\left(-jK\omega_0,\ldots,0,\ldots,jK\omega_0\right).$$

In (7), $\mathbf{P}$ and $\mathbf{Q}$ are vectors containing the Fourier coefficients of $p(y(t))$ and $q(y(t))$, respectively, and $\mathbf{G}$ and $\mathbf{C}$ denote the $(2K+1)\times(2K+1)$ conversion matrices (Toeplitz) [5, 7] corresponding to $g(y(t))$ and $c(y(t))$. If we rewrite (7) as

$$\underbrace{\mathbf{P}^{[r]}+j\Omega\mathbf{Q}^{[r]}-\mathbf{X}}_{\mathbf{F}(\mathbf{Y}^{[r]})}+\left[\underbrace{\mathbf{G}^{[r]}+j\Omega\mathbf{C}^{[r]}}_{\mathbf{J}(\mathbf{Y}^{[r]})}\right]\left[\mathbf{Y}^{[r+1]}-\mathbf{Y}^{[r]}\right]=0, \tag{9}$$

we can obtain

$$\mathbf{F}\left(\mathbf{Y}^{[r]}\right)+\left.\frac{d\mathbf{F}(\mathbf{Y})}{d\mathbf{Y}}\right|_{\mathbf{Y}=\mathbf{Y}^{[r]}}\left[\mathbf{Y}^{[r+1]}-\mathbf{Y}^{[r]}\right]=0, \tag{10}$$

in which

$$\mathbf{F}(\mathbf{Y})=\mathbf{P}(\mathbf{Y})+j\Omega\mathbf{Q}(\mathbf{Y})-\mathbf{X}=0 \tag{11}$$

is known as the *harmonic balance equation*, and the $(2K+1)\times(2K+1)$ composite conversion matrix

$$\mathbf{J}(\mathbf{Y})=\frac{d\mathbf{F}(\mathbf{Y})}{d\mathbf{Y}}=\mathbf{G}(\mathbf{Y})+j\Omega\mathbf{C}(\mathbf{Y}) \tag{12}$$

is known as the *Jacobian matrix* of the error function $\mathbf{F}(\mathbf{Y})$.

The iterative procedure of (5)–(12) is the so-called *harmonic-Newton* algorithm. In order to achieve the final solution of the problem, we have to do the following operations at each iteration r: (i) perform inverse Fourier transformation to obtain $y^{[r]}(t)$ from $\mathbf{Y}^{[r]}$; (ii) evaluate $p(y^{[r]}(t))$, $q(y^{[r]}(t))$, $g(y^{[r]}(t))$, and $c(y^{[r]}(t))$ in time domain; (iii) calculate their Fourier coefficients to obtain $\mathbf{P}(\mathbf{Y}^{[r]})$, $\mathbf{Q}(\mathbf{Y}^{[r]})$, $\mathbf{G}(\mathbf{Y}^{[r]})$, and $\mathbf{C}(\mathbf{Y}^{[r]})$, and thus $\mathbf{F}(\mathbf{Y}^{[r]})$ and $\mathbf{J}(\mathbf{Y}^{[r]})$; (iv) solve the linear system of $(2K+1)$ algebraic equations of (10) to compute the next estimate $\mathbf{Y}^{[r+1]}$. Consecutive iterations will be conducted until a final solution $\mathbf{Y}^{[f]}$ satisfies the HB equation of (11) with a desired accuracy, that is, until

$$\left\|\mathbf{F}\left(\mathbf{Y}^{[f]}\right)\right\|=\left\|\mathbf{P}\left(\mathbf{Y}^{[f]}\right)+j\Omega\mathbf{Q}\left(\mathbf{Y}^{[f]}\right)-\mathbf{X}\right\|<\text{tol}, \tag{13}$$

where tol is an allowed error ceiling and $\|\mathbf{F}(\cdot)\|$ stands for some norm of the error function $\mathbf{F}(\cdot)$.

Since in a digital computer, both time and frequency domains are represented by discrete quantities, the mathematical tools used to perform Fourier and inverse Fourier transformations are, respectively, the discrete Fourier transform (DFT) and the inverse discrete Fourier transform (IDFT) or their fast algorithms, the fast Fourier transform (FFT) and the inverse fast Fourier transform (IFFT).

The system of (10) is typically a sparse linear system in the case of a generic circuit with n state variables. In general, several methods can be used to solve this system, such as direct solvers, sparse solvers, or iterative solvers. However, for very large systems, iterative solvers are usually preferred. Krylov subspace techniques [8] are a class of iterative methods for solving sparse linear systems of equations. An advantage of Krylov techniques is that (10) does not need to be fully solved in each iteration. The iterative process needs only to proceed until $\mathbf{Y}^{[r+1]}-\mathbf{Y}^{[r]}$ is such that $\mathbf{Y}^{[r+1]}$ decreases the error function. This approach to the solution, called *inexact Newton*, can provide significantly improved efficiency. Today, there is a general consensus that a technique called the *generalized minimum residual* (GMRES) [9] is the preferred one among the many available Krylov subspace techniques, for harmonic-balance analysis [10–12].

The generalization of the above described harmonic-Newton algorithm to the case of a generic electronic circuit with n state variables is obviously straightforward. Indeed, in such case we will simply have

$$\mathbf{Y}=\left[\mathbf{Y}_1{}^T,\mathbf{Y}_2{}^T,\ldots,\mathbf{Y}_n{}^T\right]^T, \tag{14}$$

where each one of the $\mathbf{Y}_v$, $v=1,\ldots,n$, is a $(2K+1)\times 1$ vector containing the Fourier coefficients of the corresponding state variable $y_v(t)$. The $j\boldsymbol{\Omega}$ matrix will be defined as

$$j\boldsymbol{\Omega}=\operatorname{diag}\Bigg(\underbrace{-jK\omega_0,\ldots,jK\omega_0}_{v=1},\underbrace{-jK\omega_0,\ldots,jK\omega_0}_{v=2},\ldots,\underbrace{-jK\omega_0,\ldots,jK\omega_0}_{v=n}\Bigg), \tag{15}$$

and the Jacobian matrix $\mathbf{J}(\mathbf{Y})=d\mathbf{F}(\mathbf{Y})/d\mathbf{Y}$ will have a block structure, consisting of an $n\times n$ matrix of square submatrices (blocks), each of one with dimension $(2K+1)$. Each block contains information on the sensitivity of changes in a component of the error function $\mathbf{F}(\mathbf{Y})$, resulting from changes in a component of $\mathbf{Y}$. The general block of row m and column l can be expressed as

$$\frac{d\mathbf{F}_m(\mathbf{Y})}{d\mathbf{Y}_l}=\frac{d\mathbf{P}_m(\mathbf{Y})}{d\mathbf{Y}_l}+j\Omega\frac{d\mathbf{Q}_m(\mathbf{Y})}{d\mathbf{Y}_l}, \tag{16}$$

where $d\mathbf{P}_m(\mathbf{Y})/d\mathbf{Y}_l$ and $d\mathbf{Q}_m(\mathbf{Y})/d\mathbf{Y}_l$ denote, respectively, the Toeplitz conversion matrices [7] of the vectors containing the Fourier coefficients of $dp_m(y(t))/dy_l(t)$ and $dq_m(y(t))/dy_l(t)$.

3. Hybrid Time-Frequency Simulation

3.1. Modulated Signals. Signals containing components that vary at two or more widely separated rates are usually referred to as multirate signals and have a special incidence in RF and microwave applications, such as mixers (up/down converters), modulators, demodulators, power amplifiers, and so forth. Multirate signals can appear in RF systems due to the existence of excitation regimes of widely separated time scales (e.g., baseband stimuli and high frequency local oscillators) or because the stimuli can be, themselves, multirate signals (e.g., circuits driven by modulated signals). The general form of an amplitude and phase-modulated signal can be defined as

$$x(t) = e(t)\cos(\omega_C t + \phi(t)), \tag{17}$$

where $e(t)$ and $\phi(t)$ are, respectively, the amplitude, or envelope, and phase slowly varying baseband signals, modulating the $\cos(\omega_C t)$ fast-varying carrier. Circuits driven by this kind of signals, or presenting themselves state variables of this type, are common in RF and microwave applications. Since the baseband signals have a spectral content of much lower frequency than the carrier, that is, because they are typically slowly varying signals while the carrier is a fast-varying entity, simulating nonlinear circuits containing this kind of signals is often a very challenging issue. Because the aperiodic nature of the signals obviates the use of any steady-state technique, one might think that conventional time-step integration would be the natural method for simulating such circuits. However, the large time constants of the bias networks determine long transient regimes and, as a result, the obligation of simulating a large number of carrier periods. In addition, computing the RF carrier oscillations long enough to obtain information about its envelope and phase properties is, itself, a colossal task. Time-step integration is thus inadequate for simulating this kind of problems because it is computationally expensive or prohibitive.

3.2. Hybrid Time-Frequency ETHB Technique. The *envelope transient harmonic balance* (ETHB) [13–16] is a hybrid time-frequency technique that was conceived to overcome the inefficiency revealed by SPICE-like engines (time-step integration schemes) when simulating circuits driven by modulated signals or presenting state variables of this type. It consists in calculating the response of the circuit to the baseband and the carrier by treating the envelope and phase in the time domain and the carrier in the frequency domain. For that, it assumes that the envelope and phase baseband signals are extremely slow when compared to the carrier, so that they can be considered as practically constant during many carrier periods. Taking this into account, ETHB samples the baseband signals in an appropriately slow time rate and assumes a staircase version of both amplitude and phase, which will conduct to a new modulated version of these signals. The steady-state response of the circuit to this new modulated version is then computed at each time step with the frequency-domain HB engine.

In order to provide a very brief theoretical description of the ETHB technique, let us suppose that we have a circuit driven by a single source of the form of $x(t)$ in (17). If we rewrite $x(t)$ as

$$\begin{aligned} x(t) &= e(t)\sum_{k=-1}^{1} A_k e^{jk[\omega_C t + \phi(t)]} = \sum_{k=-1}^{1} e(t) A_k e^{jk\phi(t)} e^{jk\omega_C t} \\ &= \sum_{k=-1}^{1} X_k(t) e^{jk\omega_C t} \end{aligned} \tag{18}$$

and assume that the circuit is stable, then all its state variables can be expressed as time-varying Fourier series

$$y(t) = \sum_k Y_k(t) e^{jk\omega_C t}, \tag{19}$$

where $Y_k(t)$ represents the time-varying Fourier coefficients of $y(t)$, which are slowly varying in the baseband time scale. Now, if we take into consideration the disparity between the baseband and the carrier time scales and assume that they are also uncorrelated, which is normally the case, then we can rewrite (17) and (19) as

$$x(t_E, t_C) = e(t_E)\cos(\omega_C t_C + \phi(t_E)), \tag{20}$$

$$y(t_E, t_C) = \sum_k Y_k(t_E) e^{jk\omega_C t_C}, \tag{21}$$

where t_E is the slow baseband time scale and t_C is the fast carrier time scale. Then, if we discretize the slow baseband time scale using a grid of successive time instants $t_{E,i}$ and adopt a convenient harmonic truncation at some order $k = K$, we will obtain for each $t_{E,i}$ a periodic boundary value problem that can be solved in the frequency domain with HB. In order to compute the whole response of the circuit, a set of successive HB equations of the form

$$\mathbf{F}(\mathbf{Y}(t_{E,i})) = \mathbf{P}(\mathbf{Y}(t_{E,i})) + j\Omega\mathbf{Q}(\mathbf{Y}(t_{E,i})) - \mathbf{X}(t_{E,i}) = 0 \tag{22}$$

has to be solved, in which $\mathbf{X}(t_{E,i})$ and $\mathbf{Y}(t_{E,i})$ represent the vectors containing the time-varying Fourier coefficients of the excitation and the solution, respectively.

Two different ways can be conceived to evidence the system's dynamics to the time-varying envelope, depending on whether the circuit's elements' constitutive relations are described in the frequency domain or they can be formulated in the time domain.

In one possibility, we rely on the frequency-domain description of each of the constitutive elements, and so of the entire system represented in (22). Assuming that the envelope time evolution is much slower than that of the carrier, we no longer consider that each harmonic component of the carrier occupies a single frequency (constant amplitude and phase carrier) but spreads through its vicinity (slowly varying amplitude and phase modulation). For example, any dynamic linear component whose frequency-domain representation is

$$Q(Y(\omega)) = H(\omega)Y(\omega) \tag{23}$$

can be approximated by a Taylor series (or any other polynomial or rational function) in the vicinity of each of the carrier harmonics, $k\omega_C$, that is, $\omega = k\omega_C + \varpi$, where ϖ is a slight frequency perturbation, as

$$\begin{aligned} H(\omega) - H(k\omega_C) &\simeq \left.\frac{dH(\omega)}{d\omega}\right|_{\omega=k\omega_C} \varpi \\ &\quad + \frac{1}{2!}\left.\frac{dH^2(\omega)}{d\omega^2}\right|_{\omega=k\omega_C} \varpi^2 + \frac{1}{3!}\left.\frac{dH^3(\omega)}{d\omega^3}\right|_{\omega=k\omega_C} \varpi^3 + \cdots \\ &= H_1(k\omega_C)\varpi + H_2(k\omega_C)\varpi^2 + H_3(k\omega_C)\varpi^3 + \cdots \\ &= \widetilde{H}_k(\varpi), \end{aligned} \quad (24)$$

which leads to

$$\begin{aligned} Q\left(\widetilde{Y}_k(\varpi = \omega - k\omega_C)\right) &= \widetilde{H}_k(\varpi)\widetilde{Y}_k(\varpi) \\ &\simeq H_1(k\omega_C)\varpi\widetilde{Y}_k(\varpi) + H_2(k\omega_C)\varpi^2\widetilde{Y}_k(\varpi) \\ &\quad + H_3(k\omega_C)\varpi^3\widetilde{Y}_k(\varpi) + \cdots \\ &\simeq \frac{1}{j} j\varpi H_1(k\omega_C)\widetilde{Y}_k(\varpi) + \frac{1}{j^2}(j\varpi)^2 H_2(k\omega_C)\widetilde{Y}_k(\varpi) \\ &\quad + \frac{1}{j^3}(j\varpi)^3 H_3(k\omega_C)\widetilde{Y}_k(\varpi) + \cdots, \end{aligned} \quad (25)$$

with $\widetilde{H}$ and $\widetilde{Y}$ being the low-pass equivalent of H and Y. Since $H_m(k\omega_C)/j^m$ is a constant, and $(j\varpi)^m\widetilde{Y}_k(\varpi)$ can be interpreted as the m'th order derivative of the time-domain $Y_k(t_E)$ with respect to time t_E, (25) can be rewriten as

$$\begin{aligned} Q(Y_k(t_E)) \simeq \frac{H_1(k\omega_C)}{j}\frac{dY_k(t_E)}{dt_E} + \frac{H_2(k\omega_C)}{j^2}\frac{d^2Y_k(t_E)}{dt_E^2} \\ + \frac{H_3(k\omega_C)}{j^3}\frac{d^3Y_k(t_E)}{dt_E^3} + \cdots, \end{aligned} \quad (26)$$

which, substituted in (22), would evidence the desired system's dynamics to the amplitude and phase modulations. Therefore, the ETHB technique consists in the transient simulation, in an envelope time-step by time step basis, $t_{E,i}, t_{E,i+1}, \ldots$, of the harmonic balance equation of (22).

This formulation of ETHB is, nowadays, a mature technique in the RF simulation community. However, its basic assumption constitutes also its major drawback. By requiring the envelope and phase to be extremely slowly varying signals when compared to the carrier frequency, this mixed frequency-time technique becomes restricted to circuits whose stimuli occupy only a small fraction of the available bandwidth.

In an alternative ETHB formulation, we assume that every element can be described in the time domain. Hence, we can substitute the time-varying Fourier description of (21) into (1) and then treat the carrier time, t_C, in the frequency domain—converting the DAE system into an algebraic one—but keeping the envelope time, t_E, in the time domain. This way, we obtain another hybrid time-frequency description of the system that no longer suffers from the narrow bandwidth restriction just mentioned and whose formulation and solution will be discussed in more detail in Section 3.4.

3.3. Multivariate Formulation. We will now introduce a powerful strategy for analyzing nonlinear circuits handling amplitude and/or phase modulated signals, as with any other kind of multirate signals. This strategy consists in using multiple time variables to describe the multirate behavior, and it is based on the fact that multirate signals can be represented much more efficiently if they are defined as functions of two or more time variables, that is, if they are defined as *multivariate functions* [17, 18]. With this multivariate formulation, circuits will be no longer described by ordinary differential algebraic equations in the one-dimensional time t but, instead, by partial differential algebraic systems.

Let us consider the amplitude and phase-modulated signal of (17), and let us define its bivariate form as

$$\hat{x}(t_1, t_2) = e(t_1)\cos(\omega_C t_2 + \phi(t_1)), \quad (27)$$

where t_1 is the slow envelope time scale and t_2 is the fast carrier time scale. As can be seen, $\hat{x}(t_1, t_2)$ is a periodic function with respect to t_2 but not to t_1, that is,

$$\hat{x}(t_1, t_2) = \hat{x}(t_1, t_2 + T_2), \quad T_2 = \frac{2\pi}{\omega_C}, \quad (28)$$

and, in general, this bivariate form requires far fewer points to represent numerically the original signal, especially when the t_1 and t_2 time scales are widely separated [17, 18].

Let us now consider the differential algebraic equations' (DAEs) system of (1), describing the behavior of a generic RF circuit driven by the envelope-modulated signal of (17). Taking the above considerations into account, we will adopt the following procedure: for the slowly varying parts (envelope time scale) of the expressions of vectors $\mathbf{x}(t)$ and $\mathbf{y}(t)$, t is replaced by t_1; for the fast-varying parts (RF carrier time scale), t is replaced by t_2. The application of this bivariate strategy to the DAE system of (1) converts it into the following *multirate partial differential algebraic equations'* (MPDAEs) system [17, 18]:

$$\mathbf{p}(\hat{\mathbf{y}}(t_1, t_2)) + \frac{\partial \mathbf{q}(\hat{\mathbf{y}}(t_1, t_2))}{\partial t_1} + \frac{\partial \mathbf{q}(\hat{\mathbf{y}}(t_1, t_2))}{\partial t_2} = \hat{\mathbf{x}}(t_1, t_2). \quad (29)$$

The mathematical relation between (1) and (29) establishes that if $\hat{\mathbf{x}}(t_1, t_2)$ and $\hat{\mathbf{y}}(t_1, t_2)$ satisfy (29), then the univariate forms $\mathbf{x}(t) = \hat{\mathbf{x}}(t, t)$ and $\mathbf{y}(t) = \hat{\mathbf{y}}(t, t)$ satisfy (1) [18]. Therefore, the univariate solutions of (1) are available on diagonal lines $t_1 = t, t_2 = t$, along the bivariate solutions of (29), that is, $\mathbf{y}(t)$ may be retrieved from its bivariate form $\hat{\mathbf{y}}(t_1, t_2)$, by simply setting $t_1 = t_2 = t$. Consequently, if one wants to obtain the univariate solution in a generic $[0, t_{\text{Final}}]$ interval due to the periodicity of the problem in the t_2 dimension we will have

$$\mathbf{y}(t) = \widehat{\mathbf{y}}(t, t \mod T_2) \tag{30}$$

on the rectangular domain $[0, t_{\text{Final}}] \times [0, T_2]$, where $t \mod T_2$ represents the remainder of division of t by T_2. The main advantage of this MPDAE approach is that it can result in significant improvements in simulation speed when compared to DAE-based alternatives [17–20].

Envelope-modulated responses to excitations of the form of (17) correspond to a combination of initial and periodic boundary conditions for the MPDAE. This means that the bivariate forms of these solutions can be obtained by numerically solving the following initial-boundary value problem [18]

$$\begin{gathered}\mathbf{p}(\widehat{\mathbf{y}}(t_1, t_2)) + \frac{\partial \mathbf{q}(\widehat{\mathbf{y}}(t_1, t_2))}{\partial t_1} + \frac{\partial \mathbf{q}(\widehat{\mathbf{y}}(t_1, t_2))}{\partial t_2} = \widehat{\mathbf{x}}(t_1, t_2), \\ \widehat{\mathbf{y}}(0, t_2) = \mathbf{g}(t_2), \\ \widehat{\mathbf{y}}(t_1, 0) = \widehat{\mathbf{y}}(t_1, T_2),\end{gathered} \tag{31}$$

on the rectangle $[0, t_{\text{Final}}] \times [0, T_2]$. $\mathbf{g}(\cdot)$ is a given initial-condition function defined on $[0, T_2]$, satisfying $\mathbf{g}(0) = \mathbf{g}(T_2) = \mathbf{y}(0)$, and the periodic boundary condition $\widehat{\mathbf{y}}(t_1, 0) = \widehat{\mathbf{y}}(t_1, T_2)$ is due to the periodicity of the problem in the t_2 fast carrier time scale. The reason why bivariate envelope-modulated solutions do not need to be evaluated on the entire $[0, t_{\text{Final}}] \times [0, t_{\text{Final}}]$ domain (which would be computationally very expensive and would turn the multivariate strategy useless), and are restricted to the rectangle $[0, t_{\text{Final}}] \times [0, T_2]$, is because the solutions repeat along the t_2 time axis.

3.4. Multitime Envelope Transient Harmonic Balance. Multitime envelope transient harmonic balance is an improved version of the previously described ETHB technique, which is based on the multivariate formulation [21, 22]. For achieving an intuitive explanation of the multitime envelope transient harmonic balance let us consider the initial-boundary value problem of (31), and let us also consider the semidiscretization of the rectangular domain $[0, t_{\text{Final}}] \times [0, T_2]$ in the t_1 slow time dimension defined by the grid

$$\begin{gathered}0 = t_{1,0} < t_{1,1} < \cdots < t_{1,i-1} < t_{1,i} < \cdots < t_{1,K_1} = t_{\text{Final}}, \\ h_{1,i} = t_{1,i} - t_{1,i-1},\end{gathered} \tag{32}$$

where K_1 is the total number of steps in t_1. If we replace the derivatives of the MPDAE in t_1 with a finite-differences approximation (e.g., the Backward Euler rule), then we obtain for each slow time instant $t_{1,i}$, from $i = 1$ to $i = K_1$, the periodic boundary value problem defined by

$$\begin{gathered}\mathbf{p}(\widehat{\mathbf{y}}_i(t_2)) + \frac{\mathbf{q}(\widehat{\mathbf{y}}_i(t_2)) - \mathbf{q}(\widehat{\mathbf{y}}_{i-1}(t_2))}{h_{1,i}} + \frac{d\mathbf{q}(\widehat{\mathbf{y}}_i(t_2))}{dt_2} \\ = \widehat{\mathbf{x}}(t_{1,i}, t_2), \\ \widehat{\mathbf{y}}_i(0) = \widehat{\mathbf{y}}_i(T_2),\end{gathered} \tag{33}$$

where $\widehat{\mathbf{y}}_i(t_2) \simeq \widehat{\mathbf{y}}(t_{1,i}, t_2)$. This means that, once $\widehat{\mathbf{y}}_{i-1}(t_2)$ is known, the solution on the next slow time instant, $\widehat{\mathbf{y}}_i(t_2)$, is obtained by solving (33). Thus, for obtaining the whole solution $\widehat{\mathbf{y}}$ in the entire domain $[0, t_{\text{Final}}] \times [0, T_2]$, a total of K_1 boundary value problems have to be solved. With multitime ETHB, each one of these periodic boundary value problems is solved using the harmonic balance method. The corresponding HB system for each slow time instant $t_{1,i}$ is the $n \times (2K+1)$ algebraic equations set given by

$$\begin{gathered}\mathbf{P}(\widehat{\mathbf{Y}}(t_{1,i})) + \frac{\mathbf{Q}(\widehat{\mathbf{Y}}(t_{1,i})) - \mathbf{Q}(\widehat{\mathbf{Y}}(t_{1,i-1}))}{h_{1,i}} + j\mathbf{\Omega}\mathbf{Q}(\widehat{\mathbf{Y}}(t_{1,i})) \\ = \widehat{\mathbf{X}}(t_{1,i}),\end{gathered} \tag{34}$$

where $\widehat{\mathbf{X}}(t_{1,i})$ and $\widehat{\mathbf{Y}}(t_{1,i})$ are the vectors containing the Fourier coefficients of the excitation sources and of the solution (the state variables), respectively, at $t_1 = t_{1,i}$. $\mathbf{P}(\cdot)$ and $\mathbf{Q}(\cdot)$ are unknown functions, $j\mathbf{\Omega}$ is the diagonal matrix (15), and the $\widehat{\mathbf{Y}}(t_{1,i})$ vector can be expressed as

$$\widehat{\mathbf{Y}}(t_{1,i}) = \left[\widehat{\mathbf{Y}}_1(t_{1,i})^T, \widehat{\mathbf{Y}}_2(t_{1,i})^T, \ldots, \widehat{\mathbf{Y}}_n(t_{1,i})^T\right]^T, \tag{35}$$

where each one of the state variable frequency components, $\widehat{\mathbf{Y}}_v(t_{1,i})$, $v = 1, \ldots, n$, is a $(2K+1) \times 1$ vector defined as

$$\widehat{\mathbf{Y}}_v(t_{1,i}) = [Y_{v,-K}(t_{1,i}), \ldots, Y_{v,0}(t_{1,i}), \ldots, Y_{v,K}(t_{1,i})]^T. \tag{36}$$

As seen in Section 2.3, since $\mathbf{p}(\cdot)$ and $\mathbf{q}(\cdot)$ are in general nonlinear functions, one possible way to compute $\mathbf{P}(\cdot)$ and $\mathbf{Q}(\cdot)$ in (34) consists in evaluating $\mathbf{p}(\cdot)$ and $\mathbf{q}(\cdot)$ in the time domain and then calculate its Fourier coefficients. The HB system of (34) can be rewriten as

$$\begin{gathered}\mathbf{F}(\widehat{\mathbf{Y}}(t_{1,i})) = \mathbf{P}(\widehat{\mathbf{Y}}(t_{1,i})) + \frac{\mathbf{Q}(\widehat{\mathbf{Y}}(t_{1,i})) - \mathbf{Q}(\widehat{\mathbf{Y}}(t_{1,i-1}))}{h_{1,i}} \\ + j\mathbf{\Omega}\mathbf{Q}(\widehat{\mathbf{Y}}(t_{1,i})) - \widehat{\mathbf{X}}(t_{1,i}) = 0,\end{gathered} \tag{37}$$

or, in its simplified form, as

$$\mathbf{F}(\widehat{\mathbf{Y}}(t_{1,i})) = 0, \tag{38}$$

in which $\mathbf{F}(\widehat{\mathbf{Y}}(t_{1,i}))$ is the error function at $t_1 = t_{1,i}$. In order to solve the nonlinear algebraic system of (38) a Newton-Raphson iterative solver is usually used. In this case, the Newton-Raphson algorithm conducts us to

$$\begin{gathered}\mathbf{F}(\widehat{\mathbf{Y}}^{[r]}(t_{1,i})) \\ + \left.\frac{d\mathbf{F}(\widehat{\mathbf{Y}}(t_{1,i}))}{d\widehat{\mathbf{Y}}(t_{1,i})}\right|_{\widehat{\mathbf{Y}}(t_{1,i}) = \widehat{\mathbf{Y}}^{[r]}(t_{1,i})} \left[\widehat{\mathbf{Y}}^{[r+1]}(t_{1,i}) - \widehat{\mathbf{Y}}^{[r]}(t_{1,i})\right] = 0,\end{gathered} \tag{39}$$

which means that at each iteration r, we have to solve a linear system of $n \times (2K + 1)$ equations to compute the new estimate $\widehat{\mathbf{Y}}^{[r+1]}(t_{1,i})$. Consecutive Newton iterations will be computed until a desired accuracy is achieved, that is, until $\|\mathbf{F}(\widehat{\mathbf{Y}}(t_{1,i}))\| < \text{tol}$, where tol is the allowed error ceiling.

The system of (39) involves the derivative of the vector $\mathbf{F}(\widehat{\mathbf{Y}}(t_{1,i}))$, with respect to the vector $\widehat{\mathbf{Y}}(t_{1,i})$. The result is a matrix, the so-called Jacobian of $\mathbf{F}(\widehat{\mathbf{Y}}(t_{1,i}))$,

$$\mathbf{J}\left(\widehat{\mathbf{Y}}\left(t_{1,i}\right)\right) = \frac{d\mathbf{F}\left(\widehat{\mathbf{Y}}\left(t_{1,i}\right)\right)}{d\widehat{\mathbf{Y}}\left(t_{1,i}\right)} = \begin{bmatrix} \frac{d\mathbf{F}_1\left(\widehat{\mathbf{Y}}\left(t_{1,i}\right)\right)}{d\widehat{\mathbf{Y}}_1\left(t_{1,i}\right)} & \frac{d\mathbf{F}_1\left(\widehat{\mathbf{Y}}\left(t_{1,i}\right)\right)}{d\widehat{\mathbf{Y}}_2\left(t_{1,i}\right)} & \cdots & \frac{d\mathbf{F}_1\left(\widehat{\mathbf{Y}}\left(t_{1,i}\right)\right)}{d\widehat{\mathbf{Y}}_n\left(t_{1,i}\right)} \\ \frac{d\mathbf{F}_2\left(\widehat{\mathbf{Y}}\left(t_{1,i}\right)\right)}{d\widehat{\mathbf{Y}}_1\left(t_{1,i}\right)} & \frac{d\mathbf{F}_2\left(\widehat{\mathbf{Y}}\left(t_{1,i}\right)\right)}{d\widehat{\mathbf{Y}}_2\left(t_{1,i}\right)} & \cdots & \frac{d\mathbf{F}_2\left(\widehat{\mathbf{Y}}\left(t_{1,i}\right)\right)}{d\widehat{\mathbf{Y}}_n\left(t_{1,i}\right)} \\ \cdots & \cdots & \cdots & \cdots \\ \frac{d\mathbf{F}_n\left(\widehat{\mathbf{Y}}\left(t_{1,i}\right)\right)}{d\widehat{\mathbf{Y}}_1\left(t_{1,i}\right)} & \frac{d\mathbf{F}_n\left(\widehat{\mathbf{Y}}\left(t_{1,i}\right)\right)}{d\widehat{\mathbf{Y}}_2\left(t_{1,i}\right)} & \cdots & \frac{d\mathbf{F}_n\left(\widehat{\mathbf{Y}}\left(t_{1,i}\right)\right)}{d\widehat{\mathbf{Y}}_n\left(t_{1,i}\right)} \end{bmatrix}. \tag{40}$$

In the same way as in Section 2.3, this matrix has a block structure, consisting of an $n \times n$ matrix of square submatrices (blocks), each one with dimension $(2K + 1)$. The general block of row m and column l can now be expressed as

$$\frac{d\mathbf{F}_m\left(\widehat{\mathbf{Y}}\left(t_{1,i}\right)\right)}{d\widehat{\mathbf{Y}}_l\left(t_{1,i}\right)} = \frac{d\mathbf{P}_m\left(\widehat{\mathbf{Y}}\left(t_{1,i}\right)\right)}{d\widehat{\mathbf{Y}}_l\left(t_{1,i}\right)} + \frac{1}{h_{1.i}}\frac{d\mathbf{Q}_m\left(\widehat{\mathbf{Y}}\left(t_{1,i}\right)\right)}{d\widehat{\mathbf{Y}}_l\left(t_{1,i}\right)} + j\Omega\frac{d\mathbf{Q}_m\left(\widehat{\mathbf{Y}}\left(t_{1,i}\right)\right)}{d\widehat{\mathbf{Y}}_l\left(t_{1,i}\right)}. \tag{41}$$

In summary, multitime ETHB handles the solution dependence on t_2 in frequency domain, while treating the course of the solution to t_1 in time domain. So, it is a hybrid time-frequency technique which is similar to the ETHB engine previously reported in Section 3.2. However, an important advantage of multitime ETHB over conventional ETHB is that it does not suffer from bandwidth limitations [21]. For example, in circuits driven by envelope modulated signals, the only restriction that has to be imposed is that the modulating signal and the carrier must not be correlated in time (which is typically the case).

4. Advanced Hybrid Time-Frequency Simulation

One limitation of the ETHB and multitime ETHB engines is that they do not perform any distinction between nodes or blocks within the circuit, that is to say that they treat all the circuit's state variables in the same way. Thus, if the circuit evidences some heterogeneity, as is the case of modern wireless architectures combining radio frequency, baseband analog, and digital blocks in the same circuit, these tools cannot benefit from such feature. To overcome this difficulty an innovative mixed mode time-frequency technique was recently proposed by the authors [23, 24]. This technique splits the circuit's state variables (node voltages and mesh currents) into fast and slowly varying subsets, treating the former with multitime ETHB and the later with a SPICE-like engine (a time-step integration scheme). This way, the strong nonlinearities of the circuit are appropriately evaluated in the time domain, while the moderate ones are computed in the frequency domain [23, 24].

4.1. Time-Domain Latency within the Multivariate Formulation. In order to provide an illustrative explanation of the issues under discussion in this section, let us start by considering an RF circuit in which some of its state variables (node voltages and branch currents) are fast carrier envelope-modulated waveforms, while the remaining state variables are slowly varying aperiodic signals. For concreteness, let us suppose that the signals

$$y_1(t) = \sum_{k=-K}^{K} Y_k(t)\, e^{jk\omega_C t}, \qquad y_2(t) = e(t) \tag{42}$$

are two distinct state variables in different parts of the circuit. $Y_k(t)$ represents the Fourier coefficients of $y_1(t)$, which are slowly varying in the baseband time scale, ω_C is the carrier frequency, and $e(t)$ is a slowly varying aperiodic baseband function. We will denote signals of the form of $y_1(t)$ as *active* and signals of the form of $y_2(t)$ as *latent*. The latency revealed by $y_2(t)$ indicates that this variable belongs to a circuit block where there are no fluctuations dictated by the fast carrier. Consequently, due to its slowness, it can be represented efficiently with much less sample points than $y_1(t)$. On the other hand, since it does not evidence any periodicity, it cannot be processed with harmonic balance. On the contrary, if the number of harmonics K is not too large, the fast carrier oscillation components of $y_1(t)$ can be efficiently computed in the frequency domain. Therefore, it is straightforward to conclude that if we want to simulate circuits having such signal format disparities in an efficient way, distinct numerical strategies will be required.

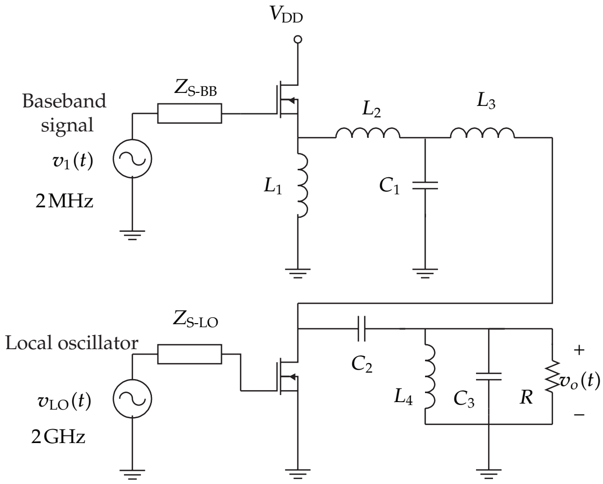

FIGURE 1: Simplified resistive FET mixer used in wireless transmitters.

Let us now consider the bivariate forms of $y_1(t)$ and $y_2(t)$ denoted by $\hat{y}_1(t_1, t_2)$ and $\hat{y}_2(t_1, t_2)$ and defined as

$$\hat{y}_1(t_1, t_2) = \sum_{k=-K}^{K} Y_k(t_1) e^{jk\omega_C t_2}, \qquad \hat{y}_2(t_1, t_2) = e(t_1), \tag{43}$$

where t_1 and t_2 are, respectively, the slow envelope time dimension and the fast carrier time dimension. As we can see, $\hat{y}_2(t_1, t_2)$ has no dependence on t_2, so it has no fluctuations in the fast time axis. In fact, it is so because $y_2(t)$ does not oscillate at the carrier frequency. Consequently, for each slow time instant $t_{1,i}$ defined on the grid of (32), while $\hat{y}_1(t_{1,i}, t_2)$ is a waveform that has to be represented by a certain quantity $k = -K, \ldots, K$ of harmonic components, $\hat{y}_2(t_{1,i}, t_2)$ is merely a constant (DC) signal that can be simply represented by the $k = 0$ component. Therefore, there is no necessity to perform the conversion between time and frequency domains for $\hat{y}_2(t_{1,i}, t_2)$, which means that this state variable can be processed in a purely time-domain scheme.

4.2. Mixed Mode Time-Frequency Technique. In the above, we illustrated that bivariate forms of latent state variables have no undulations in the t_2 fast time scale. So, while active state variables have to be represented by a set of $(2K+1)$ harmonic components arranged in vectors of the form of (36), latent state variables can be represented as scalar quantities, that is,

$$\widehat{\mathbf{Y}}_v(t_{1,i}) = Y_{v,0}(t_{1,i}) = \hat{y}_v(t_{1,i}). \tag{44}$$

By considering this, it is straightforward to conclude that the size of the $\widehat{\mathbf{Y}}(t_{1,i})$ vector defined by (35) can be considerably reduced, as can be the total number of equations

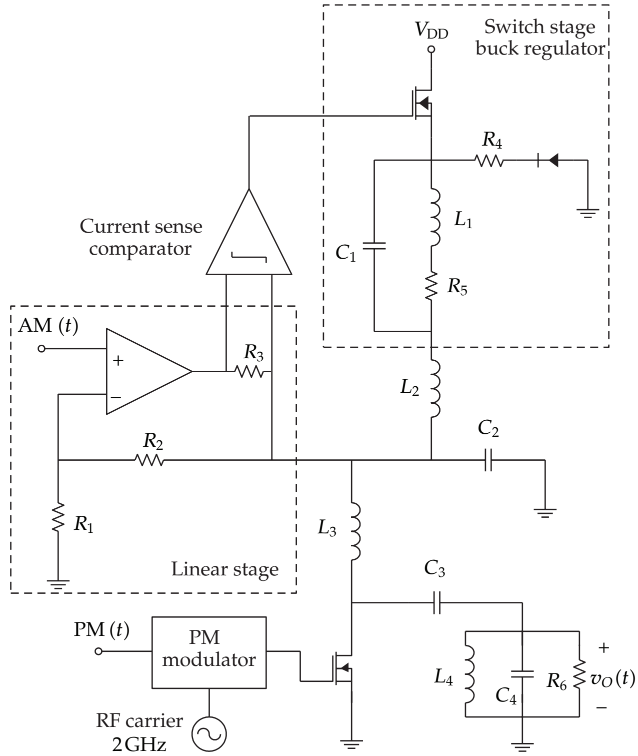

FIGURE 2: RF polar transmitter with a hybrid envelope amplifier [23].

in the HB system of (37). An additional and crucial detail is that there is no longer obligation to perform the conversion between time and frequency domains for the latent state variables expressed in the form of (44), as well as for the components of $\mathbf{F}(\widehat{\mathbf{Y}}(t_{1,i}))$ corresponding to latent blocks of the circuit. Since the $k = 0$ order Fourier coefficient $Y_{v,0}(t_{1,i})$ is exactly the same as the constant t_2 time value $\hat{y}_v(t_{1,i})$, the use of the discrete Fourier transform (DFT) and the inverse discrete Fourier transform (IDFT)—or their fast algorithms, that is, the fast Fourier transform (FFT) and the inverse fast Fourier transform (IFFT)—will be required only for components in the HB system of (37) having dependence on active state variables. Significant Jacobian matrix size reductions will be achieved, too. In effect, by taking into consideration this multirate characteristic (the subset circuit latency), some of the blocks of (40) will be merely 1×1 scalar elements that contain dc information on the sensitivity of changes in components of $\mathbf{F}(\widehat{\mathbf{Y}}(t_{1,i}))$ resulting from changes in latent components of $\widehat{\mathbf{Y}}(t_{1,i})$.

With this strategy of partitioning the circuit into active and latent subcircuits (blocks), significant computation and memory savings can be achieved when finding the solution of (37). Indeed, with the state variable $\widehat{\mathbf{Y}}(t_{1,i})$ and the error function $\mathbf{F}(\widehat{\mathbf{Y}}(t_{1,i}))$ vector size reductions, as also the resulting Jacobian $\mathbf{J}(\widehat{\mathbf{Y}}(t_{1,i}))$ matrix size reduction, it is possible to avoid dealing with large linear systems in the iterations of (39). Thus, a less computationally expensive Newton-Raphson iterative solver is required.

Table 1: Computation times—resistive FET mixer.

Simulation time interval	Mixed mode time-frequency technique	Multitime ETHB	Speedup (approx.)
[0, 0.5 μs]	2.1 s	4.6 s	2.2
[0, 5.0 μs]	19.3 s	42.5 s	2.2

Table 2: Computation times—RF polar transmitter.

Simulation time interval	Mixed mode time-frequency technique	Multitime ETHB	Speedup (approx.)
[0, 0.5 μs]	3.2 s	51.5 s	16.1
[0, 5.0 μs]	25.3 s	484.6 s	19.2

5. Performance of the Methods

The performance and the efficiency of the ETHB and multitime ETHB techniques were already attested and recognized by the RF and microwave community. In the same way, the performance and the efficiency of the advanced hybrid technique described in the previous section (the mixed mode time-frequency simulation technique) were also already demonstrated through its application to several illustrative examples of practical relevance. Indeed, electronic circuits with distinct configurations and levels of complexity were especially selected to illustrate the significant gains in computational speed that can be achieved when simulating the circuits with this method [23, 24]. Nevertheless, in order to provide the reader with a realistic idea of the potential of this recently proposed technique, we included in this section a brief comparison between this method and the previous state-of-the-art multitime ETHB. For that, we considered two distinct circuits: the resistive FET mixer depicted in Figure 1 and the RF polar transmitter described in [23] and depicted in Figure 2.

The circuits were simulated in MATLAB with the mixed mode time-frequency simulation technique versus the multitime ETHB. In our experiments a dynamic step size control tool was used in the t_1 slow time scale, and we considered $K = 9$ as the maximum harmonic order for the HB evaluations. Numerical computation times (in seconds) for simulations in the [0, 0.5 μs] and [0, 5.0 μs] intervals are presented in Tables 1 and 2.

As we can see, speedups of approximately 2 times were obtained for the simulation of the resistive FET mixer, and speedups of more than one order of magnitude were obtained for the RF polar transmitter. These efficiency gains were achieved without compromising accuracy. Indeed, for both cases, the maximum discrepancy between solutions (for all the circuits' state variables) was on the order of 10^{-8}.

The choice of these two circuits, which have different levels of complexity, was to illustrate how the computational efficiency is more evident as the ratio between the number of active and latent state variables is increased. In the first example, this ratio is 1, whereas in the second one this ratio is 4.5.

6. Conclusion

Although significant advancement has been made in RF and microwave circuit simulation along the years, the use of more elaborate functional analysis techniques has kept this subject a hot topic of scientific and practical engineering interest. Indeed, emerging wireless communication technologies continuously bring new challenges to this scientific field, as is now the case of heterogeneous RF circuits containing state variables of distinct formats and running on widely separated time scales. Taking into account the popularity of HB, but mostly ETHB, in the RF and microwave community, in this paper we have briefly reviewed the use of some functional analysis methods to address numerical simulation challenges using hybrid time-frequency techniques. A comparison between two state-of-the-art hybrid techniques in terms of computational speed is also included to evidence the efficiency gains that can be achieved by partitioning heterogeneous circuits into blocks, treating latent blocks in a one-dimensional space, and active ones in a bidimensional space.

Acknowledgment

The authors would like to acknowledge the financial support provided by the Portuguese Science and Technology Foundation (FCT) under the Project SOPAS-PTDC/EEA-TEL/114530/2009.

References

[1] R. Achar and M. S. Nakhla, "Simulation of high-speed interconnects," *Proceedings of the IEEE*, vol. 89, no. 5, pp. 693–728, 2001.

[2] L. Nagel, "Spice2: a computer program to simulate semiconductor circuits," Tech. Rep. Memo ERL-M520, Electronics Research Laboratory, University of California, Berkeley, Calif, USA, 1975.

[3] K. Kundert, J. White, and A. Sangiovanni-Vincentelli, *Steady-State Methods for Simulating Analog and Microwave Circuits*, Kluwer Academic, Norwell, Mass, USA, 1990.

[4] P. J. Rodrigues, *Computer-Aided Analysis of Nonlinear Microwave Circuits*, Artech House, Norwood, Mass, USA, 1998.

[5] S. A. Maas, *Nonlinear Microwave and RF Circuits*, Artech House, Norwood, Mass, USA, 2nd edition, 2003.

[6] W. Hayt, J. Kemmerly, and S. Durbin, *Engineering Circuit Analysis*, Artech House, Norwood, Mass, USA, 2nd edition, 2003.

[7] J. C. Pedro and N. B. Carvalho, *Intermodulation Distortion in Microwave and Wireless Circuits*, Artech House, Norwood, Mass, USA, 2003.

[8] L. Trefethen and D. Bau, *Numerical Linear Algebra*, Society for Industrial and Applied Mathematics, Philadelphia, Pa, USA, 1997.

[9] Y. Saad and M. Schultz, "GMRES: a generalized minimal residual method for solving nonsymmetric linear systems," *SIAM Journal on Scientific and Statistical Computing*, vol. 7, pp. 856–869, 1986.

[10] V. Rizzoli, F. Mastri, F. Sgallari, and G. Spaletta, "Harmonic-balance simulation of strongly nonlinear very large-size microwave circuits by inexact Newton methods," in *Proceedings of the IEEE MTT-S International Microwave Symposium Digest*, pp. 1357–1360, San Francisco, Calif, USA, June 1996.

[11] V. Rizzoli, F. Mastri, C. Cecchetti, and F. Sgallari, "Fast and robust inexact Newton approach to the harmonic-balance analysis of nonlinear microwave circuits," *IEEE Microwave and Guided Wave Letters*, vol. 7, no. 10, pp. 359–361, 1997.

[12] V. Rizzoli, F. Mastri, A. Coostanzo, and E. Montanari, "Highly efficient envelope-oriented analysis of large autonomous RF/microwave systems by a trust-region algorithm coupled with Krylov-subspace harmonic-balance," in *Proceedings of the 32th European Microwave Conference*, pp. 1–4, Milan, Italy, October 2002.

[13] E. Ngoya and R. Larcheveque, "Envelop transient analysis: a new method for the transient and steady state analysis of microwave communication circuits and systems," in *Proceedings of the IEEE MTT-S International Microwave Symposium Digest*, pp. 1365–1368, San Francisco, Calif, USA, June 1996.

[14] V. Rizzoli, A. Neri, and F. Mastri, "A modulation-oriented piecewise harmonic-balance technique suitable for transient analysis and digitally modulated analysis," in *Proceedings of the 26th European Microwave Conference*, pp. 546–550, Prague, Czech Republic, October 1996.

[15] D. Sharrit, "Method for simulating a circuit," U.S. Patent 5588142, December 24, 1996.

[16] V. Rizzoli, E. Montanari, D. Masotti, A. Lipparini, and F. Mastri, "Domain-decomposition harmonic balance with block-wise constant spectrum," in *Proceedings of the IEEE MTT-S International Microwave Symposium Digest*, pp. 860–863, San Francisco, Calif, USA, June 2006.

[17] J. Roychowdhury, "Efficient methods for simulating highly nonlinear multi-rate circuits," in *Proceedings of the 34th Design Automation Conference*, pp. 269–274, Anaheim, Calif, USA, June 1997.

[18] J. Roychowdhury, "Analyzing circuits with widely separated time scales using numerical PDE methods," *IEEE Transactions on Circuits and Systems I*, vol. 48, no. 5, pp. 578–594, 2001.

[19] J. Oliveira, "Efficient methods for solving multi-rate partial differential equations in radio frequency applications," *WSEAS Transactions on Circuits and Systems*, vol. 5, no. 1, pp. 24–31, 2006.

[20] J. Roychowdhury, "A time-domain RF steady-state method for closely spaced tones," in *Proceedings of the 39th Annual Design Automation Conference (DAC '02)*, pp. 510–513, New Orleans, La, USA, June 2002.

[21] J. C. Pedro and N. B. Carvalho, "Simulation of RF circuits driven by modulated signals without bandwidth constraints," in *Proceedings of the IEEE MTT-S International Microwave Symposium Digest*, pp. 2173–2176, Seattle, Wash, USA, June 2002.

[22] L. Zhu and C. E. Christoffersen, "Adaptive harmonic balance analysis of oscillators using multiple time scales," in *Proceedings of the 3rd International IEEE Northeast Workshop on Circuits and Systems Conference (NEWCAS '05)*, pp. 187–190, Québec City, Canada, June 2005.

[23] J. F. Oliveira and J. C. Pedro, "A new mixed time-frequency simulation method for nonlinear heterogeneous multirate RF circuits," in *Proceedings of the IEEE MTT-S International Microwave Symposium (MTT '10)*, pp. 548–551, Anaheim, Calif, USA, May 2010.

[24] J. F. Oliveira and J. C. Pedro, "Efficient RF circuit simulation using an innovative mixed time-frequency method," *IEEE Transactions on Microwave Theory and Techniques*, vol. 59, no. 4, pp. 827–836, 2011.

Hindawi Publishing Corporation
Journal of Function Spaces and Applications
Volume 2013, Article ID 651573, 11 pages
http://dx.doi.org/10.1155/2013/651573

Research Article

A Finite Difference Scheme for Pricing American Put Options under Kou's Jump-Diffusion Model

Jian Huang, Zhongdi Cen, and Anbo Le

Institute of Mathematics, Zhejiang Wanli University, Ningbo, Zhejiang 315100, China

Correspondence should be addressed to Zhongdi Cen; czdningbo@tom.com

Received 30 September 2012; Revised 15 December 2012; Accepted 17 December 2012

Academic Editor: M. Ruiz Galan

We present a stable finite difference scheme on a piecewise uniform mesh along with a penalty method for pricing American put options under Kou's jump-diffusion model. By adding a penalty term, the partial integrodifferential complementarity problem arising from pricing American put options under Kou's jump-diffusion model is transformed into a nonlinear parabolic integro-differential equation. Then a finite difference scheme is proposed to solve the penalized integrodifferential equation, which combines a central difference scheme on a piecewise uniform mesh with respect to the spatial variable with an implicit-explicit time stepping technique. This leads to the solution of problems with a tridiagonal M-matrix. It is proved that the difference scheme satisfies the early exercise constraint. Furthermore, it is proved that the scheme is oscillation-free and is second-order convergent with respect to the spatial variable. The numerical results support the theoretical results.

1. Introduction

It is widely recognized that the assumption of log-normal stock diffusion with constant volatility in the standard Black-Scholes model [1] of option pricing is not ideally consistent with that of the market price movement. In particular, the probability distribution of realized asset returns often exhibits features that are not taken into account by the standard Black-Scholes model: heavy tails, volatility clustering, and volatility smile [2]. In order to explain these phenomena, extensions of the Black-Scholes model have been proposed. Generally speaking, two different classes of models have been studied in the finance literature: the stochastic volatility models [3, 4] and the jump-diffusion models [2, 5]. Contrary to the Black-Scholes model, the jump diffusion models allow for a more realistic representation of price dynamics and greater flexibility in modeling. During the last twenty years, research on models with jumps has become very active. Most of such models have been proposed; see [2] and references therein. Here we focus on a jump-diffusion model with finite jump activity proposed by Kou in [6].

Unlike the standard Black-Scholes equation, the valuation of options under jump-diffusion models requires solving a partial integrodifferential equation. A fully implicit scheme would lead to full matrices due to the integral term, which makes many methods computationally too expensive. Several numerical methods based on the finite difference method have been proposed for pricing options under jump-diffusion models. Amin [7] gave a multinomial tree method for pricing options under jump-diffusion models, which is actually an explicit type finite difference approach. Zhang [8] and Cont and Voltchkova [9] used implicit-explicit finite difference methods for pricing options under jump-diffusion models. Andersen and Andreasen [10] and Almendral and Oosterlee [11] proposed operator splitting methods coupled with a fast Fourier transformation (FFT) technique for pricing options with jump diffusion processes. d'Halluin et al. [12, 13] developed a second-order accurate numerical method with a fixed-point iteration method and an implicit finite difference scheme along with a penalty method for pricing American options under jump diffusion processes. Toivanen et al. [14–16] introduced a high-order front-fixing finite difference method and an artificial volatility scheme along with an iterative method for pricing American options under jump-diffusion models. Zhang and Wang [17, 18] proposed fitted finite volume schemes coupled with the Crank-Nicolson time stepping method for pricing options under jump diffusion processes.

It is well known that the Black-Scholes partial differential operator at $x = 0$ is degenerative. The Black-Scholes partial differential operator becomes a convection-dominated operator when the volatility or the asset price is small. Hence, numerical difficulty can be caused when the standard methods such as the central difference and piecewise linear finite element methods are used to solve those problems. A common and widely used approach by many authors dealing with finite difference/volume/element methods for the Black-Scholes partial differential equaion is to apply an Euler transformation to remove the singularity of the differential operator when the parameters of the Black-Scholes equation are constant or space-independent; see for example, [2, 19]. As a result of the Euler transformation, the transformed interval becomes $(-\infty, \infty)$. However, the truncation on the left-hand side of the domain to artificially remove the degeneracy may cause computational errors. Furthermore, the uniform mesh on the transformed interval will lead to the originally grid points concentrating around $x = 0$ inappropriately. Moreover, when a problem is space-dependent, this transformation is impossible, and thus the Black-Scholes equation in the original form needs to be solved [20]. The same problem also appears in the partial integral-differential equations resulting from jump-diffusion models [9, 11, 18]. Wang [21] and Angermann and Wang [22] applied a stable fitted finite volume method to deal with the degeneracy and singularity of the Black-Scholes operator. In this paper, we will present a stable finite difference method with a second-order convergency with respect to the spatial variable for solving the partial integrodifferential equation defined on $(0, +\infty)$ for arbitrary volatility and arbitrary interest rate.

The penalty method was introduced by Zvan et al. [23] for pricing American options with stochastic volatility by adding a source term to the discrete equation. Nielsen et al. [24] presented a refinement of their work by adding a penalty term to the continuous equation and illustrated the performance of various numerical schemes. By adding a penalty term, the linear complementarity problem for pricing the American options can be transformed into a nonlinear parabolic partial differential equation. As the solution approaches the pay-off function at expiry, the penalty term forces the solution to stay above it. When the solution is far from the barrier, the term is small and thus the Black-Scholes equation is approximatively satisfied in this region.

In [25] we have presented a robust difference scheme for the penalized Black-Scholes equation governing American put option pricing. In this paper we present a stable finite difference scheme on a piecewise uniform mesh along with a power penalty method for pricing American put options under Kou's jump-diffusion model. By adding a penalty term the partial integrodifferential complementarity problem arising from pricing American put options under Kou's jump-diffusion model is transformed into a nonlinear parabolic integrodifferential equation. Then a finite difference scheme is proposed to solve the penalized integrodifferential equation, which combines a central difference scheme on a piecewise uniform mesh with respect to the spatial variable with an implicit-explicit time stepping technique. This leads to the solution of problems with a tridiagonal M-matrix. It is proved that the difference scheme satisfies the early exercise constraint. Furthermore, it is proved that the scheme is oscillation-free and is second-order convergent with respect to the spatial variable. Numerical results support the theoretical results.

The rest of the paper is organized as follows. In the next section, we describe some theoretical results on the continuous problem for pricing American put options under Kou's jump-diffusion model. The discretization method is described in Section 3. In Section 4 we prove that the difference scheme satisfies the early exercise constraint. In Section 5, we present a stability and error analysis for the finite difference scheme. In Section 6, numerical experiments are provided to support these theoretical results. Finally, a discussion is indicated in Section 7.

2. The Continuous Problem

Let v denote the value of an American put option with strike price E on the underlying asset x and time t. It is known that the price v under a jump-diffusion model satisfies the following partial integrodifferential complementarity problem [14–17]:

$$Lv(x,t) \geq 0, \quad x > 0, \ t \in [0, T), \tag{1}$$

$$v(x,t) - V^*(x) \geq 0, \quad x > 0, \ t \in [0, T], \tag{2}$$

$$Lv(x,t) \cdot [v(x,t) - V^*(x)] = 0, \quad x > 0, \ t \in [0, T), \tag{3}$$

$$v(x,T) = V^*(x), \quad x \geq 0, \ t = T, \tag{4}$$

$$v(0,t) = E, \quad x = 0, \ t \in [0, T], \tag{5}$$

$$v(x,t) \longrightarrow 0, \quad x \longrightarrow +\infty, \ t \in [0, T], \tag{6}$$

where L denotes the partial integrodifferential operator defined by

$$\begin{aligned} Lv(x,t) \equiv & -\frac{\partial v}{\partial t} - \frac{1}{2}\sigma^2 x^2 \frac{\partial^2 v}{\partial x^2} - (r - \lambda\zeta) x \frac{\partial v}{\partial x} \\ & + (r + \lambda) v - \lambda \int_0^\infty v(xy, t) f(y) \, \mathrm{d}y, \end{aligned} \tag{7}$$

$V^*(x)$ is the final (payoff) condition defined by

$$V^*(x) = \max\{E - x, 0\}, \tag{8}$$

σ is the volatility of the underlying asset, r is the risk free interest rate, t is the current time, T is the maturity date, and $f(y)$ is the probability function of the jump amplitude y with the obvious properties that for all y, $f(y) \geq 0$ and $\int_0^\infty f(y)\mathrm{d}y = 1$, the constant ζ is given by $\zeta = \int_0^\infty (y - 1) f(y)\mathrm{d}y$. In Kou's model, $f(y)$ is the following log-double-exponential density

$$f(y) = \begin{cases} q\alpha_2 y^{\alpha_2 - 1}, & y < 1, \\ p\alpha_1 y^{-\alpha_1 - 1}, & y \geq 1, \end{cases} \tag{9}$$

where $p, q, \alpha_1 > 1$ and α_2 are positive constants such that $p + q = 1$. It can be shown that, in this case, $\zeta = p\alpha_1/(\alpha_1 - 1) + q\alpha_2/(\alpha_2 + 1) - 1$. When the jump rate λ is zero, the partial integrodifferential operator reduces to the standard Black-Scholes operator [1]. In this paper, we assume that $r - \lambda\zeta \neq 0$.

The above linear complementarity problem (1)–(6) can be solved by a penalty approach. Let $0 < \varepsilon \ll 1$ be a small regularization parameter and consider the following initial-boundary value problem,

$$\begin{gathered} Lv(x,t) - \frac{C\varepsilon}{v(x,t) + \varepsilon - q(x)} = 0, \quad x > 0,\ t \in [0,T), \\ v(x,T) = V^*(x), \quad x \geq 0,\ t = T, \\ v(0,t) = E, \quad x = 0,\ t \in [0,T], \\ v(x,t) \longrightarrow 0, \quad x \longrightarrow +\infty,\ t \in [0,T], \end{gathered} \tag{10}$$

where $C \geq rE + \lambda S_{\max}$ is a positive constant and $q(x) = E - x$.

By adding a penalty term

$$\frac{C\varepsilon}{v(x,t) + \varepsilon - q(x)}, \tag{11}$$

the linear complementarity problem for pricing American options can be transformed into a nonlinear parabolic integrodifferential equation. Essentially, it is of order ε in regions where $v(x,t) \gg q(x)$, and hence the partial integrodifferential equation is approximately satisfied. When $v(x,t)$ approaches $q(x)$, this term is approximately equal to C assuring that the early exercise constraint is not violated. For the continuous case, the convergence and the positivity constraint of the penalty method have been proved in [26]. In this paper, we consider a second-order finite difference scheme to discretize the semilinear partial integrodifferential equation (10) and prove that the approximate option values generated by the scheme satisfies a discrete version of (2).

For applying the numerical method, we truncate the domain $(0, +\infty)$ into $(0, S_{\max})$. Based on Wilmott et al.'s estimate [19] that the upper bound of the asset price is typically three or four times the strike price, it is reasonable for us to set $S_{\max} = 4E$. The boundary condition at $x = S_{\max}$ is chosen to be $v(S_{\max}, t) = 0$. Normally, this truncation of the domain leads to a negligible error in the value of the option [27].

Therefore, in the remaining of this paper, we will consider the following nonlinear parabolic integrodifferential equation:

$$\begin{gathered} Lv(x,t) - \frac{C\varepsilon}{v(x,t) + \varepsilon - q(x)} = 0, \\ (x,t) \in (0, S_{\max}) \times (0,T), \end{gathered} \tag{12}$$

$$v(x,T) = V^*(x), \quad x \in [0, S_{\max}], \tag{13}$$

$$v(0,t) = E, \quad v(S_{\max}, t) = 0, \quad t \in [0,T]. \tag{14}$$

3. Discretization

We now consider the approximation of the solution to the semilinear partial integrodifferential equation (12)–(14) by a central difference scheme for the spatial derivatives.

The use of central difference scheme on a uniform mesh may produce nonphysical oscillations in the computed solution. To overcome this oscillation, we use a piecewise uniform mesh Ω^N on the space interval $[0, S_{\max}]$:

$$x_i = \begin{cases} h, & i = 1, \\ h\left[1 + \dfrac{\sigma^2}{|r - \lambda\zeta|}(i-1)\right], & i = 2, \dots, N, \end{cases} \tag{15}$$

where

$$h = \frac{S_{\max}}{1 + (\sigma^2/|r - \lambda\zeta|)(N-1)}. \tag{16}$$

For the time discretization, we use a uniform mesh Ω^K on $[0,T]$ with K mesh elements. Then the piecewise uniform mesh $\Omega^{N\times K}$ on $\Omega = (0, S_{\max}) \times (0,T)$ is defined to be the tensor product $\Omega^{N\times K} = \Omega^N \times \Omega^K$. It is easy to see that the mesh sizes $h_i = x_i - x_{i-1}$ and $\tau_j = t_j - t_{j-1}$ satisfy

$$h_i = \begin{cases} h, & i = 1, \\ \dfrac{\sigma^2}{|r - \lambda\zeta|}h, & i = 2, \dots, N, \end{cases} \tag{17}$$

$$\tau = \tau_j = \frac{T}{K}, \quad j = 1, \dots, K, \tag{18}$$

respectively.

The space derivatives of (12) are approximated with central differences on the above piecewise-uniform mesh:

$$\begin{gathered} \frac{\partial v}{\partial x}(x_i, t) \approx \frac{v_{i+1}(t) - v_{i-1}(t)}{h_i + h_{i+1}}, \\ \frac{\partial^2 v}{\partial x^2}(x_i, t) \approx \frac{2}{h_i + h_{i+1}}\left(\frac{v_{i+1}(t) - v_i(t)}{h_{i+1}} - \frac{v_i(t) - v_{i-1}(t)}{h_i}\right). \end{gathered} \tag{19}$$

The integral term

$$I = \int_0^\infty v(xy,t) f(y)\,\mathrm{d}y \tag{20}$$

of (12) can be approximated by a fast method as in [14–16]. By making the change of variable $y = s/x$, we have

$$I = \int_0^\infty v(xy,t) f(y)\,\mathrm{d}y = \int_0^\infty \frac{v(s,t) f(s/x)}{x}\mathrm{d}s. \tag{21}$$

By using the linear interpolation, we can obtain an approximation

$$I_i \approx A_i(t) = \sum_{n=0}^{N-1} \int_{x_n}^{x_{n+1}} \left(\frac{x_{n+1}-s}{h_{n+1}} v(x_n,t) + \frac{s-x_n}{h_{n+1}} v(x_{n+1},t) \right) \frac{f(s/x_i)}{x_i} \mathrm{d}s \tag{22}$$

of I at each mesh point x_i for $i = 1, 2, \ldots, N-1$.

A fully implicit scheme would lead to full matrices due to the integral term, which makes many methods computationally too expensive. Our technique is similar in some respects to Zhang [8], though less constrained in terms of stability restrictions. The integral term is treated explicitly in time, while the differential terms are treated implicitly. This leads to the solution of problems with a tridiagonal M-matrix. We will prove that the resulting time stepping method is unconditionally stable.

Our implicit-explicit scheme to discretize the integrodifferential equation (12)–(14) is

$$L^{N,K} V_i^j - \frac{C\varepsilon}{V_i^j + \varepsilon - q_i} = 0, \quad 1 \le i < N,\ 0 \le j < K, \tag{23}$$

$$V_i^K = V^*(x_i), \quad 0 \le i \le N, \tag{24}$$

$$V_0^j = E, \quad V_N^j = 0, \quad 0 \le j < K, \tag{25}$$

where

$$\begin{aligned} L^{N,K} V_i^j \equiv & -\frac{V_i^{j+1} - V_i^j}{\tau} - \frac{\sigma^2 x_i^2}{h_i + h_{i+1}} \left(\frac{V_{i+1}^j - V_i^j}{h_{i+1}} - \frac{V_i^j - V_{i-1}^j}{h_i} \right) \\ & - (r - \lambda\zeta) x_i \frac{V_{i+1}^j - V_{i-1}^j}{h_i + h_{i+1}} + (r+\lambda) V_i^j - \lambda A_i^{j+1}, \\ A_i^{j+1} = & \sum_{n=0}^{N-1} V_n^{j+1} \cdot \int_{x_n}^{x_{n+1}} \frac{x_{n+1}-s}{h_{n+1}} \cdot \frac{f(s/x_i)}{x_i} \mathrm{d}s + \sum_{n=0}^{N-1} V_{n+1}^{j+1} \cdot \int_{x_n}^{x_{n+1}} \frac{s-x_n}{h_{n+1}} \cdot \frac{f(s/x_i)}{x_i} \mathrm{d}s. \end{aligned} \tag{26}$$

Then from the above solution V_i^j, we can obtain the optimal stopping price which is the maximum asset price such that $V_i^j = V_i^*$ for each t_j.

Remark. Our method can be extended to the more general case of an infinite-activity process, like that of the Lévy-type models such as VG model [28] or CGMY model [29]. For example, the American put option price v under a generalized VG process satisfies the following partial integrodifferential complementarity problem [30, 31]:

$$\begin{gathered} \tilde{L} v(x,t) \ge 0, \quad x > 0,\ t \in [0,T), \\ v(x,t) - V^*(x) \ge 0, \quad x > 0,\ t \in [0,T], \\ \tilde{L} v(x,t) \cdot [v(x,t) - V^*(x)] = 0, \quad x > 0,\ t \in [0,T), \\ v(x,T) = V^*(x), \quad x \ge 0,\ t = T, \\ v(0,t) = E, \quad x = 0,\ t \in [0,T], \\ v(x,t) \to 0, \quad x \to +\infty,\ t \in [0,T], \end{gathered} \tag{27}$$

where $\tilde{L}$ denotes the partial integrodifferential operator defined by

$$\begin{aligned} \tilde{L} v(x,t) \equiv & -\frac{\partial v}{\partial t} - \frac{1}{2}\sigma^2 x^2 \frac{\partial^2 v}{\partial x^2} - (r+w) x \frac{\partial v}{\partial x} \\ & + rv - \int_{\mathbb{R}} [v(xe^y,t) - v(x,t)] g(y) \mathrm{d}y, \end{aligned} \tag{28}$$

w is some "compensation constant" given by

$$w = \int_{\mathbb{R}} (1 - e^y) g(y) \mathrm{d}y, \tag{29}$$

$g(y)$ is known as the Lévy density. It is noted in Cont and Tankov [2] and Cont and Voltchkova [9] that for the Lévy densities (in the usual case where the density decays exponentially for large jumps) an infinite-activity process can be arbitrarily well approximated by a finite-activity process and an adjusted volatility. Having done this, our numerical method for the finite-activity process can be used to value options under infinite-activity processes. However, the matrix associated with a discrete operator may not be an M-matrix.

4. Positivity Constraint

In this section, we will prove that our scheme satisfies the early exercise constraint.

Let

$$\begin{gathered} a_i = \frac{\sigma^2 x_i^2}{(h_i + h_{i+1}) h_i} - \frac{(r - \lambda\zeta) x_i}{h_i + h_{i+1}}, \qquad b_i = \frac{\sigma^2 x_i^2}{h_i h_{i+1}}, \\ c_i = \frac{\sigma^2 x_i^2}{(h_i + h_{i+1}) h_{i+1}} + \frac{(r - \lambda\zeta) x_i}{h_i + h_{i+1}}, \quad i = 1, \ldots, N-1. \end{gathered} \tag{30}$$

We can obtain

$$\begin{aligned}a_i &> \frac{\sigma^2 x_1 x_i}{(h_i+h_{i+1})h_i} - \frac{(r-\lambda\zeta)x_i}{h_i+h_{i+1}} = \frac{\sigma^2 x_1 - (r-\lambda\zeta)h_i}{(h_i+h_{i+1})h_i} x_i \\ &= \frac{\sigma^2 h - (r-\lambda\zeta)\left(\sigma^2/|r-\lambda\zeta|\right)h}{(h_i+h_{i+1})h_i} x_i \geq 0, \quad 1 < i \leq N-1, \\ c_i &> \frac{\sigma^2 x_1 x_i}{(h_i+h_{i+1})h_{i+1}} + \frac{(r-\lambda\zeta)x_i}{h_i+h_{i+1}} = \frac{\sigma^2 x_1 + (r-\lambda\zeta)h_{i+1}}{(h_i+h_{i+1})h_{i+1}} x_i \\ &= \frac{\sigma^2 h + (r-\lambda\zeta)\left(\sigma^2/|r-\lambda\zeta|\right)h}{(h_i+h_{i+1})h_{i+1}} x_i \geq 0, \quad 1 \leq i < N-1.\end{aligned} \tag{31}$$

Theorem 1. *The approximate option values generated by the implicit-explicit difference scheme* (23)–(25) *satisfy*

$$V_i^j \geq V^*(x_i), \quad (i,j) \in \Omega^{N\times K}, \tag{32}$$

provided that $C \geq rE + \lambda S_{\max}$.

Proof. We apply the similar technique of [24] to give the proof.

The schemes (23) can be written as

$$\begin{aligned}\left(\frac{1}{\tau} + b_i + r + \lambda\right) V_i^j = \frac{1}{\tau} V_i^{j+1} + a_i V_{i-1}^j + c_i V_{i+1}^j \\ + \lambda A_i^{j+1} + \frac{C\varepsilon}{V_i^j + \varepsilon - q_i}.\end{aligned} \tag{33}$$

The difference

$$u_i^j = V_i^j - q_i \tag{34}$$

satisfies the following equation:

$$\begin{aligned}&\left(\frac{1}{\tau} + b_i + r + \lambda\right) u_i^j \\ &= \frac{1}{\tau} u_i^{j+1} + a_i u_{i-1}^j + c_i u_{i+1}^j + \frac{C\varepsilon}{u_i^j + \varepsilon} + \lambda(\zeta+1)x_i \\ &\quad - (r+\lambda)E + \lambda\left(\sum_{n=0}^{N-1} u_n^{j+1} \cdot \int_{x_n}^{x_{n+1}} \frac{x_{n+1}-s}{h_{n+1}} \cdot \frac{f(s/x_i)}{x_i} ds \right. \\ &\quad \left. + \sum_{n=0}^{N-1} u_{n+1}^{j+1} \cdot \int_{x_n}^{x_{n+1}} \frac{s-x_n}{h_{n+1}} \cdot \frac{f(s/x_i)}{x_i} ds \right) \\ &\quad + \lambda\left(\sum_{n=0}^{N-1} q_n \cdot \int_{x_n}^{x_{n+1}} \frac{x_{n+1}-s}{h_{n+1}} \cdot \frac{f(s/x_i)}{x_i} ds \right. \\ &\quad \left. + \sum_{n=0}^{N-1} q_{n+1} \cdot \int_{x_n}^{x_{n+1}} \frac{s-x_n}{h_{n+1}} \cdot \frac{f(s/x_i)}{x_i} ds \right).\end{aligned} \tag{35}$$

Next, by defining

$$u^j = \min_i u_i^j, \tag{36}$$

let k be an index such that

$$u_k^j = u^j. \tag{37}$$

For $i = k$, it follows from (35) that

$$\begin{aligned}&\left(\frac{1}{\tau} + b_k + r + \lambda\right) u^j \\ &\geq \frac{1}{\tau} u_k^{j+1} + (a_k + c_k) u^j + \frac{C\varepsilon}{u^j + \varepsilon} + \lambda(\zeta+1)x_k \\ &\quad - (r+\lambda)E + \lambda\left(\sum_{n=0}^{N-1} u_n^{j+1} \cdot \int_{x_n}^{x_{n+1}} \frac{x_{n+1}-s}{h_{n+1}} \cdot \frac{f(s/x_k)}{x_k} ds \right. \\ &\quad \left. + \sum_{n=0}^{N-1} u_{n+1}^{j+1} \cdot \int_{x_n}^{x_{n+1}} \frac{s-x_n}{h_{n+1}} \cdot \frac{f(s/x_k)}{x_k} ds \right) \\ &\quad + \lambda\left(\sum_{n=0}^{N-1} q_n \cdot \int_{x_n}^{x_{n+1}} \frac{x_{n+1}-s}{h_{n+1}} \cdot \frac{f(s/x_k)}{x_k} ds \right. \\ &\quad \left. + \sum_{n=0}^{N-1} q_{n+1} \cdot \int_{x_n}^{x_{n+1}} \frac{s-x_n}{h_{n+1}} \cdot \frac{f(s/x_k)}{x_k} ds \right),\end{aligned} \tag{38}$$

where we have used (31). Since

$$\begin{aligned}&\sum_{n=0}^{N-1} q_n \cdot \int_{x_n}^{x_{n+1}} \frac{x_{n+1}-s}{h_{n+1}} \cdot \frac{f(s/x_k)}{x_k} ds \\ &\quad + \sum_{n=0}^{N-1} q_{n+1} \cdot \int_{x_n}^{x_{n+1}} \frac{s-x_n}{h_{n+1}} \cdot \frac{f(s/x_k)}{x_k} ds \\ &> (E - S_{\max}) \cdot \int_0^{x_N} \frac{f(s/x_k)}{x_k} ds \\ &= (E - S_{\max}) \cdot \int_0^{x_N/x_k} f(y)\, dy \\ &\geq E - S_{\max}, \\ \zeta + 1 &= \int_0^{\infty} (y-1) f(y)\, dy + 1 \\ &= \int_0^{\infty} y f(y)\, dy > 0,\end{aligned} \tag{39}$$

we conclude that

$$\begin{aligned}
&\left(\frac{1}{\tau}+r+\lambda\right)u^j-\frac{C\varepsilon}{u^j+\varepsilon}+\left(rE+\lambda S_{\max}\right)\\
&\quad\geq\frac{1}{\tau}u_k^{j+1}+\lambda\left(\sum_{n=1}^{N-1}u_n^{j+1}\cdot\int_{x_n}^{x_{n+1}}\frac{x_{n+1}-s}{h_{n+1}}\cdot\frac{f\left(s/x_k\right)}{x_k}ds\right.\\
&\qquad\left.+\sum_{n=1}^{N-1}u_{n+1}^{j+1}\cdot\int_{x_n}^{x_{n+1}}\frac{s-x_n}{h_{n+1}}\cdot\frac{f\left(s/x_k\right)}{x_k}ds\right)\\
&\quad\geq\frac{1}{\tau}u^{j+1}+\lambda u^{j+1}\left(\sum_{n=1}^{N-1}\int_{x_n}^{x_{n+1}}\frac{x_{n+1}-s}{h_{n+1}}\cdot\frac{f\left(s/x_k\right)}{x_k}ds\right.\\
&\qquad\left.+\sum_{n=1}^{N-1}\int_{x_n}^{x_{n+1}}\frac{s-x_n}{h_{n+1}}\cdot\frac{f\left(s/x_k\right)}{x_k}ds\right).
\end{aligned}\tag{40}$$

If we assume that

$$u^{j+1}\geq 0,\tag{41}$$

from (40) we can get

$$F\left(u^j\right)\geq 0,\tag{42}$$

where

$$F(u)=\left(\frac{1}{\tau}+r+\lambda\right)u-\frac{C\varepsilon}{u+\varepsilon}+\left(rE+\lambda S_{\max}\right).\tag{43}$$

Obviously,

$$\begin{aligned}
F'(u)&=\left(\frac{1}{\tau}+r+\lambda\right)+\frac{C\varepsilon}{(u+\varepsilon)^2}\geq 0,\\
F(0)&=-C+\left(rE+\lambda S_{\max}\right)\leq 0,
\end{aligned}\tag{44}$$

where we have used the assumption $C\geq(rE+\lambda S_{\max})$. Hence, from (42) we can obtain

$$u^j\geq 0.\tag{45}$$

Consequently, by induction on j, it follows from (34) that

$$V_i^j\geq q_i,\quad 0\leq i\leq N,\tag{46}$$

for $j=K,\ldots,1,0$.

Next we prove that $V_i^j\geq 0$. As above, we define

$$V^j=\min_i V_i^j,\tag{47}$$

and let k be an index such that

$$V_k^j=V^j.\tag{48}$$

For $i=k$, from (33) we obtain

$$\begin{aligned}
\left(\frac{1}{\tau}+b_k+r+\lambda\right)V_k^j&\geq\frac{1}{\tau}V^{j+1}+\left(a_k+c_k\right)V^j\\
&\quad+\lambda A_k^{j+1}+\frac{C\varepsilon}{V_k^j+\varepsilon-q_k}.
\end{aligned}\tag{49}$$

Hence, we have

$$\left(\frac{1}{\tau}+r+\lambda\right)V_k^j\geq\frac{1}{\tau}V^{j+1}+\lambda A_k^{j+1}+\frac{C\varepsilon}{V_k^j+\varepsilon-q_k}.\tag{50}$$

Since we have proved that $V_i^j\geq q_i$, we get

$$\begin{aligned}
&\left(\frac{1}{\tau}+r+\lambda\right)V_k^j\\
&\quad\geq\frac{1}{\tau}V^{j+1}+\lambda\left(\sum_{n=0}^{N-1}V_n^{j+1}\cdot\int_{x_n}^{x_{n+1}}\frac{x_{n+1}-s}{h_{n+1}}\cdot\frac{f\left(s/x_k\right)}{x_k}ds\right.\\
&\qquad\left.+\sum_{n=0}^{N-1}V_{n+1}^{j+1}\cdot\int_{x_n}^{x_{n+1}}\frac{s-x_n}{h_{n+1}}\cdot\frac{f\left(s/x_k\right)}{x_k}ds\right).
\end{aligned}\tag{51}$$

By the above inequality. Hence, by induction on j, we can obtain

$$V_i^j\geq 0,\quad (i,j)\in\Omega^{N\times K},\tag{52}$$

for $j=K,\ldots,1,0$.

Combine (46) with (52) to complete the proof. □

5. Error Estimates

To investigate the convergence of the method, note that the error functions $z_i^j=V_i^j-v_i^j$ $(0\leq i\leq N, 0\leq j\leq K)$ are the solutions of the discrete problem

$$\begin{aligned}
&-\frac{z_i^{j+1}-z_i^j}{\tau}-\frac{\sigma^2x_i^2}{h_i+h_{i+1}}\left(\frac{z_{i+1}^j-z_i^j}{h_{i+1}}-\frac{z_i^j-z_{i-1}^j}{h_i}\right)\\
&\quad-(r-\lambda\zeta)\,x_i\frac{z_{i+1}^j-z_{i-1}^j}{h_i+h_{i+1}}\\
&\quad+(r+\lambda)\,z_i^j+\frac{C\varepsilon}{\left(\xi_i^j+\varepsilon-q_i\right)^2}z_i^j\\
&\quad-\lambda\left(\sum_{n=0}^{N-1}z_n^{j+1}\cdot\int_{x_n}^{x_{n+1}}\frac{x_{n+1}-s}{h_{n+1}}\cdot\frac{f\left(s/x_i\right)}{x_i}ds\right.\\
&\qquad\left.+\sum_{n=0}^{N-1}z_{n+1}^{j+1}\cdot\int_{x_n}^{x_{n+1}}\frac{s-x_n}{h_{n+1}}\cdot\frac{f\left(s/x_i\right)}{x_i}ds\right)\\
&=R_i^j,\quad 1\leq i<N,\ 0\leq j<K,\\
&\qquad z_i^K=0,\quad 0\leq i\leq N,\\
&\qquad z_0^j=z_N^j=0,\quad 0\leq j<K,
\end{aligned}\tag{53}$$

where $\xi_i^j = v_i^j + \kappa z_i^j$, $0 < \kappa < 1$, and

$$R_i^j \equiv \left(\frac{v_i^{j+1} - v_i^j}{\tau} - \frac{\partial v}{\partial t}\left(x_i, t_j\right)\right) + \frac{1}{2}\sigma^2 x_i^2 \left[\frac{2}{h_i + h_{i+1}}\left(\frac{v_{i+1}^j - v_i^j}{h_{i+1}} - \frac{v_i^j - v_{i-1}^j}{h_i}\right) - \frac{\partial^2 v}{\partial x^2}\left(x_i, t_j\right)\right] + (r - \lambda\zeta) x_i \left(\frac{v_{i+1}^j - v_{i-1}^j}{h_i + h_{i+1}} - \frac{\partial v}{\partial x}\left(x_i, t_j\right)\right) + \lambda\left[\sum_{n=0}^{N-1} v\left(x_n, t_{j+1}\right) \cdot \int_{x_n}^{x_{n+1}} \frac{x_{n+1} - s}{h_{n+1}} \cdot \frac{f\left(s/x_i\right)}{x_i} ds + \sum_{n=0}^{N-1} v\left(x_{n+1}, t_{j+1}\right) \cdot \int_{x_n}^{x_{n+1}} \frac{s - x_n}{h_{n+1}} \cdot \frac{f\left(s/x_i\right)}{x_i} ds - \int_0^{S_{\max}} v\left(s, t_j\right) \frac{f\left(s/x_i\right)}{x_i} ds\right]. \tag{54}$$

Let

$$L_\varepsilon^{N,K} z_i^j \equiv -\frac{z_i^{j+1} - z_i^j}{\tau} - \frac{\sigma^2 x_i^2}{h_i + h_{i+1}}\left(\frac{z_{i+1}^j - z_i^j}{h_{i+1}} - \frac{z_i^j - z_{i-1}^j}{h_i}\right) - (r - \lambda\zeta) x_i \frac{z_{i+1}^j - z_{i-1}^j}{h_i + h_{i+1}} + (r + \lambda) z_i^j + \frac{C\varepsilon}{\left(\xi_i^j + \varepsilon - q_i\right)^2} z_i^j - \lambda\left(\sum_{n=0}^{N-1} z_n^{j+1} \cdot \int_{x_n}^{x_{n+1}} \frac{x_{n+1} - s}{h_{n+1}} \cdot \frac{f\left(s/x_i\right)}{x_i} ds + \sum_{n=0}^{N-1} z_{n+1}^{j+1} \cdot \int_{x_n}^{x_{n+1}} \frac{s - x_n}{h_{n+1}} \cdot \frac{f\left(s/x_i\right)}{x_i} ds\right). \tag{55}$$

The operator $L_\varepsilon^{N,K}$ satisfies the following discrete maximum principle. Hence, the difference scheme is stable and oscillation-free for arbitrary volatility and arbitrary interest rate.

Lemma 2 (discrete maximum principle). *The operator $L_\varepsilon^{N,K}$ defined by* (55) *on the piecewise uniform mesh $\Omega^{N\times K}$ satisfies a discrete maximum principle; that is, if u_i^j and w_i^j are mesh functions that satisfy $u_0^j \geq w_0^j$, $u_N^j \geq w_N^j$ $(0 \leq j < K)$, $u_i^K \geq w_i^K$ $(0 \leq i \leq N)$, and $L_\varepsilon^{N,K} u_i^j \geq L_\varepsilon^{N,K} w_i^j$ $(1 \leq i < N,\ 0 \leq j < K)$, then $u_i^j \geq w_i^j$ for all i, j.*

Proof. The discrete operator $L_\varepsilon^{N,K}$ can be written as follows:

$$L_\varepsilon^{N,K} z_i^j = -\frac{z_i^{j+1} - z_i^j}{\tau_{j+1}} - a_i z_{i-1}^j + \left[b_i + r + \lambda + \frac{C\varepsilon}{\left(\xi_i^j + \varepsilon - q_i\right)^2}\right] z_i^j - c_i z_{i+1}^j - \lambda\left(\sum_{n=0}^{N-1} z_n^{j+1} \cdot \int_{x_n}^{x_{n+1}} \frac{x_{n+1} - s}{h_{n+1}} \cdot \frac{f\left(s/x_i\right)}{x_i} ds + \sum_{n=0}^{N-1} z_{n+1}^{j+1} \cdot \int_{x_n}^{x_{n+1}} \frac{s - x_n}{h_{n+1}} \cdot \frac{f\left(s/x_i\right)}{x_i} ds\right), \tag{56}$$

where a_i, b_i, and c_i are defined in Section 4. From (31) we have

$$a_i > 0 \quad \text{for } 1 < i \leq N - 1, \qquad c_i > 0 \quad \text{for } 1 \leq i < N - 1. \tag{57}$$

Clearly,

$$b_i + r + \lambda + \frac{C\varepsilon}{\left(\xi_i^j + \varepsilon - q_i\right)^2} > 0 \quad \text{for } 1 \leq i \leq N - 1, \quad b_1 + c_1 > 0, \quad a_i + b_i + c_i > 0, \quad 2 \leq i \leq N - 2, \quad a_{N-1} + b_{N-1} > 0. \tag{58}$$

Furthermore, we have

$$\lambda - \lambda\left(\sum_{n=0}^{N-1} \int_{x_n}^{x_{n+1}} \frac{x_{n+1} - s}{h_{n+1}} \cdot \frac{f\left(s/x_i\right)}{x_i} ds + \sum_{n=0}^{N-1} \int_{x_n}^{x_{n+1}} \frac{s - x_n}{h_{n+1}} \cdot \frac{f\left(s/x_i\right)}{x_i} ds\right) = \lambda\left(1 - \int_0^{x_N} \frac{f\left(s/x_i\right)}{x_i} ds\right) = \lambda\left(1 - \int_0^{x_N/x_i} f\left(y\right) dy\right) > 0. \tag{59}$$

Hence, we verify that the matrix associated with $L_\varepsilon^{N,K}$ is an M-matrix; see for example [32]. Thus, by the same argument as [33, Lemma 3.1] the result follows. □

Now we can get the following error estimates.

Theorem 3. *Let v be the solution of* (12)–(14) *and V the solution of the finite difference scheme* (23)–(25). *Then one has the following error estimates,*

$$\left|V_i^j - v\left(x_i, t_j\right)\right| \leq C_1\left(\tau + N^{-2}\right), \quad 0 \leq i \leq N,\ 0 \leq j \leq K, \tag{60}$$

where C_1 is a positive constant independent of τ and N.

Proof. Under the regularity assumption on v, the linear interpolation error for any $s \in [x_i, x_{i+1}]$ is

$$v(s,t) - \left(\frac{x_{i+1} - s}{h_{i+1}} v(x_i, t) + \frac{s - x_i}{h_{i+1}} v(x_{i+1}, t) \right) = \frac{1}{2} \frac{\partial^2 v}{\partial x^2} (\eta, t)(s - x_i)(s - x_{i+1}) \tag{61}$$

for some $\eta \in [x_i, x_{i+1}]$. Thus, we get

$$\left| v(s,t) - \left(\frac{x_{i+1} - s}{h_{i+1}} v(x_i, t) + \frac{s - x_i}{h_{i+1}} v(x_{i+1}, t) \right) \right| \le C_2 N^{-2}, \tag{62}$$

where C_2 is a positive constant independent of τ and N. Using this, we have

$$\begin{aligned}
&\left| \sum_{n=0}^{N-1} v(x_n, t_{j+1}) \cdot \int_{x_n}^{x_{n+1}} \frac{x_{n+1} - s}{h_{n+1}} \cdot \frac{f(s/x_i)}{x_i} \mathrm{d}s \right. \\
&\quad + \sum_{n=0}^{N-1} v(x_{n+1}, t_{j+1}) \cdot \int_{x_n}^{x_{n+1}} \frac{s - x_n}{h_{n+1}} \\
&\quad \left. \cdot \frac{f(s/x_i)}{x_i} \mathrm{d}s - \int_0^{S_{\max}} v(s, t_j) \frac{f(s/x_i)}{x_i} \mathrm{d}s \right| \\
&\quad \le \left| \sum_{n=0}^{N-1} v(x_n, t_{j+1}) \cdot \int_{x_n}^{x_{n+1}} \frac{x_{n+1} - s}{h_{n+1}} \cdot \frac{f(s/x_i)}{x_i} \mathrm{d}s \right. \\
&\qquad + \sum_{n=0}^{N-1} v(x_{n+1}, t_{j+1}) \cdot \int_{x_n}^{x_{n+1}} \frac{s - x_n}{h_{n+1}} \\
&\qquad \left. \cdot \frac{f(s/x_i)}{x_i} \mathrm{d}s - \int_0^{S_{\max}} v(s, t_{j+1}) \frac{f(s/x_i)}{x_i} \mathrm{d}s \right| \\
&\qquad + \int_0^{S_{\max}} \left| v(s, t_{j+1}) - v(s, t_j) \right| \frac{f(s/x_i)}{x_i} \mathrm{d}s \\
&\quad \le C_2 N^{-2} \int_0^{S_{\max}} \frac{f(s/x_i)}{x_i} \mathrm{d}s + C_3 \tau \int_0^{S_{\max}} \frac{f(s/x_i)}{x_i} \mathrm{d}s \\
&\quad \le C_4 (\tau + N^{-2}) \int_0^{S_{\max}/x_i} f(y) \mathrm{d}y \le C_4 (\tau + N^{-2}),
\end{aligned} \tag{63}$$

where C_3 and C_4 are positive constants independent of τ and N. Hence, we use the Taylor expansion to obtain

$$\begin{aligned}
\left| R_i^j \right| &\le C_5 \int_{t_j}^{t_{j+1}} \left| \frac{\partial^2 v}{\partial t^2} (x_i, t) \right| \mathrm{d}t \\
&\quad + C_6 h \int_{x_{i-1}}^{x_{i+1}} \left[x_i^2 \left| \frac{\partial^4 v}{\partial x^4} (x, t_j) \right| + x_i \left| \frac{\partial^3 v}{\partial x^3} (x, t_j) \right| \right] \mathrm{d}x \\
&\quad + C_4 (\tau + N^{-2}) \\
&\le C_6 (\tau + N^{-2}),
\end{aligned} \tag{64}$$

for $0 < i < N$, $0 \le j < K$, where C_5 and C_6 are also positive constants independent of τ and N. Therefore, using the barrier function $W_i^j = C_1(\tau + N^{-2})$ (with the constant C_1 sufficiently large), Lemma 2 implies that

$$\left| V_i^j - v(x_i, t_j) \right| \le C_1 (\tau + N^{-2}), \quad 0 \le i \le N, \ 0 \le j \le K, \tag{65}$$

which completes the proof. □

6. Numerical Experiments

In this section, we verify experimentally the theoretical results obtained in the preceding section. Errors and convergence rates for the finite difference scheme are presented for two test problems.

Test 1. American put option under Kou's jump-diffusion model with parameters:

$$\begin{aligned}
&\sigma = 0.15, && r = 0.06, && T = 1, \\
&E = 25, && S_{\max} = 100, && \lambda = 0.1, \\
&\alpha_1 = 2.0465, && \alpha_2 = 3.0775, && p = 0.3445.
\end{aligned} \tag{66}$$

Test 2. American put option under Kou's jump-diffusion model with parameters:

$$\begin{aligned}
&\sigma = 0.4, && r = 0.06, && T = 1, \\
&E = 25, && S_{\max} = 100, && \lambda = 0.1, \\
&\alpha_1 = 2.0465, && \alpha_2 = 3.0775, && p = 0.3445.
\end{aligned} \tag{67}$$

To solve the nonlinear problem (23)–(25), we use Newton iterative method. The initial guesses for Tests 1 and 2 are taken as $[V_i^j]^{(0)} = V_i^{j+1}$ for time mesh point j and the stoping criterion is

$$\max_i \left| \left[V_i^j \right]^{(m)} - \left[V_i^j \right]^{(m-1)} \right| \le 10^{-5}. \tag{68}$$

For Tests 1 and 2 we choose $\varepsilon = 0.0001$, $C = rE + \lambda S_{\max}$. The computed option value V and the constraint $V - V^*$ with $N = 128$ and $K = 64$ for Test 1 are depicted in Figures 1 and 2, respectively. The computed option value V and the constraint $V - V^*$ with $N = 128$ and $K = 64$ for Test 2 are depicted in Figures 3 and 4, respectively.

The exact solutions of our test problems are not available. We use the approximated solution of $N = 1024$ and $K = 4096$ as the exact solution. We present the error estimates for different N and K at $t = 0$. Because we only know "the exact solution" on mesh points, we use the linear interpolation to get solutions at other points. In this paper $\overline{V}(x,t)$ denotes "the exact solution" which is a linear interpolation of the approximated solution $V^{1024,4096}$. We

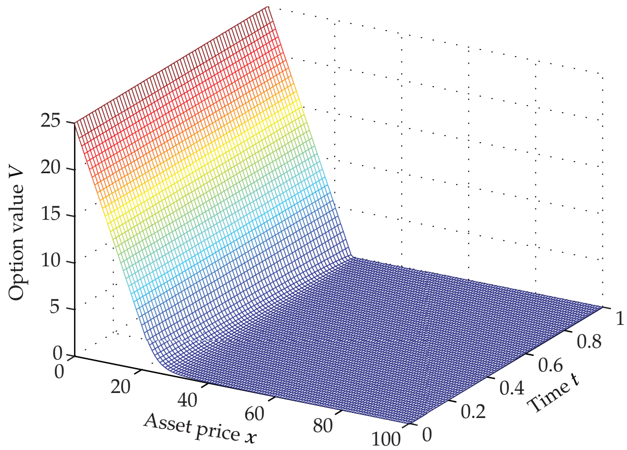

Figure 1: Computed option value V for Test 1.

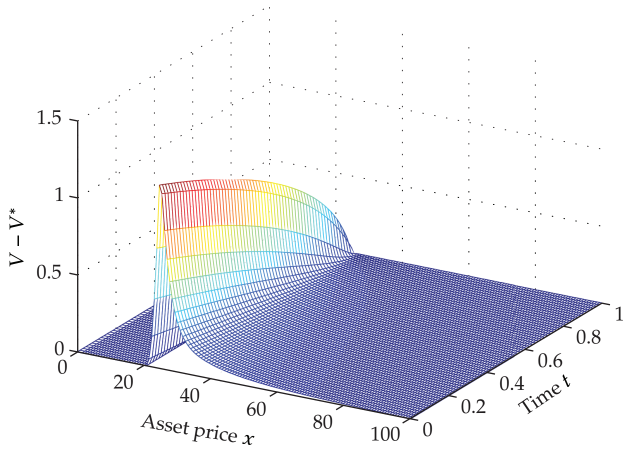

Figure 2: The constraint $V - V^*$ for Test 1.

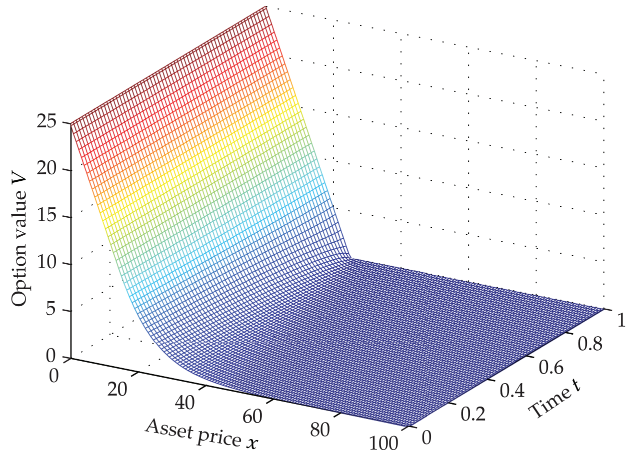

Figure 3: Computed option value V for Test 2.

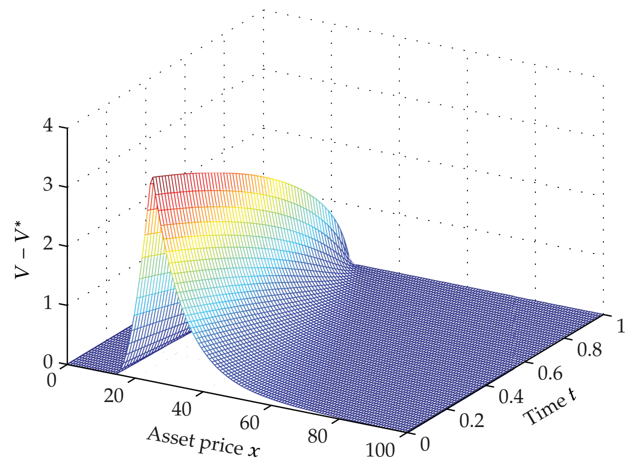

Figure 4: The constraint $V - V^*$ for Test 2.

measure the accuracy in the discrete maximum norm

$$e^{N,K} = \max_i \left| V_{i,0}^{N,K} - \overline{V}(x_i, 0) \right|, \tag{69}$$

and the convergence rate

$$R^{N,K} = \log_2 \left(\frac{e^{N,K}}{e^{2N,4K}} \right). \tag{70}$$

The error estimates and the convergence rates in our computed solutions of Tests 1 and 2 are listed in Tables 1 and 2, respectively.

From the figures, it is seen that the numerical solutions by our method are nonoscillatory. From Tables 1 and 2, we see that $e^{N,K}/e^{2N,4K}$ is close to 4, which supports the convergence estimate of Theorem 3. The numerical results of Zhang and Wang [17, 18] verify that their schemes are also second-order convergent. However, their penalty term is nonsmooth and a smoothing technique is needed for solving the nonlinear discretization system.

7. Discussion

7.1. The Crank-Nicolson Scheme. For the time discretization, we can use the Crank-Nicolson scheme to improve the accuracy of the scheme. Then the implicit finite difference scheme on the above piecewise-uniform mesh for the integrodifferential equation (12)–(14) is

$$\begin{gathered}
\overline{L}^{N,K} V_i^j - \frac{1/2C\varepsilon}{V_i^j + \varepsilon - q_i} - \frac{1/2C\varepsilon}{V_i^{j+1} + \varepsilon - q_i} = 0, \\
1 \le i < N, \ 0 \le j < K, \\
V_i^K = V^*(x_i), \quad 0 \le i \le N, \\
V_0^j = E, \quad V_N^j = 0, \quad 0 \le j < K,
\end{gathered} \tag{71}$$

Table 1: Numerical results for Test 1.

N	K	error	rate
64	16	$2.8859e-2$	—
128	64	$8.3456e-3$	1.780
256	256	$2.1187e-3$	1.978
512	1024	$5.5979e-4$	1.920

Table 2: Numerical results for Test 2.

N	K	error	rate
64	16	$4.8818e-2$	—
128	64	$1.3125e-2$	1.895
256	256	$3.3288e-3$	1.979
512	1024	$7.2756e-4$	2.194

where

$$\begin{aligned}\overline{L}^{N,K}V_i^j \equiv & -\frac{V_i^{j+1}-V_i^j}{\tau} \\ & -\frac{\sigma^2 x_i^2}{h_i+h_{i+1}}\left[\frac{1}{2}\left(\frac{V_{i+1}^j-V_i^j}{h_{i+1}}+\frac{V_{i+1}^{j+1}-V_i^{j+1}}{h_{i+1}}\right)\right. \\ & \left.-\frac{1}{2}\left(\frac{V_i^j-V_{i-1}^j}{h_i}+\frac{V_i^{j+1}-V_{i-1}^{j+1}}{h_i}\right)\right] \\ & -\frac{1}{2}(r-\lambda\zeta)x_i\left(\frac{V_{i+1}^j-V_{i-1}^j}{h_i+h_{i+1}}+\frac{V_{i+1}^{j+1}-V_{i-1}^{j+1}}{h_i+h_{i+1}}\right) \\ & +(r+\lambda)\frac{V_i^j+V_i^{j+1}}{2}-\lambda\frac{A_i^j+A_i^{j+1}}{2}, \\ A_i^j = & \sum_{n=0}^{N-1}V_n^j\cdot\int_{x_n}^{x_{n+1}}\frac{x_{n+1}-s}{h_{n+1}}\cdot\frac{f(s/x_i)}{x_i}ds \\ & +\sum_{n=0}^{N-1}V_{n+1}^j\cdot\int_{x_n}^{x_{n+1}}\frac{s-x_n}{h_{n+1}}\cdot\frac{f(s/x_i)}{x_i}ds.\end{aligned} \tag{72}$$

The implicit scheme would lead to full matrices due to the integral term, which makes many methods computationally expensive. Furthermore, in order to satisfy the positivity constraint and to avoid spurious oscillations in the Crank-Nicolson method [34–36], the time mesh size should satisfy the following constraint condition [24, 35]

$$\tau \le \frac{2h_i^2}{\sigma^2 S_{\max}^2 + rS_{\max}h_i + rh_i^2 + (2rE/\varepsilon)h_i^2}. \tag{73}$$

7.2. Power Penalty Methods. Some papers [12, 22, 37] have used power penalty methods to the linear complementarity problem arising from pricing American options. Wang et al. [37] prove that the solution to their penalized equation converges to that of the variational inequality problem with an arbitrary order. The power penalty methods [12, 22, 37] can also be applied to valuate American options under Kou's jump-diffusion model. The discretization method can be same as that of Section 3. Therefore, our difference scheme for the power penalty equation is

$$\begin{aligned}&\widehat{L}^{N,K}V_i^j+\lambda\left[\max\left(V^*(x_i)-V_i^j,0\right)\right]^{1/s}=0, \\ &\qquad 1\le i<N,\ 0\le j<K, \\ &V_i^K = V^*(x_i),\quad 0\le i\le N, \\ &V_0^j = E,\quad V_N^j=0,\quad 0\le j<K,\end{aligned} \tag{74}$$

where

$$\begin{aligned}\widehat{L}^{N,K}V_i^j \equiv & -\frac{V_i^{j+1}-V_i^j}{\tau} \\ & -\frac{\sigma^2x_i^2}{h_i+h_{i+1}}\left(\frac{V_{i+1}^j-V_i^j}{h_{i+1}}-\frac{V_i^j-V_{i-1}^j}{h_i}\right) \\ & -(r-\lambda\zeta)x_i\frac{V_{i+1}^j-V_{i-1}^j}{h_i+h_{i+1}} \\ & +(r+\lambda)V_i^j-\lambda A_i^{j+1}, \\ A_i^{j+1} = & \sum_{n=0}^{N-1}V_n^{j+1}\cdot\int_{x_n}^{x_{n+1}}\frac{x_{n+1}-s}{h_{n+1}}\cdot\frac{f(s/x_i)}{x_i}ds \\ & +\sum_{n=0}^{N-1}V_{n+1}^{j+1}\cdot\int_{x_n}^{x_{n+1}}\frac{s-x_n}{h_{n+1}}\cdot\frac{f(s/x_i)}{x_i}ds,\end{aligned} \tag{75}$$

λ and s are the penalty parameters. Since the power penalty term is nonsmooth, a smoothing technique is needed for solving the nonlinear discretization system.

Acknowledgments

The authors would like to thank the anonymous referees for their helpful comments and suggestions for the improvement of this paper. The work was supported by the Zhejiang Province Natural Science Foundation (Grant nos. Y6100021, Y6110310), Research Project (Grant no. Y201016720) of the Zhejiang Provincial Education Department and the Ningbo Municipal Natural Science Foundation (Grant nos. 2012A610035, 2012A610036).

References

[1] F. Black and M. Scholes, "The pricing of options and corporate liabilities," *Journal of Political Economy*, vol. 81, no. 3, pp. 637–654, 1973.

[2] R. Cont and P. Tankov, *Financial Modelling with Jump Processes*, Chapman & Hall/CRC Press, Boca Raton, Fla, USA, 2004.

[3] S. Heston, "A closed-form solution for options with stochastic volatility with applications to bond and currency options," *Reviews of Financial Studies*, vol. 6, no. 2, pp. 327–343, 1993.

[4] J. Hull and A. White, "The pricing of options on assets with stochastic volatilities," *Journal of Finance*, vol. 42, no. 2, pp. 281–300, 1987.

[5] R. C. Merton, "Option pricing when underlying stock return are discontinuous," *Journal of Financial Economics*, vol. 3, no. 1-2, pp. 125–144, 1976.

[6] S. G. Kou, "A jump-diffusion model for option pricing," *Management Science*, vol. 48, no. 8, pp. 1086–1101, 2002.

[7] K. Amin, "Jump diffusion option valuation in discrete time," *Journal of Finance*, vol. 48, no. 5, pp. 1883–1863, 1993.

[8] X. L. Zhang, "Numerical analysis of American option pricing in a jump-diffusion model," *Mathematics of Operations Research*, vol. 22, no. 3, pp. 668–690, 1997.

[9] R. Cont and E. Voltchkova, "A finite difference scheme for option pricing in jump diffusion and exponential Lévy models," *SIAM Journal on Numerical Analysis*, vol. 43, no. 4, pp. 1596–1626, 2005.

[10] L. Andersen and J. Andreasen, "Jump-diffusion processes: volatility smile fitting and numerical methods for option pricing," *Review of Derivatives Research*, vol. 4, no. 3, pp. 231–262, 2000.

[11] A. Almendral and C. W. Oosterlee, "Numerical valuation of options with jumps in the underlying," *Applied Numerical Mathematics*, vol. 53, no. 1, pp. 1–18, 2005.

[12] Y. d'Halluin, P. A. Forsyth, and G. Labahn, "A penalty method for American options with jump diffusion processes," *Numerische Mathematik*, vol. 97, no. 2, pp. 321–352, 2004.

[13] Y. d'Halluin, P. A. Forsyth, and K. R. Vetzal, "Robust numerical methods for contingent claims under jump diffusion processes," *IMA Journal of Numerical Analysis*, vol. 25, no. 1, pp. 87–112, 2005.

[14] S. Salmi and J. Toivanen, "An iterative method for pricing American options under jump-diffusion models," *Applied Numerical Mathematics*, vol. 61, no. 7, pp. 821–831, 2011.

[15] J. Toivanen, "Numerical valuation of European and American options under Kou's jump-diffusion model," *SIAM Journal on Scientific Computing*, vol. 30, no. 4, pp. 1949–1970, 2008.

[16] J. Toivanen, "A high-order front-tracking finite difference method for pricing American options under jump-diffusion models," *Journal of Computational Finance*, vol. 13, no. 3, pp. 61–79, 2010.

[17] K. Zhang and S. Wang, "Pricing options under jump diffusion processes with fitted finite volume method," *Applied Mathematics and Computation*, vol. 201, no. 1-2, pp. 398–413, 2008.

[18] K. Zhang and S. Wang, "A computational scheme for options under jump diffusion processes," *International Journal of Numerical Analysis and Modeling*, vol. 6, no. 1, pp. 110–123, 2009.

[19] P. Wilmott, J. Dewynne, and S. Howison, *Option Pricing: Mathematical Models and Computation*, Oxford Financial Press, Oxford, UK, 1993.

[20] Z. Cen and A. Le, "A robust and accurate finite difference method for a generalized Black-Scholes equation," *Journal of Computational and Applied Mathematics*, vol. 235, no. 13, pp. 3728–2733, 2011.

[21] S. Wang, "A novel fitted finite volume method for the Black-Scholes equation governing option pricing," *IMA Journal of Numerical Analysis*, vol. 24, no. 4, pp. 699–720, 2004.

[22] L. Angermann and S. Wang, "Convergence of a fitted finite volume method for the penalized Black-Scholes equation governing European and American option pricing," *Numerische Mathematik*, vol. 106, no. 1, pp. 1–40, 2007.

[23] R. Zvan, P. A. Forsyth, and K. R. Vetzal, "Penalty methods for American options with stochastic volatility," *Journal of Computational and Applied Mathematics*, vol. 91, no. 2, pp. 199–218, 1998.

[24] B. F. Nielsen, O. Skavhaug, and A. Tveito, "Penalty and front-fixing methods for the numerical solution of American option problems," *Journal of Computational Finance*, vol. 5, pp. 69–97, 2002.

[25] Z. Cen, A. Le, and A. Xu, "A second-order difference scheme for the penalized Black-Scholes equation governing American put option pricing," *Computational Economics*, vol. 40, no. 1, pp. 49–62, 2012.

[26] K. Zhang and S. Wang, "Convergence property of an interior penalty approach to pricing American option," *Journal of Industrial and Management Optimization*, vol. 7, no. 2, pp. 435–447, 2011.

[27] R. Kangro and R. Nicolaides, "Far field boundary conditions for Black-Scholes equations," *SIAM Journal on Numerical Analysis*, vol. 38, no. 4, pp. 1357–1368, 2000.

[28] D. B. Madan and E. Seneta, "The variance gamma (V.G.) model for share market returns," *Journal of Business*, vol. 63, no. 4, pp. 511–524, 1990.

[29] P. Carr, H. Geman, D. B. Madan, and M. Yor, "The fine structure of asset returns: an empirical investigation," *Journal of Business*, vol. 75, no. 2, pp. 305–332, 2002.

[30] A. Almendral and C. W. Oosterlee, "On American options under the variance gamma process," *Applied Mathematical Finance*, vol. 14, no. 2, pp. 131–152, 2007.

[31] D. B. Madan, P. Carr, and E. C. Chang, "The variance Gamma process and option pricing," *European Finance Review*, vol. 2, no. 1, pp. 79–105, 1998.

[32] R. S. Varga, *Matrix Iterative Analysis*, Prentice-Hall, Englewood Cliffs, NJ, USA, 1962.

[33] R. B. Kellogg and A. Tsan, "Analysis of some difference approximations for a singular perturbation problem without turning points," *Mathematics of Computation*, vol. 32, no. 144, pp. 1025–1039, 1978.

[34] M. Giles and R. Carter, "Convergence analysis of Crank-Nicolson and Rannacher time marching," *Journal of Computational Finance*, vol. 9, no. 4, pp. 89–112, 2006.

[35] A. Q. M. Khaliq, D. A. Voss, and K. Kazmi, "Adaptive θ-methods for pricing American options," *Journal of Computational and Applied Mathematics*, vol. 222, no. 1, pp. 210–227, 2008.

[36] D. M. Pooley, K. R. Vetzal, and P. A. Forsyth, "Convergence remedies for non-smooth payoffs in option pricing," *Journal of Computational Finance*, vol. 6, no. 4, pp. 25–40, 2003.

[37] S. Wang, X. Q. Yang, and K. L. Teo, "Power penalty method for a linear complementarity problem arising from American option valuation," *Journal of Optimization Theory and Applications*, vol. 129, no. 2, pp. 227–254, 2006.

Hindawi Publishing Corporation
Journal of Function Spaces and Applications
Volume 2012, Article ID 242870, 12 pages
doi:10.1155/2012/242870

Research Article

Analysis of the Error in a Numerical Method Used to Solve Nonlinear Mixed Fredholm-Volterra-Hammerstein Integral Equations

D. Gámez

Departamento de Matemática Aplicada, E. T. S. Ingeniería de Edificación, Universidad de Granada, c/Severo Ochoa, s/n, 18071 Granada, Spain

Correspondence should be addressed to D. Gámez, domingo@ugr.es

Received 19 October 2012; Accepted 27 November 2012

Academic Editor: Manuel Ruiz Galan

This work presents an analysis of the error that is committed upon having obtained the approximate solution of the nonlinear Fredholm-Volterra-Hammerstein integral equation by means of a method for its numerical resolution. The main tools used in the study of the error are the properties of Schauder bases in a Banach space.

1. Introduction

In this paper we consider the following nonlinear mixed Fredholm-Volterra-Hammerstein integral equation:

$$x(t) = y_0(t) + \int_{\alpha}^{\alpha+\beta} k_1(t,s)g_1(s,x(s))ds + \int_{\alpha}^{t} k_2(t,s)g_2(s,x(s))ds, \quad t \in [\alpha, \alpha+\beta], \tag{1.1}$$

where $y_0 : [\alpha, \alpha+\beta] \to \mathbb{R}$, $g_1, g_2 : [\alpha, \alpha+\beta] \times \mathbb{R} \to \mathbb{R}$ and the kernels $k_1, k_2 : [\alpha, \alpha+\beta]^2 \to \mathbb{R}$ are assumed to be known continuous functions, and $x : [\alpha, \alpha+\beta] \to \mathbb{R}$ is the unknown function to be determined.

Equation (1.1) arises in a variety of applications in many fields, including continuum mechanics, potential theory, electricity and magnetism, three-dimensional contact problems, and fluid mechanics, and so forth (see, e.g., [1–4]). Several numerical methods for approximating the solution of integral, and integrodifferential equations are known (see, e.g., [5–8]). For Fredholm-Volterra-Hammerstein integral equations, the classical method of successive approximations was introduced in [9]. An optimal control problem method was presented in [10], and a collocation-type method was developed in [11–13]. Computational methods based on Bernstein operational matrices and the Chebyshev approximation method were presented in [14, 15], respectively.

The use of fixed point techniques and Schauder bases, in the field of numerical resolution of differential, integral and integro-differential equations, allows for the development of new methods providing significant improvements upon other known methods (see [16–23]).

In this work we make an analysis of the error committed upon having obtained the approximate solution of the nonlinear Fredholm-Volterra-Hammerstein integral equation, using the theorem of Banach fixed point and Schauder bases (see [21], for a detailed description of the numerical method used in a more general equation).

In order to recall the aforementioned numerical method, let $C([\alpha,\alpha+\beta])$ and $C([\alpha,\alpha+\beta]^2)$ be the Banach spaces of all continuous and real-valued functions on $[\alpha,\alpha+\beta]$ and $[\alpha,\alpha+\beta]^2$ endowed with their usual supnorms. Throughout this paper we will make the following assumptions on k_i and g_i for $i\in\{1,2\}$.

(i) Since $k_i\in C([\alpha,\alpha+\beta]^2)$, there exists $M_{k_i}\geq 0$ such that $|k_i(t,s)|\leq M_{k_i}$ for all $(t,s)\in[\alpha,\alpha+\beta]^2$.

(ii) $g_i:[\alpha,\alpha+\beta]\times\mathbb{R}\to\mathbb{R}$ are functions such that there exists $L_{g_i}>0$ such that $|g_i(s,y)-g_i(s,z)|\leq L_{g_i}|y-z|$ for $s\in[\alpha,\alpha+\beta]$ and for all $y,z\in\mathbb{R}$.

(iii) $\beta\sum_{i=1}^{2}M_{k_i}L_{g_i}<1$.

We organize this paper as follows. In Section 2, we reformulate (1.1) in terms of a convenient integral operator T and we describe the numerical method used. The study of the error is described in Section 3. Finally, in Section 4 we show some illustrative examples.

2. Analytical Preliminaries

In this section we recall, in a summarized form, the concepts and results relative to the numerical method used for the study of the error that we carried out.

Let us start by observing that (1.1) is equivalent to the problem of finding fixed points of the operator $T:C([\alpha,\alpha+\beta])\to C([\alpha,\alpha+\beta])$ defined by

$$\begin{aligned}(Tx)(t) := y_0(t) &+ \int_{\alpha}^{\alpha+\beta} k_1(t,s)g_1(s,x(s))\,ds\\ &+ \int_{\alpha}^{t} k_2(t,s)g_2(s,x(s))\,ds,\quad t\in[\alpha,\alpha+\beta],\ x\in C([\alpha,\alpha+\beta]).\end{aligned}\tag{2.1}$$

A direct calculation over T leads to

$$\|Ty_1-Ty_2\|\leq M\|y_1-y_2\|\tag{2.2}$$

for all $y_1,y_2\in C([\alpha,\alpha+\beta])$, where we denote $M:=\beta\sum_{i=1}^{2}M_{k_i}L_{g_i}$. As the operator T defined in (2.1) satisfies (2.2), under condition (iii) and from the Banach fixed-point theorem, it follows that there exists a unique fixed point $x \in C([\alpha, \alpha+\beta])$ for T that is the unique solution of (1.1). In addition, for each $\tilde{x} \in C([\alpha, \alpha+\beta])$, we have

$$\|T^m \tilde{x} - x\| \leq \frac{M^m}{1-M} \|T\tilde{x} - \tilde{x}\| \tag{2.3}$$

and in particular $x = \lim_m T^m \tilde{x}$.

But it is not possible, in an explicit way, to calculate the sequence of iterations $\{T^m\}_{m\geq 1}$, to obtain the unique sequence x of (1.1), for which reason a numerical method is needed in order to approximate the fixed point of T.

Now we recall the concrete Schauder bases in the spaces $C([\alpha, \alpha+\beta])$ and $C([\alpha, \alpha+\beta]^2)$. Let $\{t_n\}_{n\geq 1}$ be a dense sequence of distinct points in $[\alpha, \alpha+\beta]$ such that $t_1 = \alpha$ and $t_2 = \alpha+\beta$. We set $b_1(t) := 1$ for $t \in [\alpha, \alpha+\beta]$, and for $n \geq 1$, and we let b_n be a piecewise linear continuous function on $[\alpha, \alpha+\beta]$ with nodes at $\{t_j : 1 \leq j \leq n\}$, uniquely determined by the relations $b_n(t_n) = 1$ and $b_n(t_k) = 0$ for $k < n$. We denote by $\{P_n\}_{n\geq 1}$ the sequence of associated projections and $\{b_n^*\}_{n\geq 1}$ the coordinate functionals. It is easy to check that $\{b_n\}_{n\geq 1}$ is a Schauder basis in $C([\alpha, \alpha+\beta])$ (see [24]).

From the Schauder basis $\{b_n\}_{n\geq 1}$ in $C([\alpha, \alpha+\beta])$, we can build another Schauder basis $\{B_n\}_{n\geq 1}$ of $C([\alpha, \alpha+\beta]^2)$ (see [25, 26]). It is sufficient to consider $B_n(t,s) := b_i(t)b_j(s)$ for all $t, s \in [\alpha, \alpha+\beta]$, with $\tau(n) = (i,j)$, where for a real number p, $[p]$ will denote its integer part and $\tau = (\tau_1, \tau_2) : \mathbb{N} \to \mathbb{N}\times\mathbb{N}$ is the bijective mapping defined by

$$\tau(n) := \begin{cases} \left(\sqrt{n}, \sqrt{n}\right), & \text{if } \left[\sqrt{n}\right] = \sqrt{n}, \\ \left(n - \left[\sqrt{n}\right]^2, \left[\sqrt{n}\right]+1\right), & \text{if } 0 < n - \left[\sqrt{n}\right]^2 \leq \left[\sqrt{n}\right], \\ \left(\left[\sqrt{n}\right]+1, n - \left[\sqrt{n}\right]^2 - \left[\sqrt{n}\right]\right), & \text{if } \left[\sqrt{n}\right] < n - \left[\sqrt{n}\right]^2. \end{cases} \tag{2.4}$$

We denote by $\{Q_n\}_{n\geq 1}$ the sequence of associated projections and by $\{B_n^*\}_{n\geq 1}$ the coordinate functionals. The Schauder basis $\{B_n\}_{n\geq 1}$ of $C([\alpha, \alpha+\beta]^2)$ has similar properties to the ones for the one-dimensional case. See Table 1 and note under some weak conditions (see the last row, which is derived easily from the third row of Table 1, resp., and the Mean-Value theorems for one and two variables) we can estimate the rate of the convergence of the sequence of projections in the one and two-dimensional cases, where we consider the dense subset $\{t_i\}_{i\geq 1}$ of distinct points in $[\alpha, \alpha+\beta]$, T_n as the set $\{t_1, \ldots, t_n\}$ ordered in an increasing way for $n \geq 2$, and ΔT_n denotes the maximum distance between two consecutive points of T_n.

Let us consider the continuous integral operator $T : C([\alpha, \alpha+\beta]) \to C([\alpha, \alpha+\beta])$ defined in (2.1). Let $\tilde{x} \in C([\alpha, \alpha+\beta])$, and the functions $\phi_1, \phi_2 \in C([\alpha, \alpha+\beta]^2)$, defined for $\phi_1(t,s) = k_1(t,s)g_1(s, \tilde{x}(s))$, $\phi_2(t,s) = k_2(t,s)g_2(s, \tilde{x}(s))$. Let $\{\lambda_n\}_{n\geq 1}$ and $\{\mu_n\}_{n\geq 1}$ be the sequences of scalars satisfying $\phi_1 = \sum_{n\geq 1} \lambda_n B_n$, $\phi_2 = \sum_{n\geq 1} \mu_n B_n$. Then for all $t \in [\alpha, \alpha+\beta]$, we have that

$$(T\tilde{x})(t) = y_0(t) + \sum_{n\geq 1} \lambda_n \int_\alpha^{\alpha+\beta} B_n(t,s)\,ds + \sum_{n\geq 1} \mu_n \int_\alpha^t B_n(t,s)\,ds. \tag{2.5}$$

The equality (2.5) enables us to determine, in an elemental way, the image of any continuous function under the operator T. However, it does not seem to be a usable expression due to the two infinite sums appearing in it. For this reason, the aforementioned sums are truncated.

3. Study of the Error

In this section we realize a new study of the error, obtaining one bound of it. Supposing conditions of regularity in the functions data, we improve and complete the study realized in [21].

Let $\tilde{x} \in C([\alpha, \alpha+\beta])$ and consider

$$x_0(t) := \tilde{x}(t) \in C([\alpha, \alpha+\beta]), \tag{3.1}$$

and for $m \in \mathbb{N}$, define inductively for $r \in \{1, \dots, m\}$ the following functions:

$$\sigma_{r-1}(t,s) := k_1(t,s) g_1(s, x_{r-1}(s)), \tag{3.2}$$

$$\varphi_{r-1}(t,s) := k_2(t,s) g_2(s, x_{r-1}(s)), \tag{3.3}$$

$$x_r(t) := y_0(t) + \int_\alpha^{\alpha+\beta} Q_{n_r^2}(\sigma_{r-1}(t,s))\,ds + \int_\alpha^{t} Q_{n_r^2}(\varphi_{r-1}(t,s))\,ds, \tag{3.4}$$

where $t, s \in [\alpha, \alpha+\beta]$ and $n_r \in \mathbb{N}$.

Proposition 3.1. *The sequence $\{x_r\}_{r\geq 1}$ is uniformly bounded.*

Proof. Let $R = \max\{|g_1(s,0)| : s \in [\alpha, \alpha+\beta]\}$, $S = \max\{|g_2(s,0)| : s \in [\alpha, \alpha+\beta]\}$, and we have for all $r \geq 1$ and $(t,s) \in [\alpha, \alpha+\beta]^2$

$$\begin{aligned}
|\sigma_{r-1}(t,s)| &= |k_1(t,s)|\left|g_1(s, x_{r-1}(s))\right| \\
&\leq M_{k_1}\left(\left|g_1(s, x_{r-1}(s)) - g_1(s,0)\right| + \left|g_1(s,0)\right|\right) \\
&\leq M_{k_1}\left(L_{g_1}|x_{r-1}(s)| + R\right), \\
\left|\varphi_{r-1}(t,s)\right| &= |k_2(t,s)|\left|g_2(s, x_{r-1}(s))\right| \\
&\leq M_{k_2}\left(\left|g_2(s, x_{r-1}(s)) - g_2(s,0)\right| + \left|g_2(s,0)\right|\right) \\
&\leq M_{k_2}\left(L_{g_2}|x_{r-1}(s)| + S\right).
\end{aligned} \tag{3.5}$$

For the monotonicity of the Schauder basis, we have

$$\begin{aligned}|x_r(t)| &\leq |y_0(t)| + \int_\alpha^{\alpha+\beta} \left|Q_{n_r^2}(\sigma_{r-1}(t,s))\right| ds + \int_\alpha^t \left|Q_{n_r^2}(\psi_{r-1}(t,s))\right| ds \\ &\leq |y_0(t)| + \int_\alpha^{\alpha+\beta} \|\sigma_{r-1}\| ds + \int_\alpha^t \|\psi_{r-1}\| ds \\ &\leq |y_0(t)| + \beta(M_{k_1}R + M_{k_2}S) + M_{k_1}L_{g_1}\int_\alpha^{\alpha+\beta} \|x_{r-1}\| ds + M_{k_2}L_{g_2}\int_\alpha^t \|x_{r-1}\| ds.\end{aligned} \tag{3.6}$$

Therefore,

$$\|x_r\| \leq \|y_0\| + \beta(M_{k_1}R + M_{k_2}S) + M\|x_{r-1}\|. \tag{3.7}$$

Applying recursively this process we get

$$\begin{aligned}\|x_r\| &\leq (\|y_0\| + \beta(M_{k_1}R + M_{k_2}S))\left(1 + M + \cdots + M^{r-1}\right) + M^r\|x_0\| \\ &\leq (\|y_0\| + \beta(M_{k_1}R + M_{k_2}S))\frac{1-M^r}{1-M} + M^r\|x_0\|\end{aligned} \tag{3.8}$$

for all $r \geq 1$. Then $\{x_r\}_{r\geq 1}$ is uniformly bounded. □

Remark 3.2. For $i \in \{1,2\}$, the sequence $\{g_i(\cdot, x_r(\cdot)\}_{r\geq 1}$ is uniformly bounded, as it follows Proposition 3.1 and the fact that g_i for $i \in \{1,2\}$ is Lipschitz in its second variable.

Proposition 3.3. *Let $y_0 \in C^1([\alpha, \alpha+\beta])$, and for $i \in \{1,2\}$, $k_i \in C^1([\alpha,\alpha+\beta]^2)$, $g_i \in C^1([\alpha,\alpha+\beta] \times \mathbb{R})$ such that $\partial g_i/\partial s$ and $\partial g_i/\partial x$ satisfy a global Lipschitz condition in the last variable. Let $x_0(t) := \tilde{x}(t) \in C^1([\alpha,\alpha+\beta])$, and define inductively as in* (3.2), (3.3), *and* (3.4) *the functions σ_{r-1}, ψ_{r-1} and x_r, respectively. Then*

$$\left\{\frac{\partial \sigma_{r-1}}{\partial t}\right\}_{r\geq 1}, \quad \left\{\frac{\partial \sigma_{r-1}}{\partial s}\right\}_{r\geq 1}, \quad \left\{\frac{\partial \psi_{r-1}}{\partial t}\right\}_{r\geq 1}, \quad \left\{\frac{\partial \psi_{r-1}}{\partial s}\right\}_{r\geq 1} \tag{3.9}$$

are uniformly bounded.

Proof. From (3.2) and (3.3), we have, respectively, that for all $r \geq 1$, $(\partial\sigma_{r-1}/\partial t)(t,s) = (\partial k_1/\partial t)(t,s)g_1(s,x_{r-1}(s))$, $(\partial\psi_{r-1}/\partial t)(t,s) = (\partial k_2/\partial t)(t,s)g_2(s,x_{r-1}(s))$, and therefore by the conditions over k_1, k_2, and Remark 3.2, $\{\partial\sigma_{r-1}/\partial t\}_{r\geq 1}$, $\{\partial\psi_{r-1}/\partial t\}_{r\geq 1}$ are uniformly bounded.

Observe that

$$\begin{aligned}\left|x_r'(t)\right| \leq \left|y_0'(t)\right| &+ \int_\alpha^{\alpha+\beta} \left|\frac{\partial}{\partial t} Q_{n_r^2}(\sigma_{r-1}(t,s))\right| ds \\ &+ \left|Q_{n_r^2}(\psi_{r-1}(t,t))\right| + \int_\alpha^t \left|\frac{\partial}{\partial t} Q_{n_r^2}(\psi_{r-1}(t,s))\right| ds.\end{aligned} \tag{3.10}$$

In view of the monotonicity of the Schauder basis, we have

$$\left\|x_r'\right\| \le \left\|y_0'\right\| + \left\|\varphi_{r-1}\right\| + \beta\left(\left\|\frac{\partial\sigma_{r-1}}{\partial t}\right\| + \left\|\frac{\partial\varphi_{r-1}}{\partial t}\right\|\right), \tag{3.11}$$

and hence the sequence $\{x_r'\}_{r\ge1}$ is uniformly bounded.

On the other hand from (3.2) and (3.3), respectively, we have

$$\begin{aligned}\frac{\partial\sigma_{r-1}}{\partial s}(t,s) &= \frac{\partial k_1}{\partial s}(t,s)g_1(s,x_{r-1}(s)) \\ &\quad + k_1(t,s)\left(\frac{\partial g_1}{\partial s}(s,x_{r-1}(s)) + \frac{\partial g_1}{\partial x}(s,x_{r-1}(s))x_{r-1}'(s)\right), \\ \frac{\partial\varphi_{r-1}}{\partial s}(t,s) &= \frac{\partial k_2}{\partial s}(t,s)g_2(s,x_{r-1}(s)) \\ &\quad + k_2(t,s)\left(\frac{\partial g_2}{\partial s}(s,x_{r-1}(s)) + \frac{\partial g_2}{\partial x}(s,x_{r-1}(s))x_{r-1}'(s)\right).\end{aligned} \tag{3.12}$$

For $i \in \{1,2\}$, let $U = \max\{|(\partial g_i/\partial s)(s,0)| : s \in [\alpha,\alpha+\beta]\}$, and we have for all $r \ge 1$ and $s \in [\alpha,\alpha+\beta]$

$$\left|\frac{\partial g_i}{\partial s}(s,x_{r-1}(s))\right| \le \left|\frac{\partial g_i}{\partial s}(s,x_{r-1}(s)) - \frac{\partial g_i}{\partial s}(s,0)\right| + \left|\frac{\partial g_i}{\partial s}(s,0)\right| \le l_{g_i}|x_{r-1}(s)| + U \tag{3.13}$$

with l_{g_i} as the Lipschitz constant of $\partial g_i/\partial s$ in the last variable.

By repeating the previous argument, we have

$$\left|\frac{\partial g_i}{\partial x}(s,x_{r-1}(s))\right| \le q_{g_i}|x_{r-1}(s)| + V, \tag{3.14}$$

where $V = \max\{|(\partial g_i/\partial x)(s,0)| : s \in [\alpha,\alpha+\beta]\}$, and q_{g_i} is the Lipschitz constant of $\partial g_i/\partial x$ in the last variable.

Therefore by the conditions over k_1, k_2, Proposition 3.1, Remark 3.2, and (3.11),

$$\left\{\frac{\partial\sigma_{r-1}}{\partial s}\right\}_{r\ge1}, \qquad \left\{\frac{\partial\varphi_{r-1}}{\partial s}\right\}_{r\ge1} \tag{3.15}$$

are uniformly bounded. □

Proposition 3.4. *With the previous notation and the same hypothesis as in Proposition 3.3, there is $\rho_1,\rho_2 > 0$ such that for all $r \ge 1$ and $n_r \ge 2$, we have*

$$\begin{aligned}\left\|\sigma_{r-1} - Q_{n_r^2}(\sigma_{r-1})\right\| &\le \rho_1\Delta T_{n_r}, \\ \left\|\varphi_{r-1} - Q_{n_r^2}(\varphi_{r-1})\right\| &\le \rho_2\Delta T_{n_r}.\end{aligned} \tag{3.16}$$

Table 1: Properties of the univariate and bivariate Schauder bases.

$b_1(t) = 1$ $n \geq 2 \Rightarrow b_n(t_k) = \begin{cases} 1, & \text{if } k = n \\ 0, & \text{if } k < n \end{cases}$	$B_1(t,s) = 1$ $n \geq 2 \Rightarrow B_n(t_i,t_j) = \begin{cases} 1, & \text{if } \tau(n) = (i,j) \\ 0, & \text{if } \tau^{-1}(i,j) < n \end{cases}$
$y \in C([\alpha, \alpha+\beta])$ $\Downarrow$ $b_1^*(y) = y(t_1)$ $n \geq 2 \Rightarrow b_n^*(y) = y(t_n) - \sum_{k=1}^{n-1} b_k^*(y) b_k(t_n)$	$z \in C([\alpha, \alpha+\beta]^2)$ $\Downarrow$ $B_1^*(z) = z(t_1,t_1)$ $\left.\begin{array}{c} n \geq 2 \\ \tau(n) = (i,j) \end{array}\right\} \Rightarrow B_n^*(z) = z(t_i,t_j) - \sum_{k=1}^{n-1} B_k^*(z) B_k(t_i,t_j)$
$y \in C([\alpha, \alpha+\beta])$ $\Downarrow$ $k \leq n \Rightarrow P_n(y)(t_k) = y(t_k)$	$z \in C([\alpha, \alpha+\beta]^2)$ $\Downarrow$ $\tau^{-1}(i,j) \leq n \Rightarrow Q_n(z)(t_i,t_j) = z(t_i,t_j)$
$\{b_n\}_{n\geq 1}$ is monotone, that is, $\sup_{n\geq 1}\|P_n\| = 1$	$\{B_n\}_{n\geq 1}$ is monotone, that is, $\sup_{n\geq 1}\|Q_n\| = 1$
$y \in C^1([\alpha, \alpha+\beta]), n \geq 2$ $\Downarrow$ $\|y - P_n(y)\| \leq 2\|y'\|\Delta T_n$	$z \in C^1([\alpha, \alpha+\beta]^2), n \geq 2$ $\Downarrow$ $\|z - Q_{n^2}(z)\| \leq 4 \max\left\{ \left\| \frac{\partial z}{\partial t} \right\|, \left\| \frac{\partial z}{\partial s} \right\| \right\} \Delta T_n$

Proof. In the last property in Table 1, take $\rho_1 = 4\max\{\|\partial\sigma_{r-1}/\partial t\|, \|\partial\sigma_{r-1}/\partial s\|\}_{r\geq 1}$ and $\rho_2 = 4\max\{\|\partial\varphi_{r-1}/\partial t\|, \|\partial\varphi_{r-1}/\partial s\|\}_{r\geq 1}$. $\square$

In the result below we show that the sequence defined in (3.4) approximates the exact solution of (1.1) as well as giving an upper bound of the error committed.

Theorem 3.5. *With the previous notation and the same hypothesis as in Proposition 3.3, let $m \in \mathbb{N}$, $n_r \in \mathbb{N}$, $n_r \geq 2$, and $\{\varepsilon_1, \ldots, \varepsilon_m\}$ be a set of positive numbers such that for all $r \in \{1, \ldots, m\}$ we have*

$$\Delta T_{n_r} \leq \frac{\varepsilon_r}{\beta(\rho_1 + \rho_2)}. \tag{3.17}$$

Then,

$$\|T x_{r-1} - x_r\| \leq \varepsilon_r. \tag{3.18}$$

Moreover, if x is the exact solution of the integral equation (1.1)*, then the error $\|x - x_m\|$ is given by*

$$\|x - x_m\| \leq \frac{M^m}{1-M}\|T\tilde{x} - \tilde{x}\| + \sum_{r=1}^{m} M^{m-r}\varepsilon_r. \tag{3.19}$$

Proof. First we deal with proving (3.18). For all $r \in \{1, \ldots, m\}$ and $t \in [\alpha, \alpha+\beta]$, Proposition 3.4 gives

$$\begin{aligned} |Tx_{r-1}(t) - x_r(t)| &\leq \int_{\alpha}^{\alpha+\beta} \left|\sigma_{r-1}(t,s) - Q_{n_r^2}(\sigma_{r-1}(t,s))\right| ds \\ &\quad + \int_{\alpha}^{t} \left|\varphi_{r-1}(t,s) - Q_{n_r^2}(\varphi_{r-1}(t,s))\right| ds \\ &\leq \rho_1 \Delta T_{n_r} \beta + \rho_2 \Delta T_{n_r} \beta = \Delta T_{n_r} \beta(\rho_1 + \rho_2) \leq \varepsilon_r. \end{aligned} \tag{3.20}$$

To conclude the proof, we derive (3.19). From (2.3), we have

$$\|x - T^m \tilde{x}\| \leq \frac{M^m}{1-M} \|T\tilde{x} - \tilde{x}\|, \tag{3.21}$$

and in addition, on the other hand, applying recursively (2.2) and (3.18), we obtain

$$\begin{aligned} \|T^m \tilde{x} - x_m\| &\leq \sum_{r=1}^{m} \left\| T^{m-r+1} x_{r-1} - T^{m-r} x_r \right\| \\ &= \sum_{r=1}^{m} \left\| T^{m-r} T x_{r-1} - T^{m-r} x_r \right\| \\ &\leq \sum_{r=1}^{m} M^{m-r} \|T x_{r-1} - x_r\| \leq \sum_{r=1}^{m} M^{m-r} \varepsilon_r. \end{aligned} \tag{3.22}$$

Then we use the triangular inequality

$$\|x - x_m\| \leq \|x - T^m \tilde{x}\| + \|T^m \tilde{x} - x_m\|, \tag{3.23}$$

and the proof is complete in view of (3.21) and (3.22). □

Remark 3.6. Under the hypotheses of Theorem 3.5, let us observe that by the inequality (3.19) we have

$$\|x - x_m\| \leq \frac{M^m}{1-M} \|T\tilde{x} - \tilde{x}\| + \frac{1-M^m}{1-M} \max_{r \geq 1}\{\varepsilon_r\}. \tag{3.24}$$

The first sumand on the right hand side approximates zero when m increases; with respect to the second sumand, since the points of the partition can be chosen in such a way that ΔT_{n_r} becomes so close to zero as we desire, the $\varepsilon_r' s$ can become so small as we desire, arriving in this way at an explicit control of the error committed.

Therefore, given $\varepsilon > 0$, there exists $m \geq 1$ such that $\|x - x_m\| < \varepsilon$ when choosing ε_r sufficiently small.

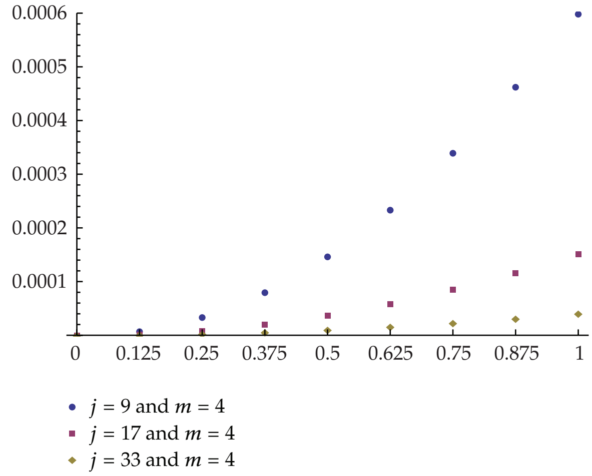

Figure 1: The plot of absolute errors for Example 4.1.

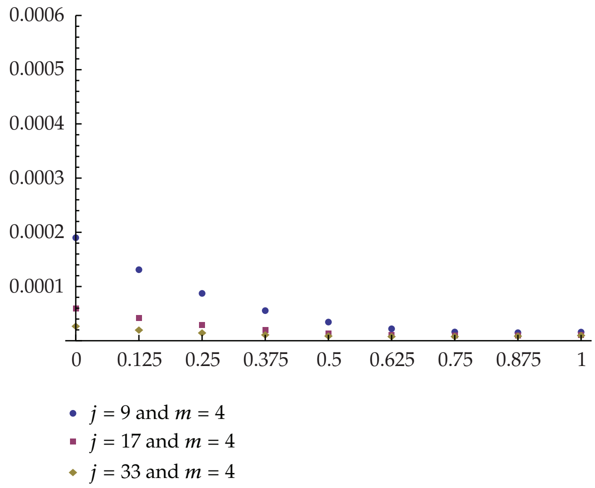

Figure 2: The plot of absolute errors for Example 4.2.

4. Numerical Examples

In this last section we illustrate the results previously developed, stressing the significance of inequality (3.19) in Theorem 3.5, as mentioned in Remark 3.6.

First of all, we show how the numerical method works, because we use it later in the estimation of the error. For solving the numerical example, Mathematica 7 is used, and to construct the Schauder basis in $C([0,1]^2)$, we considered the particular choice $t_1 = 0$, $t_2 = 1$ and for $n \in \mathbb{N} \cup \{0\}$, $t_{i+1} = (2k+1)/2^{n+1}$ if $i = 2^n + k + 1$ where $0 \le k < 2^n$ are integers. To define the sequence $\{x_r\}_{r\ge1}$, we take $x_0(t) = y_0(t)$ and $n_r = j$ (for all $r \ge 1$). In Tables 2 and 3, we exhibit, for $j = 9$, 17, and 33, the absolute errors committed in eight representative points of $[0,1]$ when we approximate the exact solution x by the iteration x_4. Its numerical results are also given in Figures 1 and 2, respectively.

Table 2: Absolute errors for Example 4.1.

t	$j = 9$ $\lvert x_4(t) - x(t)\rvert$	$j = 17$ $\lvert x_4(t) - x(t)\rvert$	$j = 33$ $\lvert x_4(t) - x(t)\rvert$
0.0	0.0	0.0	0.0
0.125	7.64×10^{-6}	2.13×10^{-6}	7.49×10^{-7}
0.250	3.40×10^{-5}	8.93×10^{-6}	2.65×10^{-6}
0.375	8.03×10^{-5}	2.07×10^{-5}	5.79×10^{-6}
0.5	1.47×10^{-4}	3.75×10^{-5}	1.02×10^{-5}
0.625	2.34×10^{-4}	5.95×10^{-5}	1.59×10^{-5}
0.750	3.40×10^{-4}	8.63×10^{-5}	2.29×10^{-5}
0.875	4.63×10^{-4}	1.17×10^{-4}	3.10×10^{-5}
1	5.99×10^{-4}	1.52×10^{-4}	4.04×10^{-5}

Table 3: Absolute errors for Example 4.2.

t	$j = 9$ $\lvert x_4(t) - x(t)\rvert$	$j = 17$ $\lvert x_4(t) - x(t)\rvert$	$j = 33$ $\lvert x_4(t) - x(t)\rvert$
0.	1.91×10^{-4}	6.05×10^{-5}	2.78×10^{-5}
0.125	1.32×10^{-4}	4.31×10^{-5}	2.08×10^{-5}
0.250	8.83×10^{-5}	3.00×10^{-5}	1.55×10^{-5}
0.375	5.65×10^{-5}	2.08×10^{-5}	1.19×10^{-5}
0.5	3.54×10^{-5}	1.48×10^{-5}	9.77×10^{-6}
0.625	2.30×10^{-5}	1.16×10^{-5}	8.82×10^{-6}
0.750	1.71×10^{-5}	1.05×10^{-5}	8.86×10^{-6}
0.875	1.58×10^{-5}	1.08×10^{-5}	9.64×10^{-6}
1	1.69×10^{-5}	1.20×10^{-5}	1.08×10^{-5}

Example 4.1. We solve (1.1) with $k_1(t,s) = ts/5$, $g_1(s,x(s)) = \cos(x(s))$, $k_2(t,s) = s/3$, $g_2(s,x(s)) = \sin(x(s))$, and $y_0(t) = 1 + t - (t/5)(\cos(2) - \cos(1) + \sin(2)) + (1/3)(t\cos(1 + t) - \sin(1+t) + \sin(1))$ with the exact solution $x(t) = 1 + t$.

Example 4.2. We solve (1.1) with $k_1(t,s) = (1/4)(1-t)^3$, $g_1(s,x(s)) = \arctan(x(s))$, $k_2(t,s) = 1/8$, $g_2(s,x(s)) = x(s)$, and $y_0(t) = t - (t^2/16) - ((\pi - \ln(4))/16)(t-1)^3$ with the exact solution $x(t) = t$.

Now we realize that the choice of a particular j, determining the dyadic partition of the interval $[0,1]$ from the first $2^j + 1$ nodes, and in such a way that the error is less than a fixed positive ε, that is, $\|x - x_m\| < \varepsilon$, can be easily determined practically: it suffices to compute, once again by means of Mathematica 7, the error. To this end, since it is measured in terms of the supnorm, we consider the nodes 0, 0.125, 0.25, 0.375, 0.5, 0.625, 0.75, 0.875, 1 and maximum of the absolute values of the differences between the values of the exact solution and the approximation obtained for the third iteration ($m = 3$). The numerical tests are given in Table 4 and correspond to the nonlinear mixed Fredhol-Volterra-Hammerstein equations considered in Examples 4.1 and 4.2, respectively.

Table 4: Number of nodes (j) from error (ε) and for $m = 3$.

ε	Example 4.1	Example 4.2
10^{-2}	$j = 5$	$j = 5$
10^{-3}	$j = 9$	$j = 9$
10^{-4}	$j = 33$	$j = 33$

Acknowledgment

This paper is partially supported by Junta de Andaluca Grant FQM359.

References

[1] M. A. Abdou, "On a symptotic methods for Fredholm-Volterra integral equation of the second kind in contact problems," *Journal of Computational and Applied Mathematics*, vol. 154, no. 2, pp. 431–446, 2003.
[2] S. Jiang and V. Rokhlin, "Second kind integral equations for the classical potential theory on open surfaces. II," *Journal of Computational Physics*, vol. 195, no. 1, pp. 1–16, 2004.
[3] K. V. Kotetishvili, G. V. Kekelia, G. S. Kevanishvili, I. G. Kevanishvili, and B. G. Midodashvili, "Development and solution of the integral equation for axial current of a center-driven dipole," *Journal of Applied Electromagnetism*, vol. 12, no. 3, pp. 1–14, 2010.
[4] X. Zhang, J. Luo, and Z. Zhao, "The iterative solution for electromagnetic field coupling to buried wires," *Mathematical Problems in Engineering*, vol. 2011, Article ID 165032, 8 pages, 2011.
[5] P. Baratella, "A Nyström interpolant for some weakly singular nonlinear Volterra integral equations," *Journal of Computational and Applied Mathematics*, vol. 237, no. 1, pp. 542–555, 2013.
[6] M. B. Dhakne and G. B. Lamb, "On an abstract nonlinear second order integrodifferential equation," *Journal of Function Spaces and Applications*, vol. 5, no. 2, pp. 167–174, 2007.
[7] M. Hadizadeh and M. Mohamadsohi, "Numerical solvability of a class of Volterra-Hammerstein integral equations with noncompact kernels," *Journal of Applied Mathematics*, no. 2, pp. 171–181, 2005.
[8] J. Zhu, Y. Yu, and V. Postolică, "Initial value problems for first order impulsive integro-differential equations of Volterra type in Banach spaces," *Journal of Function Spaces and Applications*, vol. 5, no. 1, pp. 9–26, 2007.
[9] F. G. Tricomi, *Integral Equations*, Dover, New York, NY, USA, 1985.
[10] M. A. El-Ameen and M. El-Kady, "A new direct method for solving nonlinear Volterra-Fredholm-Hammerstein integral equations via optimal control problem," *Journal of Applied Mathematics*, vol. 2012, Article ID 714973, 10 pages, 2012.
[11] H. R. Marzban, H. R. Tabrizidooz, and M. Razzaghi, "A composite collocation method for the nonlinear mixed Volterra-Fredholm-Hammerstein integral equations," *Communications in Nonlinear Science and Numerical Simulation*, vol. 16, no. 3, pp. 1186–1194, 2011.
[12] Y. Ordokhani and M. Razzaghi, "Solution of nonlinear Volterra-Fredholm-Hammerstein integral equations via a collocation method and rationalized Haar functions," *Applied Mathematics Letters*, vol. 21, no. 1, pp. 4–9, 2008.
[13] K. Parand and J. A. Rad, "Numerical solution of nonlinear Volterra-Fredholm-Hammerstein integral equations via collocation method based on radial basis functions," *Applied Mathematics and Computation*, vol. 218, no. 9, pp. 5292–5309, 2012.
[14] K. Maleknejad, E. Hashemizadeh, and B. Basirat, "Computational method based on Bernstein operational matrices for nonlinear Volterra-Fredholm-Hammerstein integral equations," *Communications in Nonlinear Science and Numerical Simulation*, vol. 17, no. 1, pp. 52–61, 2012.
[15] E. Babolian, F. Fattahzadeh, and E. G. Raboky, "A Chebyshev approximation for solving nonlinear integral equations of Hammerstein type," *Applied Mathematics and Computation*, vol. 189, no. 1, pp. 641–646, 2007.
[16] M. I. Berenguer, A. I. Garralda-Guillem, and M. R. Galán, "Biorthogonal systems approximating the solution of the nonlinear Volterra integro-differential equation," *Fixed Point Theory and Applications*, vol. 2010, Article ID 470149, 9 pages, 2010.
[17] M. I. Berenguer, D. Gámez, A. I. Garralda-Guillem, and M. C. S. Pérez, "Nonlinear Volterra integral equation of the second kind and biorthogonal systems," *Abstract and Applied Analysis*, vol. 2010, Article ID 135216, 11 pages, 2010.

[18] M. I. Berenguer, D. Gámez, A. I. Garralda-Guillem, M. R. Galán, and M. C. S. Pérez, "Biorthogonal systems for solving Volterra integral equation systems of the second kind," *Journal of Computational and Applied Mathematics*, vol. 235, no. 7, pp. 1875–1883, 2011.

[19] M. I. Berenguer, D. Gámez, and A. J. López Linares, "Fixed-point iterative algorithm for the linear Fredholm-Volterra integro-differential equation," *Journal of Applied Mathematics*, vol. 2010, Article ID 370894, 12 pages, 2012.

[20] M. I. Berenguer, D. Gámez, and A. J. López Linares, "Fixed point techniques and Schauder bases to approximate the solution of the first order nonlinear mixed Fredholm-Volterra integro-differential equation," *Journal of Computational and Applied Mathematics*, 2012. In press.

[21] F. Caliò, A.I. Garralda-Guillem, E. Marchetti, and M. Ruiz Galán, "About some numerical approaches for mixed integral equations," *Applied Mathematics and Computation*, vol. 219, no. 2, pp. 464–474, 2012.

[22] D. Gámez, A. I. G. Guillem, and M. R. Galán, "High-order nonlinear initial-value problems countably determined," *Journal of Computational and Applied Mathematics*, vol. 228, no. 1, pp. 77–82, 2009.

[23] D. Gámez, A. I. G. Guillem, and M. R. Galán, "Nonlinear initial-value problems and Schauder bases," *Nonlinear Analysis: Theory, Methods & Applications*, vol. 63, no. 1, pp. 97–105, 2005.

[24] G. J. O. Jameson, *Topology and Normed Spaces*, Chapman & Hall, London, UK, 1974.

[25] B. R. Gelbaum and J. G. de Lamadrid, "Bases of tensor products of Banach spaces," *Pacific Journal of Mathematics*, vol. 11, pp. 1281–1286, 1961.

[26] Z. Semadeni, "Product Schauder bases and approximation with nodes in spaces of continuous functions," *Bulletin de l'Académie Polonaise des Sciences*, vol. 11, pp. 387–391, 1963.

Hindawi Publishing Corporation
Journal of Function Spaces and Applications
Volume 2012, Article ID 984682, 23 pages
doi:10.1155/2012/984682

Research Article

Explicit Solution of Telegraph Equation Based on Reproducing Kernel Method

Mustafa Inc,[1] Ali Akgül,[2] and Adem Kiliçman[3]

[1] *Department of Mathematics, Science Faculty, Firat University, 23119 Elazig, Turkey*
[2] *Department of Mathematics, Education Faculty, Dicle University, 21280 Diyarbakir, Turkey*
[3] *Department of Mathematics and Institute for Mathematical Research, University Putra Malaysia, 43400 Serdang, Selangor, Malaysia*

Correspondence should be addressed to Adem Kiliçman, akilicman@putra.upm.edu.my

Received 5 August 2012; Revised 21 November 2012; Accepted 21 November 2012

Academic Editor: Gabriel N. Gatica

We propose a reproducing kernel method for solving the telegraph equation with initial conditions based on the reproducing kernel theory. The exact solution is represented in the form of series, and some numerical examples have been studied in order to demonstrate the validity and applicability of the technique. The method shows that the implement seems easy and produces accurate results.

1. Introduction

In this paper, we consider the telegraph equation of the following form:

$$\frac{\partial^2 u}{\partial t^2} + (\alpha + \beta)\frac{\partial u}{\partial t} + \alpha\beta u = c^2 \frac{\partial^2 u}{\partial x^2} + f(x,t), \tag{1.1}$$

over a region $\Omega = \{(x,t) : 0 < x < 1 \;\text{ and }\; 0 < t < T\}$ and α, β are known constant coefficients with initial conditions as

$$u(x,0) = \phi(x), \qquad \frac{\partial u(x,0)}{\partial t} = \psi(x), \tag{1.2}$$

where $u(x,t)$ can be voltage or current through the wire at position x and time t. In (1.1), we have

$$\alpha = \frac{G}{C}, \qquad \beta = \frac{R}{L}, \qquad c^2 = \frac{1}{LC}, \tag{1.3}$$

where G is conductance of resistor, R is resistance of resistor, L is inductance of capacitor, C is capacitance of capacitor, and $u(x,t)$ can be considered as a function depending on distance x and time t, and constants are depending on a given problem and f, ϕ, and ψ are known continuous functions.

The hyperbolic partial differential equations model the vibrations of structures (e.g., buildings, beams, and machines) and are the basis for fundamental equations of atomic physics. Equation (1.1), referred to as the second-order telegraph equation with constant coefficients, models a mixture between diffusion and wave propagation by introducing a term that accounts for effects of finite velocity to the standard heat or mass transport equation [1]. However, (1.1) is commonly used in signal analysis for transmission and propagation of electrical signals [2, 3].

In recent years, much attention has been given in the literature to the development, analysis, and implementation of stable methods for the numerical solution of second-order hyperbolic equations, see, for example, [4–11]. These methods are conditionally stable. In [12], Mohanty carried over a new technique to solve (1.1), which is unconditionally stable and is of second-order accuracy in both the time and space components. Mohebbi and Dehghan [13] presented a high-order accurate method for solving one-space-dimensional linear hyperbolic equations and proved the high-order accuracy due to the fourth-order discretization of spatial derivative and unconditional stability. A compact finite difference approximation was presented in [14] by using the fourth order discretizing spatial derivatives of the linear hyperbolic equation and collocation method for the time component. Another solution is approximated by suing a polynomial at each grid point such that its coefficients were determined by solving a linear system of equations [15]. By using collocation points and approximating the solution by using a thin plate splines radial basis function was presented in [16].

In [17], the author used the Chebyshev cardinal functions. Lakestani and Saray [18] used interpolating scaling function. Ding et al. [19] constructed a class of new difference scheme based on a new nonpolynomial spline method to solve (1.1) and (1.2). Lakoud and Belakroum [20] studied the existence and uniqueness of the solution with integral condition by using the Ro the time discretization method. Dehghan et al. [21] used to compute the solution for the linear, variable coefficient, fractional derivative, and multispace telegraph equations by using the variational iteration method. Further, Biazar et al. [22] obtained an approximate solution by using the variational iteration method. Recently, Yao and Lin [23] investigated a nonlinear hyperbolic telegraph equation with an integral condition by reproducing kernel space at $\alpha = \beta = 0$ in (1.1). In [24], Yousefi presented a numerical method by using Legendre multiwavelet Galerkin method.

In this paper, the RKHSM [25–47] will be used to investigate the telegraph equation (1.1). Several researches have been devoted to the application of RKHSM to a wide class of stochastic and deterministic problems involving fractional differential equation, nonlinear oscillator with discontinuity, singular nonlinear two-point periodic boundary value problems, integral equations, and nonlinear partial differential equations [27–41]. The method is well suited to physical problems.

The efficiency of the method was used by many authors to investigate several scientific applications. Geng and Cui [27] applied the RKHSM to handle the second-order boundary value problems. Yao and Cui [28] and Wang et al. [29] investigated a class of singular boundary value problems by this method and the obtained results were good. Zhou et al. [30] used the RKHSM effectively to solve second-order boundary value problems. In [31], the method was used to solve nonlinear infinite-delay-differential equations. Wang and Chao [32], Li and Cui [33], and Zhou and Cui [34] independently employed the RKHSM to variable-coefficient partial differential equations. Geng and Cui [35] and Du and Cui [36] investigated to the approximate solution of the forced Duffing equation with integral boundary conditions by combining the homotopy perturbation method and the RKHSM. Lv and Cui [37] presented a new algorithm to solve linear fifth-order boundary value problems. In [38, 39], authors developed a new existence proof of solutions for nonlinear boundary value problems. Cui and Du [40] obtained the representation of the exact solution for the nonlinear Volterra-Fredholm integral equations by using the reproducing kernel space. Wu and Li [41] applied iterative reproducing kernel method to obtain the analytical approximate solution of a nonlinear oscillator with discontinuities. Recently, the method was applied the fractional partial differential equations and the multipoint boundary value problems [42–45]. For more details about RKHSM and the modified forms and their effectiveness, see [25–47].

In the present work, we use the following equation:

$$v(x,t) = u(x,t) + h(x) + tg(x); \tag{1.4}$$

by transformation for homogeneous initial conditions of (1.1) and (1.2), we get as follows (1.5):

$$\begin{gathered}\frac{\partial^2 v}{\partial t^2} - c^2\frac{\partial^2 v}{\partial x^2} + (\alpha+\beta)\frac{\partial v}{\partial t} + \alpha\beta v = f(x,t) + M(x,t),\\ v(x,0) = 0, \qquad \frac{\partial v(x,0)}{\partial t} = 0,\end{gathered} \tag{1.5}$$

where

$$M(x,t) = (\alpha+\beta)g(x) + \alpha\beta h(x) + \alpha\beta t g(x) - c^2 h''(x) - c^2 t g''(x). \tag{1.6}$$

The paper is organized as follows. Section 2 is devoted to several reproducing kernel spaces and a linear operator is introduced. The solution representation in $W(\Omega)$ has been presented in Section 3. We prove that the approximate solution converges to the exact solution uniformly. Some numerical examples are illustrated in Section 4. We provide some conclusions in the last sections.

2. Preliminaries

Hilbert spaces can be completely classified: there is a unique Hilbert space up to isomorphism for every cardinality of the base. Since finite-dimensional Hilbert spaces are fully understood in linear algebra, and since morphisms of Hilbert spaces can always be divided into morphisms of spaces with Aleph-null ($\varkappa_0$) dimensionality, functional analysis of Hilbert spaces mostly deals with the unique Hilbert space of dimensionality Aleph-null and its morphisms. One of the open problems in functional analysis is to prove that every bounded linear operator on a Hilbert space has a proper invariant subspace. Many special cases of this invariant subspace problem have already been proven [48].

2.1. Reproducing Kernel Spaces

In this section, we define some useful reproducing kernel spaces.

Definition 2.1 (reproducing kernel). Let E be a nonempty set. A function $K : E \times E \longrightarrow \mathbb{C}$ is called a reproducing kernel of the Hilbert space H if and only if

(a) $K(\cdot, t) \in H$ for all $t \in E$,

(b) $\langle \varphi, K(\cdot, t)\rangle = \varphi(t)$ for all $t \in E$ and all $\varphi \in H$.

The last condition is called "the reproducing property" as the value of the function φ at the point t is reproduced by the inner product of φ with $K(\cdot, t)$.

Then we need some notation that we use in the development of the paper. In the next we define several spaces with inner product over those spaces. Thus the space defined as

$$W_2^3[0,1] = \left\{ v \mid v, v', v'' : [0,1] \longrightarrow \mathbb{R} \text{ are absolutely continuous}, v^{(3)} \in L^2[0,1] \right\} \tag{2.1}$$

is a Hilbert space. The inner product and the norm in $W_2^3[0,1]$ are defined by

$$\begin{gathered} \langle v, g\rangle_{W_2^3} = \sum_{i=0}^{2} v^{(i)}(0) g^{(i)}(0) + \int_0^1 v^{(3)}(x) g^{(3)}(x) dx, \quad v, g \in W_2^3[0,1], \\ \|v\|_{W_2^3} = \sqrt{\langle v, v\rangle_{W_2^3}}, \quad v \in W_2^3[0,1], \end{gathered} \tag{2.2}$$

respectively. Thus the space $W_2^3[0,1]$ is a reproducing kernel space, that is, for each fixed $y \in [0,1]$ and any $v \in W_2^3[0,1]$, there exists a function R_y such that

$$v(y) = \langle v(x), R_y(x)\rangle_{W_2^3}, \tag{2.3}$$

and similarly we define the space

$$T_2^3[\,[0,1] = \left\{ \begin{matrix} v \mid v, v', v'' : [0,1] \longrightarrow \mathbb{R} \ \text{ are absolutely continuous}, \\ v'' \in L^2[0,1], v(0) = 0, v'(0) = 0 \end{matrix} \right\}. \tag{2.4}$$

The inner product and the norm in $T_2^3[0,1]$ are defined by

$$\begin{gathered} \langle v, g\rangle_{T_2^3} = \sum_{i=0}^{2} v^{(i)}(0) g^{(i)}(0) + \int_0^1 v'''(t) g'''(t) dt, \quad v, g \in T_2^3[0,1], \\ \|v\|_{T_2^3} = \sqrt{\langle v, v\rangle_{T_2^3}}, \quad v \in T_2^3[0,1], \end{gathered} \tag{2.5}$$

respectively. The space $T_2^3[0,1]$ is a reproducing kernel Hilbert space and its reproducing kernel function r_s is given by [26] as

$$r_s = \begin{cases} \dfrac{1}{4}s^2t^2 + \dfrac{1}{12}s^2t^3 - \dfrac{1}{24}st^4 + \dfrac{1}{120}t^5, & t \le s, \\ \dfrac{1}{4}s^2t^2 + \dfrac{1}{12}s^3t^2 - \dfrac{1}{24}ts^4 + \dfrac{1}{120}s^5, & t > s, \end{cases} \tag{2.6}$$

and the space

$$G_2^1[0,1] = \left\{ v \mid v : [0,1] \longrightarrow \mathbb{R} \text{ is absolutely continuous}, v'(x) \in L^2[0,1] \right\}, \tag{2.7}$$

is a Hilbert space where the inner product and the norm in $G_2^1[0,1]$ are defined by

$$\begin{gathered} \langle v, g \rangle_{G_2^1} = v^{(i)}(0)g^{(i)}(0) + \int_0^1 v'(x)g'(x)dx, \quad v, g \in G_2^1[0,1], \\ \|v\|_{G_2^1} = \sqrt{\langle v, v \rangle_{G_2^1}}, \quad v \in G_2^1[0,1], \end{gathered} \tag{2.8}$$

respectively. The space $G_2^1[0,1]$ is a reproducing kernel space and its reproducing kernel function Q_y is given by [26] as

$$Q_y = \begin{cases} 1 + x, & x \le y, \\ 1 + y, & x > y. \end{cases} \tag{2.9}$$

Similarly, the space $H_2^1[0,1]$ defined by

$$H_2^1[0,1] = \left\{ v \mid v : [0,1] \longrightarrow \mathbb{R} \text{ is absolutely continuous}, v(t) \in L^2[0,1] \right\} \tag{2.10}$$

is a Hilbert space and then inner product and the norm in $T_2^1[0,1]$ are defined by

$$\begin{gathered} \langle v, g \rangle_{H_2^1} = v(0)g(0) + \int_0^1 v'(t)g'(t)dt, \quad v, g \in H_2^1[0,1], \\ \|v\|_{H_2^1} = \sqrt{\langle v, v \rangle_{T_2^1}}, \quad v \in H_2^1[0,1], \end{gathered} \tag{2.11}$$

respectively. The space $H_2^1[0,1]$ is a reproducing kernel space and its reproducing kernel function q_s is given by [26] as

$$q_s = \begin{cases} 1 + t, & t \le s, \\ 1 + s, & t > s. \end{cases} \tag{2.12}$$

Now we have the following theorem.

Theorem 2.2. *The space $W_2^3[0,1]$ is a complete reproducing kernel space whose reproducing kernel R_y is given by*

$$R_y(x) = \begin{cases} \sum_{i=1}^{6} c_i(y)x^{i-1}, & x \le y, \\ \sum_{i=1}^{6} d_i(y)x^{i-1}, & x > y, \end{cases} \tag{2.13}$$

where

$$\begin{gathered} c_1(y) = 1, \quad c_2(y) = \quad y, \quad c_3(y) = \frac{y^2}{4}, \quad c_4(y) = \frac{y^2}{12}, \quad c_5(y) = -\frac{1}{24}y, \quad c_6(y) = \frac{1}{120}, \\ d_1(y) = 1 + \frac{y^5}{120}, \quad d_2(y) = -\frac{y^4}{24} + y, \quad d_3(y) = \frac{y^2}{4} + \frac{y^3}{12}, \quad d_4(y) = d_5(y) = d_6(y) = 0. \end{gathered} \tag{2.14}$$

Proof. Since

$$\langle v, R_y \rangle_{W_2^3} = \sum_{i=0}^{2} v^{(i)}(0) R_y^{(i)}(0) + \int_0^1 v^{(3)}(x) R_y^{(3)}(x) dx, \quad \left(v, R_y \in W_2^3[0,1]\right) \tag{2.15}$$

through iterative integrations by parts for (2.15), we have

$$\begin{aligned} \langle v(x), R_y(x) \rangle_{W_2^4} = & \sum_{i=0}^{2} v^{(i)}(0) \left[R_y^{(i)}(0) - (-1)^{(2-i)} R_y^{(5-i)}(0) \right] \\ & + \sum_{i=0}^{2} (-1)^{(2-i)} v^{(i)}(1) R_y^{(5-i)}(1) + \int_0^1 v(x) R_y^{(6)}(x) dx. \end{aligned} \tag{2.16}$$

Note the property of the reproducing kernel as

$$\langle v(x), R_y(x) \rangle_{W_2^3} = v(y). \tag{2.17}$$

If

$$\begin{aligned}
R_y(0) - R_y^{(5)}(0) &= 0, \\
R'_y(0) + R_y^{(4)}(0) &= 0, \\
R''_y(0) - R'''_y(0) &= 0, \\
R_y^{(3)}(1) &= 0, \\
R_y^{(4)}(1) &= 0, \\
R_y^{(5)}(1) &= 0,
\end{aligned} \tag{2.18}$$

Then by (2.16) we obtain

$$R_y^{(6)}(x) = \delta(x-y), \tag{2.19}$$

when $x \neq y$,

$$R_y^{(6)}(x) = 0, \tag{2.20}$$

therefore

$$R_y(x) = \begin{cases} \sum_{i=1}^{6} c_i(y) x^{i-1}, & x \leq y, \\ \sum_{i=1}^{6} d_i(y) x^{i-1}, & x > y. \end{cases} \tag{2.21}$$

Since

$$R_y^{(6)}(x) = \delta(x-y), \tag{2.22}$$

we have

$$\begin{gathered}
\partial^k R_{y^+}(y) = \partial^k R_{y^-}(y), \quad k = 0,1,2,3,4, \\
\partial^5 R_{y^+}(y) - \partial^5 R_{y^-}(y) = -1.
\end{gathered} \tag{2.23}$$

From (2.18) and (2.23), the unknown coefficients $c_i(y)$ and $d_i(y)$ $(i = 1, 2, \ldots, 6)$ can be obtained. Thus R_y is given by

$$R_y = \begin{cases} 1 + yx + \dfrac{1}{4}y^2x^2 + \dfrac{1}{12}y^2x^3 - \dfrac{1}{24}yx^4 + \dfrac{1}{120}x^5, & x \leq y \\ 1 + yx + \dfrac{1}{4}y^2x^2 + \dfrac{1}{12}y^3x^2 - \dfrac{1}{24}xy^4 + \dfrac{1}{120}y^5, & x > y. \end{cases} \tag{2.24}$$

Now we note that the space given in [26] as

$$W(\Omega) = \left\{ \begin{array}{c} v(x,t) \mid \dfrac{\partial^4 v}{\partial x^2 \partial t^2}, \text{ is completely continuous in } \Omega = [0,1] \times [0,1], \\ \dfrac{\partial^6 v}{\partial x^3 \partial t^3} \in L^2(\Omega), v(x,0) = 0, \dfrac{\partial v(x,0)}{\partial t} = 0 \end{array} \right\}, \tag{2.25}$$

is a binary reproducing kernel Hilbert space. The inner product and the norm in $W(\Omega)$ are defined by

$$\begin{aligned} \langle v(x,t), g(x,t) \rangle_W = & \sum_{i=0}^{2} \int_0^1 \left[\frac{\partial^3}{\partial t^3} \frac{\partial^i}{\partial x^i} v(0,t) \frac{\partial^3}{\partial t^3} \frac{\partial^i}{\partial x^i} g(0,t) \right] dt \\ & + \sum_{j=0}^{2} \left\langle \frac{\partial^j}{\partial t^j} v(x,0), \frac{\partial^j}{\partial t^j} g(x,0) \right\rangle_{W_2^3} \\ & + \int_0^1 \int_0^1 \left[\frac{\partial^3}{\partial x^3} \frac{\partial^3}{\partial t^3} v(x,t) \frac{\partial^3}{\partial x^3} \frac{\partial^3}{\partial t^3} g(x,t) \right] dx\, dt, \\ \|v\|_W = & \sqrt{\langle v, v \rangle_W}, \quad v \in W(\Omega), \end{aligned} \tag{2.26}$$

respectively. □

Theorem 2.3. *The $W(\Omega)$ is a reproducing kernel space and its reproducing kernel function is*

$$K_{(y,s)} = R_y r_s, \tag{2.27}$$

such that for any $v \in W(\Omega)$,

$$\begin{aligned} v(y,s) &= \langle v(x,t), K_{(y,s)}(x,t) \rangle_W, \\ K_{(y,s)}(x,t) &= K_{(x,t)}(y,s). \end{aligned} \tag{2.28}$$

Similarly, the space

$$\widehat{W}(\Omega) = \left\{ v(x,t) \mid v(x,t) \text{ is completely continuous in } \Omega = [0,1] \times [0,1], \frac{\partial^2 v}{\partial x \partial t} \in L^2(\Omega) \right\} \tag{2.29}$$

is a binary reproducing kernel Hilbert space. The inner product and the norm in $\widehat{W}(\Omega)$ are defined by [26] as

$$
\begin{aligned}
\langle v(x,t), g(x,t)\rangle_{\widehat{W}} &= \int_0^1 \left[\frac{\partial}{\partial t} v(0,t) \frac{\partial}{\partial t} g(0,t)\right] dt + \langle v(x,0), g(x,0)\rangle_{W_2^1} \\
&\quad + \int_0^1 \int_0^1 \left[\frac{\partial}{\partial x}\frac{\partial}{\partial t} v(x,t) \frac{\partial}{\partial x}\frac{\partial}{\partial t} g(x,t)\right] dxdt, \\
\|v\|_{\widehat{W}} &= \sqrt{\langle v, v\rangle_{\widehat{W}}}, \quad v \in \widehat{W}(\Omega),
\end{aligned}
\tag{2.30}
$$

respectively. $\widehat{W}(\Omega)$ is a reproducing kernel space and its reproducing kernel function $G_{(y,s)}$ is

$$
G_{(y,s)} = Q_y q_s. \tag{2.31}
$$

3. Solution Representation in $W(\Omega)$

In this section, the solution of (1.1) is given in the reproducing kernel space $W(\Omega)$. We define the linear operator $L : W(\Omega) \to \widehat{W}(\Omega)$ as

$$
Lv = \frac{\partial^2 v}{\partial t^2} - c^2 \frac{\partial^2 v}{\partial x^2} + (\alpha + \beta)\frac{\partial v}{\partial t} + \alpha\beta v. \tag{3.1}
$$

Model problem (1.1) changes to the following problem:

$$
\begin{aligned}
&Lv = f(x,t) + M(x,t), \quad x,t \in [0,1], \\
&v(x,0) = 0, \qquad \frac{\partial v(x,0)}{\partial t} = 0.
\end{aligned}
\tag{3.2}
$$

Lemma 3.1. *The operator L is a bounded linear operator.*

Proof. Since

$$
\begin{aligned}
\|Lv\|_{\widehat{W}}^2 &= \int_0^1 \left[\frac{\partial}{\partial t} Lv(0,t)\right]^2 dt + \langle Lv(x,0), Lv(x,0)\rangle_{W_2^1} \\
&\quad + \int_0^1 \int_0^1 \left[\frac{\partial}{\partial x}\frac{\partial}{\partial t} Lv(x,t)\right]^2 dx\, dt \\
&= \int_0^1 \left[\frac{\partial}{\partial t} Lv(0,t)\right]^2 dt + [Lv(0,0)]^2 \\
&\quad + \int_0^1 \left[\frac{\partial}{\partial x} Lv(x,0)\right]^2 + \int_0^1 \int_0^1 \left[\frac{\partial}{\partial x}\frac{\partial}{\partial t} Lv(x,t)\right]^2 dx\, dt,
\end{aligned}
\tag{3.3}
$$

$$
v(x,t) = \langle v(\xi,\eta), K_{(x,t)}(\xi,\eta)\rangle_W, \qquad Lv(x,t) = \langle v(\xi,\eta), LK_{(x,t)}(\xi,\eta)\rangle_W,
$$

by continuity of $K_{(x,t)}(\xi,\eta)$, we have

$$|Lv(x,t)| \leq \|v\|_W \left\|LK_{(x,t)}(\xi,\eta)\right\|_W \leq a_0\|v\|_W. \tag{3.4}$$

Now similarly for $i = 0, 1$, we obtain

$$\begin{aligned} \frac{\partial^i}{\partial x^i} Lv(x,t) &= \left\langle v(\xi,\eta), \frac{\partial^i}{\partial x^i} LK_{(x,t)}(\xi,\eta) \right\rangle_W, \\ \frac{\partial}{\partial t}\frac{\partial^i}{\partial x^i} Lv(x,t) &= \left\langle v(\xi,\eta), \frac{\partial}{\partial t}\frac{\partial^i}{\partial x^i} LK_{(x,t)}(\xi,\eta) \right\rangle_W, \end{aligned} \tag{3.5}$$

and then

$$\begin{aligned} \left|\frac{\partial^i}{\partial x^i} Lv(x,t)\right| &\leq e_i\|v\|_W, \\ \left|\frac{\partial}{\partial t}\frac{\partial^i}{\partial x^i} Lv(x,t)\right| &\leq f_i\|v\|_W. \end{aligned} \tag{3.6}$$

Therefore we conclude

$$\|Lv(x,t)\|^2_{\widehat{W}} \leq \sum_{i=0}^{1}\left(e_i^2 + f_i^2\right)\|v\|^2_W \leq a^2\|v\|^2_W. \tag{3.7}$$

□

Now, if we choose a countable dense subset $\{(x_1,t_1),(x_2,t_2),\ldots\}$ in $\Omega = [0,1]\times[0,1]$ and define

$$\Phi_i(x,t) = G_{(x_i,t_i)}(x,t), \qquad \Psi_i(x,t) = L^*\Phi_i(x,t), \tag{3.8}$$

where L^* is the adjoint operator of L, then the orthonormal system $\{\widehat{\Psi}_i(x,t)\}_{i=1}^{\infty}$ of $W(\Omega)$ can be derived from the process of Gram-Schmidt orthogonalization of $\{\Psi_i(x,t)\}_{i=1}^{\infty}$ as

$$\widehat{\Psi}_i(x,t) = \sum_{k=1}^{i}\beta_{ik}\Psi_k(x,t). \tag{3.9}$$

Then we have the following theorem.

Theorem 3.2. *Suppose that $\{(x_i,t_i)\}_{i=1}^{\infty}$ is dense in Ω, then $\{\Psi_i(x,t)\}_{i=1}^{\infty}$ is complete system in $W(\Omega)$ and*

$$\Psi_i(x,t) = L_{(y,s)}K_{(y,s)}(x,t)\big|_{(y,s)=(x_i,t_i)}. \tag{3.10}$$

Proof. We have

$$\begin{aligned}
\Psi_i(x,t) = (L^*\Phi_i)(x,t) &= \left\langle (L^*\Phi_i)(y,s), K_{(x,t)}(y,s) \right\rangle_W \\
&= \left\langle \Phi_i(y,s), L_{(y,s)} K_{(x,t)}(y,s) \right\rangle_{\widehat{W}} \\
&= L_{(y,s)} K_{(x,t)}(y,s) \Big|_{(y,s)=(x_i,t_i)} \\
&= L_{(y,s)} K_{(y,s)}(x,t) \Big|_{(y,s)=(x_i,t_i)}.
\end{aligned} \tag{3.11}$$

That is clearly $\Psi_i(x,t) \in W(\Omega)$. For each fixed $v(x,t) \in W(\Omega)$, if

$$\langle v(x,t), \Psi_i(x,t) \rangle_W = 0, \quad i = 1, 2, \ldots \tag{3.12}$$

then

$$\begin{aligned}
\langle v(x,t), (L^*\Phi_i)(x,t) \rangle_W &= \langle Lv(x,t), \Phi_i(x,t) \rangle_{\widehat{W}} \\
&= (Lv)(x_i,t_i) = 0, \quad i = 1, 2, \ldots.
\end{aligned} \tag{3.13}$$

Note that $\{(x_i,t_i)\}_{i=1}^{\infty}$ is dense in Ω, hence, $(Lv)(x,t) = 0$. It follows that $v = 0$ from the existence of L^{-1}. So the proof is complete. □

Theorem 3.3. *If* $\{(x_i,t_i)\}_{i=1}^{\infty}$ *is dense in* Ω*, then the solution of* (1.5) *is given as*

$$v(x,t) = \sum_{i=1}^{\infty} \sum_{k=1}^{i} \beta_{ik} \left[f(x_k,t_k) + M(x_k,t_k) \right] \widehat{\Psi}_i(x,t). \tag{3.14}$$

Proof. Since $\{\Psi_i(x,t)\}_{i=1}^{\infty}$ is complete system in Ω, we have

$$\begin{aligned}
v(x,t) &= \sum_{i=1}^{\infty} \left\langle v(x,t), \widehat{\Psi}_i(x,t) \right\rangle_W \widehat{\Psi}_i(x,t) \\
&= \sum_{i=1}^{\infty} \sum_{k=1}^{i} \beta_{ik} \langle v(x,t), \Psi_k(x,t) \rangle_W \widehat{\Psi}_i(x,t)
\end{aligned}$$

$$
\begin{aligned}
&= \sum_{i=1}^{\infty}\sum_{k=1}^{i}\beta_{ik}\langle v(x,t), L^{*}\Phi_k(x,t)\rangle_W \widehat{\Psi}_i(x,t) \\
&= \sum_{i=1}^{\infty}\sum_{k=1}^{i}\beta_{ik}\langle Lv(x,t), \Phi_k(x,t)\rangle_{\widehat{W}} \widehat{\Psi}_i(x,t) \\
&= \sum_{i=1}^{\infty}\sum_{k=1}^{i}\beta_{ik}\langle Lv(x,t), G_{(x_k,t_k)}(x,t)\rangle_{\widehat{W}} \widehat{\Psi}_i(x,t) \\
&= \sum_{i=1}^{\infty}\sum_{k=1}^{i}\beta_{ik} Lv(x_k,t_k)\widehat{\Psi}_i(x,t) \\
&= \sum_{i=1}^{\infty}\sum_{k=1}^{i}\beta_{ik}\left[f(x_k,t_k)+M(x_k,t_k)\right]\widehat{\Psi}_i(x,t).
\end{aligned}
\tag{3.15}
$$

□

Now the approximate solution $v_n(x,t)$ can be obtained from the n-term intercept of the exact solution $v(x,t)$ and

$$v_n(x,t) = \sum_{i=1}^{n}\sum_{k=1}^{i}\beta_{ik}\left[f(x_k,t_k)+M(x_k,t_k)\right]\widehat{\Psi}_i(x,t). \tag{3.16}$$

Of course it is also easy to show that

$$\|v_n(x,t) - v(x,t)\| \longrightarrow 0, \quad (n \longrightarrow \infty). \tag{3.17}$$

3.1. Convergence Analysis

We assume that $\{x_i, t_i\}_{i=1}^{\infty}$ is dense in $\Omega = [0,1] \times [0,1]$. We discuss the convergence of the approximate solutions constructed in Section 3. Let v be the exact solution of (1.1) and v_n the n-term approximation solution of (1.1). Then we have the following theorem.

Theorem 3.4. *If $v \in W(\Omega)$, then*

$$\|v - v_n\|_{W(\Omega)} \longrightarrow 0, \quad n \longrightarrow \infty. \tag{3.18}$$

Moreover a sequence $\|v - v_n\|_{W(\Omega)}$ is monotonically decreasing in n.

Proof. From (3.14) and (3.16), it follows that

$$\|v - v_n\|_{W(\Omega)} = \|v - v_n\|_{W(\Omega)} = \left\| \sum_{i=n+1}^{\infty}\sum_{k=1}^{i}\beta_{ik}\left[f(x_k,t_k)+M(x_k,t_k)\right]\overline{\varphi}_i(x,t)\right\|_{W(\Omega)}. \tag{3.19}$$

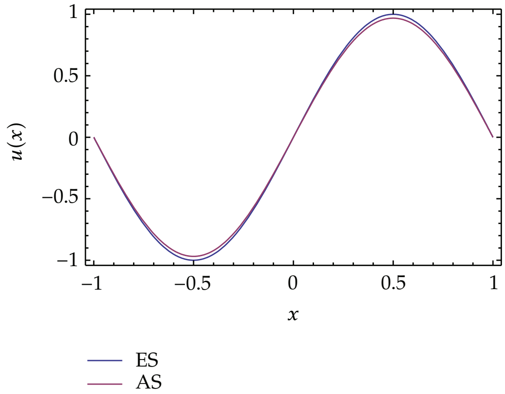

Figure 1: The compared results of the analytical and numerical solutions of Example 4.1 for $t = 0.5$.

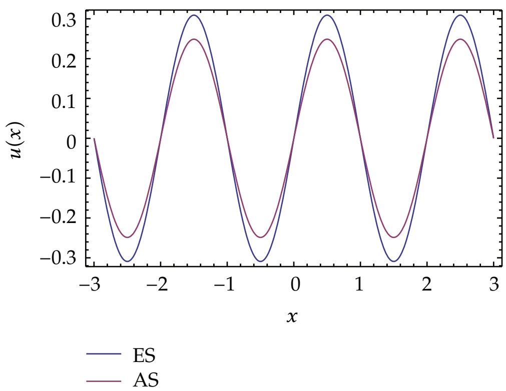

Figure 2: The compared results of the analytical and numerical solutions of Example 4.1 for $t = 1.0$.

Thus

$$\|v - v_n\|_{W(\Omega)} \longrightarrow 0, \quad n \longrightarrow \infty. \tag{3.20}$$

In addition,

$$\begin{aligned} \|v - v_n\|^2_{W(\Omega)} &= \left\| \sum_{i=n+1}^{\infty} \sum_{k=1}^{i} \beta_{ik} \left[f(x_k, t_k) + M(x_k, t_k) \right] \overline{\varphi}_i(x, t) \right\|^2_{W(\Omega)} \\ &= \sum_{i=n+1}^{\infty} \left(\sum_{k=1}^{i} \beta_{ik} \left[f(x_k, t_k) + M(x_k, t_k) \right] \right)^2. \end{aligned} \tag{3.21}$$

Then clearly, $\|v - v_n\|_{W(\Omega)}$ is monotonically decreasing in n.

□

Table 1: The exact solution, approximate solution, absolute error, and relative error of Example 4.1 for initial conditions at $t = 0.5$.

x	Exact solution	Approximate solution	Absolute error	Relative error
0.2	0.5877852524	0.5877852576	5.21×10^{-9}	$8.846768405 \times 10^{-9}$
0.4	0.9510565165	0.951056525	8.52×10^{-9}	$8.937428904 \times 10^{-9}$
0.6	0.9510565163	0.95105657	5.37×10^{-8}	$5.646352144 \times 10^{-8}$
0.8	0.5877852522	0.587785294	4.18×10^{-8}	$7.111440759 \times 10^{-8}$

Table 2: The absolute error ofExample 7 for difference schemes and our scheme at $t = 0.5$.

x	Difference scheme [13]	Difference scheme [21]	Present scheme
0.2	5.859×10^{-1}	1.167×10^{-5}	5.21×10^{-9}
0.4	9.480×10^{-1}	1.889×10^{-5}	8.52×10^{-9}
0.6	9.480×10^{-1}	1.889×10^{-5}	5.37×10^{-8}
0.8	5.859×10^{-1}	1.167×10^{-5}	4.18×10^{-8}

Table 3: The exact solution, approximate solution, absolute error, and relative error of Example 4.2 for initial conditions at $t = 0.8$.

x	Exact solution	Approximate solution	Absolute error	Relative error
0.2	0.04761212907	0.047612168	3.8931×10^{-8}	$8.176487958 \times 10^{-7}$
0.4	0.07703804312	0.07703791	1.3312×10^{-7}	0.000001727977433
0.6	0.07703804310	0.077037983	6.0101×10^{-8}	$7.801340426 \times 10^{-7}$
0.8	0.04761212906	0.04761256075	4.3169×10^{-7}	0.000009066807314

Table 4: The absolute error of Example 4.2 for difference schemes and our scheme at $t = 0.8$.

x	Difference scheme [13]	Difference scheme [21]	Our scheme
0.2	5.119×10^{-2}	2.334×10^{-6}	3.8931×10^{-8}
0.4	8.283×10^{-1}	3.776×10^{-6}	1.3312×10^{-7}
0.6	8.283×10^{-1}	3.776×10^{-6}	6.0101×10^{-8}
0.8	5.119×10^{-2}	2.334×10^{-6}	4.3169×10^{-7}

Table 5: The exact solution, approximate solution, absolute error, and relative error of Example 4.3 for initial conditions at $t = 1$.

x	Exact solution	Approximate solution	Absolute error	Relative error
0.2	0.004842491805	0.00484215485	3.36955×10^{-7}	0.00006958297785
0.4	0.02451511476	0.024515542	4.2724×10^{-7}	0.00001742761575
0.6	0.02451511476	0.02451574136	6.2660×10^{-7}	0.00002555974166
0.8	0.004842491805	0.004843445	9.53195×10^{-7}	0.0001968397756

Table 6: The absolute error of Example 4.3 for difference schemes and our scheme at $t = 1.0$.

x	Difference scheme [13]	Difference scheme [21]	Our scheme
0.2	4.956×10^{-3}	5.138×10^{-7}	3.36955×10^{-7}
0.4	2.392×10^{-2}	3.550×10^{-7}	4.27242×10^{-7}
0.6	2.392×10^{-2}	3.550×10^{-7}	6.26601×10^{-7}
0.8	4.956×10^{-3}	5.138×10^{-7}	9.53195×10^{-7}

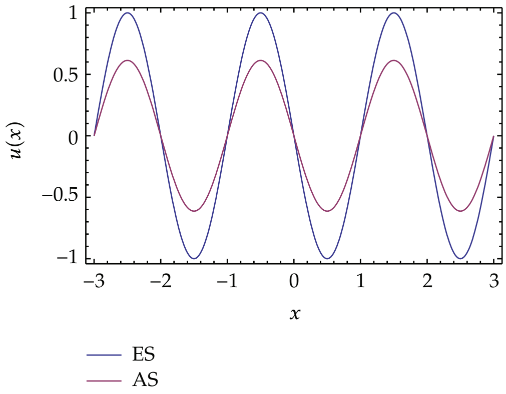

Figure 3: The compared results of the analytical and numerical solutions of Example 4.1 for $t = 1.5$.

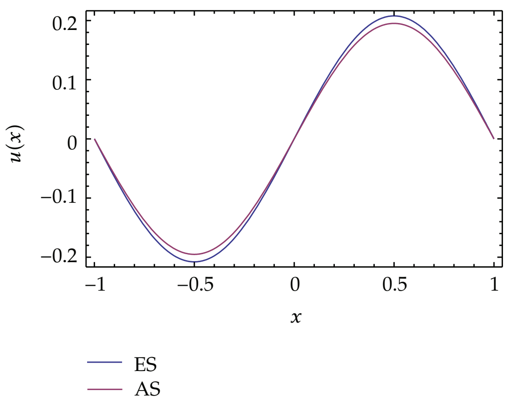

Figure 4: The compared results of the analytical and numerical solutions of Example 4.2 for $t = 0.5$.

4. Experimental Results for the Telegraph Equation

In this section, three numerical examples are provided to show the accuracy of the present method. All the computations were performed by Maple 13. Since, the RKHSM does not require discretization of the variables, that is, time and space, it is also not effected by computation round-off errors and no need to face with necessity of large computer memory and time. The accuracy of the RKHSM for the problem (1.1) is controllable and absolute errors are small with present choice of x and t (see Tables 1, 2, 3, 4, 5, and 6). Thus the numerical results which we obtain justify the advantage of this methodology.

Note that the solutions are very rapidly convergent by utilizing the RKHSM. Further, the series solution methodology can be applied to various types of linear or nonlinear system of partial differential equations and single partial differential equations, see, for example, [25–30].

Using our method we choose 100 points in $[0,1]\times[0,1]$. In Tables 2, 4 and 6 we compute the absolute errors $|u(x,t) - u_n(x,t)|$ at the following points:

$$\{(x_i, t_i) : x_i = 2i, i = 0.1, 0.2, 0.3, 0.4;\ \ t = 0.5, 0.8, 1.0\}. \tag{4.1}$$

Table 7: The relative errors and computational times for Examples 4.1–4.3 at different values of x and t.

x	t	Example 5.1	Time	Example 5.2	Time	Example 5.3	Time
0.1	0.1	5.57×10^{-9}	1.685	5.20963×10^{-5}	1.809	5.13216×10^{-6}	1.716
0.2	0.2	3.02×10^{-8}	1.857	2.07422×10^{-5}	1.732	6.82234×10^{-7}	1.872
0.3	0.3	3.250×10^{-7}	1.841	7.17823×10^{-4}	1.934	6.74863×10^{-7}	1.669
0.4	0.4	5.56×10^{-8}	1.857	6.44910×10^{-4}	1.872	5.73933×10^{-6}	1.716
0.5	0.5	$3. \times 10^{-6}$	1.622	2.481×10^{-7}	1.841	3.93839×10^{-6}	1.716
0.6	0.6	1.632×10^{-7}	1.826	4.54×10^{-8}	1.654	5.35112×10^{-6}	1.701
0.7	0.7	2.01×10^{-8}	1.731	9.19×10^{-9}	1.560	9.26055×10^{-6}	1.638
0.8	0.8	2.9613×10^{-6}	1.747	4.3169×10^{-7}	1.591	9.6449×10^{-9}	1.763
0.9	0.9	4.9767×10^{-7}	1.701	1.781×10^{-8}	1.653	6.3701×10^{-9}	1.669
1.0	1.0	4.2964×10^{-5}	1.623	1.61644×10^{-10}	1.513	2.75453×10^{-4}	1.732

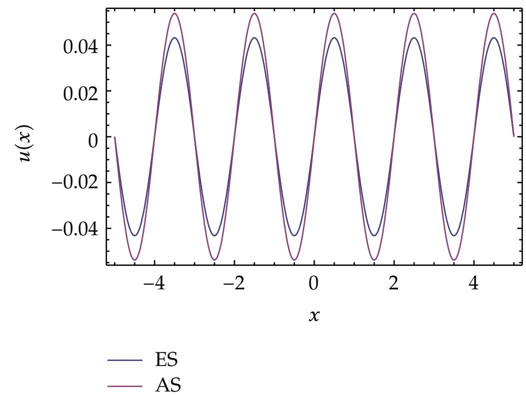

Figure 5: The compared results of the analytical and numerical solutions of Example 4.2 for $t = 1.0$.

In Table 7, we compute the following relative errors:

$$\frac{|u(x,t) - u_n(x,t)|}{|u(x,t)|} \tag{4.2}$$

at the points $\{(x_i, t_i) : x_i = t_i = i, i = 0.1, \ldots, 1.0\}$. It is possible to refine the result by increasing the intensive points.

We constructed the figures for different values of x and t. It can be concluded by figures that the speed of convergence is decreasing by increasing the values of x and t.

Example 4.1. Consider the following telegraph equation with initial conditions:

$$\begin{gathered}\frac{\partial^2 u}{\partial t^2} + 2\pi \frac{\partial u}{\partial t} + \pi^2 u = \frac{\partial^2 u}{\partial x^2} + \pi^2 \sin \pi x (\sin \pi t + 2 \cos \pi t), \\ 0 \le x \le 1, \quad 0 \le t \le 1, \\ u(x,0) = 0, \qquad \frac{\partial u(x,0)}{\partial t} = \pi \sin \pi x.\end{gathered} \tag{4.3}$$

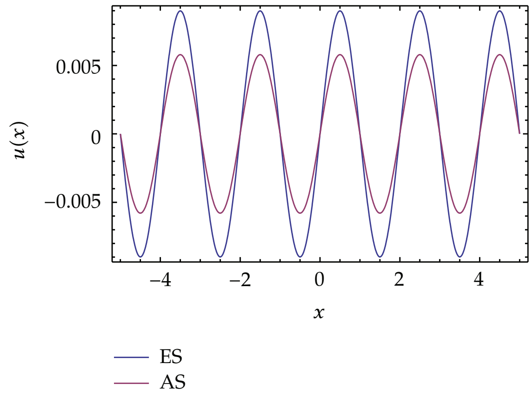

Figure 6: The compared results of the analytical and numerical solutions of Example 4.2 for $t = 1.5$.

Then the exact solution is given as

$$u(x,t) = \sin(\pi x)\sin(\pi t). \tag{4.4}$$

If we apply $v(x,t) = u(x,t) - t\sin(\pi x)$ to (4.3), then we obtain the following equation:

$$\frac{\partial^2 v}{\partial t^2} - \frac{\partial^2 v}{\partial x^2} + 2\pi\frac{\partial v}{\partial t} + \pi^2 v = -2\pi^2 \sin\pi x - 2t\pi^3 \sin\pi x + \pi^2 \sin\pi x(\sin\pi t + 2\cos\pi t),$$

$$0 \le x \le 1, \quad 0 \le t \le 1 \tag{4.5}$$

$$v(x,0) = 0, \qquad \frac{\partial v(x,0)}{\partial t} = 0.$$

Then we have the estimation in Table 1.

Now if we compare [13, 21] and the present scheme we have Table 2.

We have Figures 1, 2, and 3 for this example, where ES = exact solution and AS = approximate solution.

Example 4.2. Consider the following telegraph equation with initial conditions:

$$\frac{\partial^2 u}{\partial t^2} + 4\pi\frac{\partial u}{\partial t} + 3\pi^2 u = 4\frac{\partial^2 u}{\partial x^2} + 4\pi^2 e^{-\pi t}\sin\pi x, \quad 0 \le x \le 1, 0 \le t \le 1,$$
$$u(x,0) = \sin\pi x, \qquad \frac{\partial u(x,0)}{\partial t} = -\pi\sin\pi x. \tag{4.6}$$

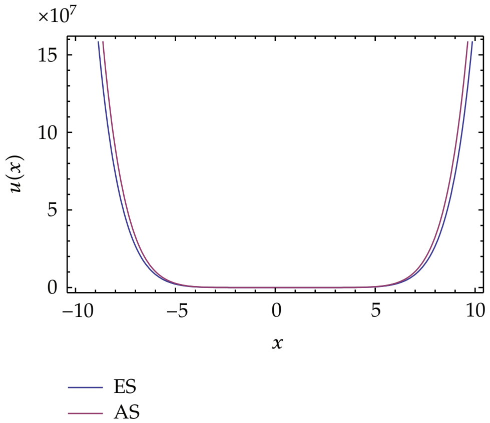

Figure 7: The compared results of the analytical and numerical solutions of Example 4.3 for $t = 0.5$.

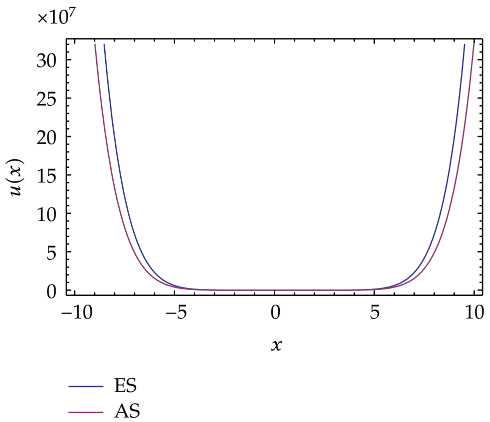

Figure 8: The compared results of the analytical and numerical solutions of Example 4.3 for $t = 1.0$.

The exact solution $u(x,t) = e^{-\pi t}\sin \pi x$. If we apply $v(x,t) = u(x,t) - \sin \pi x + t\pi \sin \pi x$ to (4.6), then we obtain

$$\frac{\partial^2 v}{\partial t^2} - \frac{\partial^2 v}{\partial x^2} + 4\pi \frac{\partial v}{\partial t} + 3\pi^2 v = 4t\pi^3 \sin \pi x + 4\pi^2 e^{-\pi t}\sin \pi x, \quad 0 \le x \le 1, 0 \le t \le 1,$$
$$v(x,0) = 0, \qquad \frac{\partial v(x,0)}{\partial t} = 0, \tag{4.7}$$

then similarly, in Table 3 we have the estimation among the exact and approximate solutions and the error terms.

Then the comparison yields in Table 4.

We have Figures 4, 5, and 6 for this example.

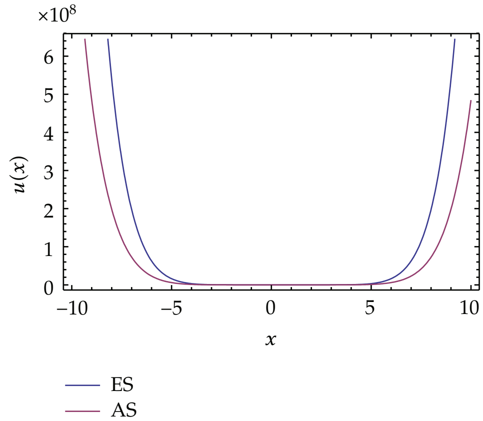

Figure 9: The compared results of the analytical and numerical solutions of Example 4.3 for $t = 1.5$.

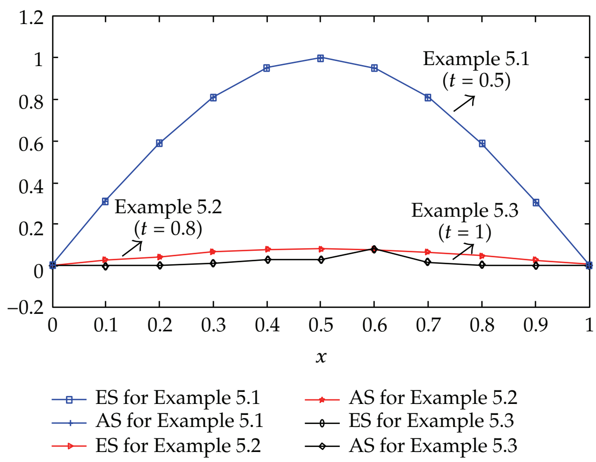

Figure 10: The compared results of the analytical and numerical solutions of Examples 4.1–4.3.

Example 4.3. Consider the following telegraph equation with initial conditions:

$$\frac{\partial^2 u}{\partial t^2} + 10\frac{\partial u}{\partial t} + 24u = \frac{\partial^2 u}{\partial x^2} + 4x^2(x-1)^2\left(12x^4 - 24x^3 - 2x^2 + 14x - 3\right)e^{2t},$$
$$0 \le x \le 1, \quad 0 \le t \le 1, \tag{4.8}$$
$$u(x,0) = x^4(x-1)^4, \qquad \frac{\partial u(x,0)}{\partial t} = 2x^4(x-1)^4.$$

The exact solution $u(x,t) = e^{2t}x^4(x-1)^4$. If we apply

$$v(x,t) = u(x,t) - x^4(x-1)^4 - 2tx^4(x-1)^4 \tag{4.9}$$

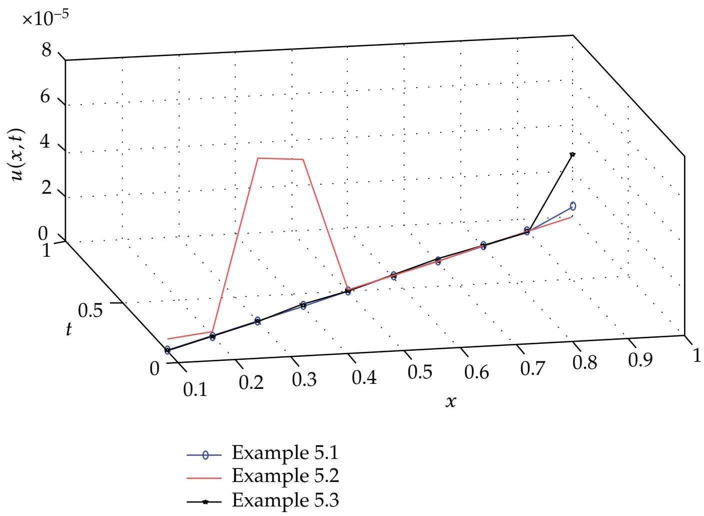

Figure 11: The compared results of the relative errors for Examples 4.1–4.3.

to (4.8) then (4.10) is obtained as

$$\frac{\partial^2 v}{\partial t^2} - \frac{\partial^2 v}{\partial x^2} + 10\frac{\partial v}{\partial t} + 3\pi^2 v = 4t\pi^3 \sin \pi x + 4\pi^2 e^{-\pi t} \sin \pi x,$$
$$0 \le x \le 1, \quad 0 \le t \le 1, \tag{4.10}$$
$$v(x,0) = 0, \qquad \frac{\partial v(x,0)}{\partial t} = 0.$$

We have Figures 7, 8, 9, 10, and 11 for this example.

Remark 4.4. Ding et al. [19] has solved Examples 4.1–4.3 by using new polynomial spline methods. In our method the numerical solutions are in good agreement with analytical solutions (see Figures 1–11). In addition, the figure of the relative error is drawn for the value of x, t and also for three examples (see Figure 11).

One may view Tables 1, 2, 3, 4, 5 and 6 for the confidence of the method and the comparison with the other methods. In Table 7, computing time with relative error is also given for each example.

5. Conclusion

In this paper, the RKHSM was used for the telegraph equation with initial conditions. The approximate solutions to the equations have been calculated by using the RKHSM without any need to transformation techniques and linearization or perturbation of the equations. In closing, the RKHSM avoids the difficulties and massive computational work by determining the analytic solutions. We compare our solutions with the exact solutions and the results of [19].

A clear conclusion can be drawn from the numerical results as the RKHSM algorithm provides highly accurate numerical solutions without spatial discretizations for the nonlinear partial differential equations. It is also worth noting that the advantage of this methodology displays a fast convergence of the solutions. The illustrations show the dependence of the rapid convergence depends on the character and behavior of the solutions just as in a closed form solutions.

Acknowledgments

The authors express their sincere thanks to the referees for the careful and detailed reading of the paper and the very helpful suggestions that improved the paper substantially. The third author gratefully acknowledges that this paper was partially supported by the University Putra Malaysia under the ERGS Grant Scheme having project no. 5527068.

References

[1] M. S. El-Azab and M. El-Gamel, "A numerical algorithm for the solution of telegraph equations," *Applied Mathematics and Computation*, vol. 190, no. 1, pp. 757–764, 2007.

[2] A. C. Metaxas and R. J. Meredith, *Industrial Microwave, Heating*, Peter Peregrinus, London, UK, 1993.

[3] G. Roussy and J. A. Pearcy, *Foundations and Industrial Applications of Microwaves and Radio Frequency Fields*, John Wiley, New York, NY, USA, 1995.

[4] M. Dehghan, "On the solution of an initial-boundary value problem that combines Neumann and integral condition for the wave equation," *Numerical Methods for Partial Differential Equations*, vol. 21, no. 1, pp. 24–40, 2005.

[5] R. K. Mohanty, M. K. Jain, and K. George, "On the use of high order difference methods for the system of one space second order nonlinear hyperbolic equations with variable coefficients," *Journal of Computational and Applied Mathematics*, vol. 72, no. 2, pp. 421–431, 1996.

[6] E. H. Twizell, "An explicit difference method for the wave equation with extended stability range," *Nordisk Tidskrift for Informationsbehandling (BIT)*, vol. 19, no. 3, pp. 378–383, 1979.

[7] F. Gao and C. Chi, "Unconditionally stable difference schemes for a one-space-dimensional linear hyperbolic equation," *Applied Mathematics and Computation*, vol. 187, no. 2, pp. 1272–1276, 2007.

[8] A. Saadatmandi and M. Dehghan, "Numerical solution of the one-dimensional wave equation with an integral condition," *Numerical Methods for Partial Differential Equations*, vol. 23, no. 2, pp. 282–292, 2007.

[9] A. Borhanifar and R. Abazari, "An unconditionally stable parallel difference scheme for telegraph equation," *Mathematical Problems in Engineering*, vol. 2009, Article ID 969610, 17 pages, 2009.

[10] A. Saadatmandi and M. Dehghan, "Numerical solution of hyperbolic telegraph equation using the Chebyshev tau method," *Numerical Methods for Partial Differential Equations*, vol. 26, no. 1, pp. 239–252, 2010.

[11] M. A. Abdou, "Adomian decomposition method for solving the telegraph equation in charged particle transport," *Journal of Quantitative Spectroscopy and Radiative Transfer*, vol. 95, no. 3, pp. 407–414, 2005.

[12] R. K. Mohanty, "An unconditionally stable difference scheme for the one-space-dimensional linear hyperbolic equation," *Applied Mathematics Letters*, vol. 17, no. 1, pp. 101–105, 2004.

[13] A. Mohebbi and M. Dehghan, "High order compact solution of the one-space-dimensional linear hyperbolic equation," *Numerical Methods for Partial Differential Equations*, vol. 24, no. 5, pp. 1222–1235, 2008.

[14] M. Dehghan, "Finite difference procedures for solving a problem arising in modeling and design of certain optoelectronic devices," *Mathematics and Computers in Simulation*, vol. 71, no. 1, pp. 16–30, 2006.

[15] M. Dehghan, "Implicit collocation technique for heat equation with non-classic initial condition," *International Journal of Nonlinear Sciences and Numerical Simulation*, vol. 7, no. 4, pp. 461–466, 2006.

[16] M. Dehghan and A. Shokri, "A numerical method for solving the hyperbolic telegraph equation," *Numerical Methods for Partial Differential Equations*, vol. 24, no. 4, pp. 1080–1093, 2008.

[17] M. Dehghan and M. Lakestani, “The use of Chebyshev cardinal functions for solution of the second-order one-dimensional telegraph equation,” *Numerical Methods for Partial Differential Equations*, vol. 25, no. 4, pp. 931–938, 2009.
[18] M. Lakestani and B. N. Saray, “Numerical solution of telegraph equation using interpolating scaling functions,” *Computers & Mathematics with Applications*, vol. 60, no. 7, pp. 1964–1972, 2010.
[19] H.-F. Ding, Y.-X. Zhang, J.-X. Cao, and J.-H. Tian, “A class of difference scheme for solving telegraph equation by new non-polynomial spline methods,” *Applied Mathematics and Computation*, vol. 218, no. 9, pp. 4671–4683, 2012.
[20] A. G. Lakoud and D. Belakroum, “Rothe’s method for a telegraph equation with integral conditions,” *Nonlinear Analysis. Theory, Methods & Applications*, vol. 70, no. 11, pp. 3842–3853, 2009.
[21] M. Dehghan, S. A. Yousefi, and A. Lotfi, “The use of He’s variational iteration method for solving the telegraph and fractional telegraph equations,” *International Journal for Numerical Methods in Biomedical Engineering*, vol. 27, no. 2, pp. 219–231, 2011.
[22] J. Biazar, H. Ebrahimi, and Z. Ayati, “An approximation to the solution of telegraph equation by variational iteration method,” *Numerical Methods for Partial Differential Equations*, vol. 25, no. 4, pp. 797–801, 2009.
[23] H. Yao and Y. Lin, “New algorithm for solving a nonlinear hyperbolic telegraph equation with an integral condition,” *International Journal for Numerical Methods in Biomedical Engineering*, vol. 27, no. 10, pp. 1558–1568, 2011.
[24] S. A. Yousefi, “Legendre multiwavelet Galerkin method for solving the hyperbolic telegraph equation,” *Numerical Methods for Partial Differential Equations*, vol. 26, no. 3, pp. 535–543, 2010.
[25] M. Cui and Z. Deng, “Solutions to the define solution problem of differential equations in space $W_2^1[0,1]$,” *Advances in Mathematics*, vol. 17, pp. 327–328, 1986.
[26] M. Cui and Y. Lin, *Nonlinear Numerical Analysis in the Reproducing Kernel Space*, Nova Science Publishers, New York, NY, USA, 2009.
[27] F. Geng and M. Cui, “Solving a nonlinear system of second order boundary value problems,” *Journal of Mathematical Analysis and Applications*, vol. 327, no. 2, pp. 1167–1181, 2007.
[28] H. Yao and M. Cui, “A new algorithm for a class of singular boundary value problems,” *Applied Mathematics and Computation*, vol. 186, no. 2, pp. 1183–1191, 2007.
[29] W. Wang, M. Cui, and B. Han, “A new method for solving a class of singular two-point boundary value problems,” *Applied Mathematics and Computation*, vol. 206, no. 2, pp. 721–727, 2008.
[30] Y. Zhou, Y. Lin, and M. Cui, “An efficient computational method for second order boundary value problems of nonlinear differential equations,” *Applied Mathematics and Computation*, vol. 194, no. 2, pp. 354–365, 2007.
[31] X. Lü and M. Cui, “Analytic solutions to a class of nonlinear infinite-delay-differential equations,” *Journal of Mathematical Analysis and Applications*, vol. 343, no. 2, pp. 724–732, 2008.
[32] Y.-L. Wang and L. Chao, “Using reproducing kernel for solving a class of partial differential equation with variable-coefficients,” *Applied Mathematics and Mechanics*, vol. 29, no. 1, pp. 129–137, 2008.
[33] F. Li and M. Cui, “A best approximation for the solution of one-dimensional variable-coefficient Burgers’ equation,” *Numerical Methods for Partial Differential Equations*, vol. 25, no. 6, pp. 1353–1365, 2009.
[34] S. Zhou and M. Cui, “Approximate solution for a variable-coefficient semilinear heat equation with nonlocal boundary conditions,” *International Journal of Computer Mathematics*, vol. 86, no. 12, pp. 2248–2258, 2009.
[35] F. Geng and M. Cui, “New method based on the HPM and RKHSM for solving forced Duffing equations with integral boundary conditions,” *Journal of Computational and Applied Mathematics*, vol. 233, no. 2, pp. 165–172, 2009.
[36] J. Du and M. Cui, “Solving the forced Duffing equation with integral boundary conditions in the reproducing kernel space,” *International Journal of Computer Mathematics*, vol. 87, no. 9, pp. 2088–2100, 2010.
[37] X. Lv and M. Cui, “An efficient computational method for linear fifth-order two-point boundary value problems,” *Journal of Computational and Applied Mathematics*, vol. 234, no. 5, pp. 1551–1558, 2010.
[38] W. Jiang and M. Cui, “Constructive proof for existence of nonlinear two-point boundary value problems,” *Applied Mathematics and Computation*, vol. 215, no. 5, pp. 1937–1948, 2009.
[39] J. Du and M. Cui, “Constructive proof of existence for a class of fourth-order nonlinear BVPs,” *Computers & Mathematics with Applications*, vol. 59, no. 2, pp. 903–911, 2010.
[40] M. Cui and H. Du, “Representation of exact solution for the nonlinear Volterra-Fredholm integral equations,” *Applied Mathematics and Computation*, vol. 182, no. 2, pp. 1795–1802, 2006.

[41] B. Wu and X. Li, “Iterative reproducing kernel method for nonlinear oscillator with discontinuity,” *Applied Mathematics Letters*, vol. 23, no. 10, pp. 1301–1304, 2010.

[42] W. Jiang and Y. Lin, “Representation of exact solution for the time-fractional telegraph equation in the reproducing kernel space,” *Communications in Nonlinear Science and Numerical Simulation*, vol. 16, no. 9, pp. 3639–3645, 2011.

[43] F. Geng and M. Cui, “A reproducing kernel method for solving nonlocal fractional boundary value problems,” *Applied Mathematics Letters*, vol. 25, no. 5, pp. 818–823, 2012.

[44] Y. Lin and M. Cui, “A numerical solution to nonlinear multi-point boundary value problems in the reproducing kernel space,” *Mathematical Methods in the Applied Sciences*, vol. 34, no. 1, pp. 44–47, 2011.

[45] F. Z. Geng, “A numerical algorithm for nonlinear multi-point boundary value problems,” *Journal of Computational and Applied Mathematics*, vol. 236, no. 7, pp. 1789–1794, 2012.

[46] M. Mohammadi and R. Mokhtari, “Solving the generalized regularized long wave equation on the basis of a reproducing kernel space,” *Journal of Computational and Applied Mathematics*, vol. 235, no. 14, pp. 4003–4014, 2011.

[47] B. Y. Wu and X. Y. Li, “A new algorithm for a class of linear nonlocal boundary value problems based on the reproducing kernel method,” *Applied Mathematics Letters*, vol. 24, no. 2, pp. 156–159, 2011.

[48] L. M. Surhone, M. T. Tennoe, and S. F. Henssonow, *Reproducing Kernel Hilbert Space*, Betascript Publishing, Berlin, Germany, 2010.

Hindawi Publishing Corporation
Journal of Function Spaces and Applications
Volume 2012, Article ID 405368, 14 pages
doi:10.1155/2012/405368

Research Article

Note on Boehmians for Class of Optical Fresnel Wavelet Transforms

S. K. Q. Al-Omari[1] and A. Kılıçman[2]

[1] *Department of Applied Sciences, Faculty of Engineering Technology, Al-Balqa Applied University, Amman 11134, Jordan*
[2] *Department of Mathematics and Institute of Mathematical Research, Universiti Putra Malaysia (UPM), Selangor, 43400 Serdang, Malaysia*

Correspondence should be addressed to A. Kılıçman, akilicman@putra.upm.edu.my

Received 4 July 2012; Accepted 27 August 2012

Academic Editor: Manuel Ruiz Galan

We extend the Fresnel-wavelet transform to the context of generalized functions, namely, Boehmians. At first, we study the Fresnel-wavelet transform in the sense of distributions of compact support. Based on this concept, we introduce two new spaces of Boehmians and proving certain related results. Further, we show that the extended transform establishes a linear and an isomorphic mapping between the Boehmian spaces. Moreover, conditions of continuity of the extended transform and its inverse with respect to δ and Δ convergence are discussed in some details.

1. Introduction

Optical integral transforms have been studied in several works, for example, [1–8]. However, is the Fresnel transform among all the great importance [5, 9] where for which the kernel takes the form of a complex exponential function $\exp[(i/2c)(ax_1^2 + bx_2^2)]$, for some constants a, b and c. The generalization of the Fresnel transform called the linear canonical transform was introduced in [10] and has recently attracted considerable attention in optics, see [4, 11]. One of the very well-known linear transform is the wavelet transform, see [12, 13] we have

$$\Omega_f(\mu, \lambda) = \frac{1}{\sqrt{\mu}} \int_{\mathbf{R}} f(x) \psi^* \left(\frac{x - \lambda}{\mu} \right) dx, \tag{1.1}$$

where $\psi(x)$ is named as the mother wavelet such that

$$\int_{\mathbf{R}} dx \psi(x) = 0, \tag{1.2}$$

$\mu \in \mathbf{R}_+$ and $\lambda \in \mathbf{R}$ are the transform dilate and translate of the wavelet ψ and ψ^* being the complex conjugate of ψ. The optical diffraction transform is described by the Fresnel integration in [5, 9] as follows:

$$f_w(x_2) = \frac{1}{\sqrt{2\pi i \gamma_1}} \int_{\mathbf{R}} \exp\left[\frac{i}{2\gamma_1}\left(\alpha_1 x_1^2 - 2x_1 x_2 + \alpha_2 x_2^2\right)\right] f(x_1) dx_1. \tag{1.3}$$

The parameters (α_1, γ_1, γ_2, and α_2) are elements of more ray transfer Matrix M describing optical systems, $\alpha_1\alpha_2 - \gamma_1\gamma_2 = 1$. For a details of Fresnel integrals, see [14, 15].

Note that many familiar transforms can be considered as special cases of the diffraction Fresnel transform. For example, if the parameters α_1, γ_1, γ_2, and α_2 are written in the following matrix form:

$$\begin{pmatrix} \alpha_1 & \gamma_1 \\ \gamma_2 & \alpha_2 \end{pmatrix} = \begin{pmatrix} \cos\theta & \sin\theta \\ -\sin\theta & \cos\theta \end{pmatrix} \tag{1.4}$$

then the diffraction Fresnel transform, the generalized Fresnel Transform becomes a fractional Fourier transform, see [11, 16, 17].

In the present work, we consider a combined optical transform of Fresnel and wavelet transforms, namely, the optical Fresnel-wavelet transform defined by [9]

$$f_w(x_2) = \frac{1}{\sqrt{2\pi i \gamma_1}} \int_{\mathbf{R}} K_{\lambda,\mu,x_2}(x_1) f(x_1) dx. \tag{1.5}$$

with kernel

$$K_{\lambda,\mu,x_2}(x_1) = \exp\left(\frac{i}{2\gamma_1}\left(\frac{\alpha_1(x_1-\lambda)^2}{\mu^2} - \frac{2x_2(x_1-\lambda)}{\mu} + \alpha_2 x_2^2\right)\right). \tag{1.6}$$

The parameters α_1, γ_1, γ_2, and α_2 appearing in (1.5) are elements of 2×2 matrix with unit determinant.

As the general single-mode squeezing operator of the generalized Fresnel transform is in wave optics, further its applications are having a faithful representation in the optical Fresnel-wavelet transform, see [9]. Therefore the combined optical Fresnel-wavelet transform can be more conveniently studied by the general single-mode squeezed operation.

However, our discussion is somewhat different and making more interesting. Since the theory of the optical Fresnel-wavelet transform of generalized functions has not been reported in the literature. Thus, we extend the optical Fresnel-wavelet transform to a specific space of generalized functions, namely, known as Boehmian space. In Section 2, we observe that the kernel function of the Fresnel-wavelet transform is a smooth function, and therefore the optical Fresnel-wavelet transform is defined as an adjoint operator in the space of distributions. In a concrete way, Section 3 builds an appropriate space of Boehmians, whereas Section 4 constructs a new space of all images of Boehmians from Section 3. In Section 5, we define the optical Fresnel-wavelet transform of a Boehmian and study some of its general properties.

2. Optical Fresnel-Wavelet Transforms of Distributions

Let $\mathbb{E}(\mathbf{R})$ be the space of all test functions $\phi(x)$ of arbitrary support and $\mathbb{E}'(\mathbf{R})$ be its dual of distributions of bounded support, see, for example [12, 18–20]. Then, $\mathbb{E}(\mathbf{R})$ is a complete multinormed space with the set of norms as follows:

$$\xi_k(\phi)(x) = \sup_{x\in\mathbf{K}}\left|D_x^k\phi(x)\right|, \tag{2.1}$$

where $\mathbf{K}$ run through compact subsets of $\mathbf{R}$ and $\phi \in \mathbb{E}(\mathbf{R})$. It is clear that the kernel function of the optical Fresnel-wavelet transform

$$K_{\lambda,\mu,x_2}(x_1) = \exp\frac{i}{2\gamma_1}\left(\frac{\alpha_1(x_1-\lambda)^2}{\mu^2} - \frac{2x_2(x_1-\lambda)}{\mu} + \alpha_2 x_2^2\right) \tag{2.2}$$

for each $x_2, \lambda \in \mathbf{R}$, $\mu \in \mathbf{R}_+$ is an element of $\mathbb{E}(\mathbf{R})$. This describes the distributional optical Fresnel-wavelet transform of bounded support as an adjoint operator as follows:

$$f_w(x_2) = T_f(x_2) = \left\langle f(x_1), \exp\frac{i}{2\gamma_1}\left(\frac{\alpha_1(x_1-\lambda)^2}{\mu^2} - \frac{2x_2(x_1-\lambda)}{\mu} + \alpha_2 x_2^2\right)\right\rangle. \tag{2.3}$$

For convenience we sometimes write $T_f(x_2)$ instead of $f_w(x_2)$. Moreover, from (2.3), we observe that $T_f(x_2)$ is an analytic function satisfying the expression as follows:

$$D_{x_2}^k T_f(x_2) = \left\langle f(x_1), D_{x_2}^k K_{\lambda,\mu,x_2}(x_1)\right\rangle. \tag{2.4}$$

Further, $D_{x_2}^k T_f(x_2)$ is well defined since $D_{x_2}^k K_{\lambda,\mu,x_2}(x_1) \in \mathbb{E}(\mathbf{R})$, $K_{\lambda,\mu,x_2}(x_1)$ has its usual meaning where denoted by $*$ to be the usual convolution product [18, 20, 21]. Then we have the following lemma.

Lemma 2.1. *Let $f, g \in \mathbb{E}'(\mathbf{R})$ and $T_f = f_w(f(x))(x_2)$, $T_g = f_w(g(\tau))(x_2)$ be their respective optical Fresnel-wavelet transforms and $\lambda^2 = 2x\tau$ for all x and τ, then*

$$T_{f*g}(x_2) = \exp\frac{i}{2\gamma_1}\left(-\frac{2x_2\lambda}{\mu} - \alpha_2 x_2^2\right) T_f(x_2) T_g(x_2), \tag{2.5}$$

where $T_{f*g}(x_2) = f_w((f*g)(x))(x_2)$.

Proof. Let $f, g \in \mathbb{E}'(\mathbf{R})$, $T_f = f_w(f(x))(x_2)$, and $T_g = f_w(g(\tau))(x_2)$, and then

$$\begin{aligned} T_{f*g}(x_2) &= \left\langle (f*g)(x), \exp \frac{i}{2\gamma_1}\left(\frac{\alpha_1 (x-\lambda)^2}{\mu^2} - 2x_2 \frac{(x-\lambda)}{\mu} + \alpha_2 x_2^2\right)\right\rangle \\ \text{i.e.,} \quad &= \left\langle f(x), \left\langle g(\tau), \exp \frac{i}{2\gamma_1}\left(\frac{\alpha_1 (x+\tau-\lambda)^2}{\mu^2} - 2x_2 \frac{(x+\tau-\lambda)}{\mu} + \alpha_2 x_2^2\right)\right\rangle\right\rangle. \end{aligned} \tag{2.6}$$

Hence, using properties of distributions and simple calculations we get

$$T_{f*g}(x_2) = \exp \frac{i}{2\gamma_1}\left(-\frac{2x_2\lambda}{\mu} - \alpha_2 x_2^2\right) T_f(x_2) T_g(x_2). \tag{2.7}$$

The above theorem is known as the convolution theorem of the Fresnel-wavelet transform. □

Let δ be the dirac delta function. Then the Fresnel-wavelet transform of δ is described as follows:

$$T_\delta = f_w(\delta(x))(x_2) = \exp\left(\frac{i}{2\gamma_1}\left(\alpha_1 \frac{\lambda^2}{\mu^2} + \frac{2x_2\lambda}{\mu} + \alpha_2 x_2^2\right)\right), \tag{2.8}$$

Now e can easily deduce a corollary for the Lemma 2.1 as follows.

Corollary 2.2. *Let $f, g \in \mathbb{E}'(\mathbf{R})$ and δ be the dirac delta function, and then*

$$\begin{aligned} T_{f*\delta}(x_2) &= \exp \frac{i}{2\gamma_1}\left(\alpha_1 \frac{4\lambda^2 + 2x\tau}{\mu^2}\right) T_f(x_2), \\ T_{\delta*g}(x_2) &= \exp \frac{i}{2\gamma_1}\left(\alpha_1 \frac{4\lambda^2 + 2x\tau}{\mu^2}\right) T_g(x_2). \end{aligned} \tag{2.9}$$

Proof. It is a straightforward result of Lemma 2.1. □

Theorem 2.3. *The distributional optical Fresnel-wavelet transform f_w is linear.*

Proof. It is obvious. □

Lemma 2.4. *Let $f, g \in \mathbb{E}'(\mathbf{R})$, $T_g(x_2) = f_w(g(x))(x_2)$, $T_f(x_2) = f_w(f(\tau))(x_2)$, and then one has*

(1) $T_{(f*g)^{(k)}}(x_2) = \exp \dfrac{i}{2\gamma_1}\left(-\dfrac{2x_2\lambda}{\mu} - \alpha_2 x_2^2\right) T_{f^{(k)}}(x_2) T_g(x_2)$

(2) $T_{(f*g)^{(k)}}(x_2) = \exp \dfrac{i}{2\gamma_1}\left(-\dfrac{2x_2\lambda}{\mu} - \alpha_2 x_2^2\right) T_f(x_2) T_{g^{(k)}}(x_2)$.

Proof. It is a straightforward conclusion of the fact [20]. Consider

$$(f * g)^{(k)} = f^{(k)} * g = f * g^{(k)}. \tag{2.10}$$

□

3. The Boehmian Space $\mathbb{B}_1$

In this section, we assume that the reader is acquainted with the general construction of Boehmian spaces [6, 22–27]. Let $\mathbb{D}(\mathbf{R})$ be the Schwartz space of test functions of bounded support see [12, 20, 28]. The operation $\bullet$ between a distribution $f \in \mathbb{E}'(\mathbf{R})$ and a test function $\phi \in \mathbb{D}(\mathbf{R})$ is defined by

$$(f \bullet g)\psi(x) = f(g \odot \tau_x \psi), \tag{3.1}$$

where $\tau_x \psi(y) = \psi(x + y)$ and

$$(g \odot \tau_x \psi)(y) = \int_{\mathbf{R}} g(y) \tau_x \psi(y) dy. \tag{3.2}$$

A sequence (ϕ_n) of functions in $\mathbb{D}(\mathbf{R})$ is said to be a delta sequence if it satisfies Conditions (3.3)–(3.5). Consider

$$\int_{\mathbf{R}} \phi_n(x) dx = 1 \tag{3.3}$$

$$\int_{\mathbf{R}} \phi_n(x) dx \le M, \quad \exists M > 0, \tag{3.4}$$

$$\operatorname{supp} \phi_n \subset (-\varepsilon_n, \varepsilon_n) \longrightarrow 0 \quad \text{as } n \longrightarrow \infty. \tag{3.5}$$

The set of all such sequences is denoted by Δ. To see the extension to certain integral transform, see [29–31].

Lemma 3.1. *Given $\phi \in \mathbb{D}(\mathbf{R})$ and $\varphi \in \mathbb{E}(\mathbf{R})$ then*

$$\frac{d^k}{dx^k}(\phi \odot \tau_x \varphi) = \phi \odot \frac{d^k}{dx^k} \tau_x \varphi, \tag{3.6}$$

for each $k \in \mathbb{N}$.

Proof. We prove the lemma by induction on k. Let $k = 1$ and $\phi \in \mathbb{D}(\mathbf{R})$ with $\operatorname{supp} \phi \subset K$, and then

$$\frac{d}{dx}(\phi \odot \tau_x \varphi) = \lim_{x \to h} \frac{\phi \odot \tau_x \varphi - \phi \odot \tau_h \varphi}{x - h} = \phi \odot \lim_{x \to h} \frac{\tau_x \varphi - \tau_h \varphi}{x - h}. \tag{3.7}$$

Hence (3.7) reduces to

$$\frac{d}{dx}(\phi \odot \tau_x \varphi) = \phi \odot \frac{d}{dx}\tau_x \varphi. \tag{3.8}$$

□

Next, assume that the lemma satisfies for kth derivatives, then certainly we get

$$\frac{d^{k+1}}{dx^{k+1}}(\phi \odot \tau_x \varphi) = \frac{d}{dx}\left(\frac{d^k}{dx^k}(\phi \odot \tau_x \varphi)\right) = \phi \odot \frac{d^{k+1}}{dx^{k+1}}\tau_x \varphi, \tag{3.9}$$

by (3.7). Hence the lemmais as follows.

Lemma 3.2. *Let $\phi \in \mathbb{D}(\mathbf{R})$ and $\varphi \in \mathbb{E}(\mathbf{R})$, and then $\phi \odot \tau_x \varphi \in \mathbb{E}(\mathbf{R})$.*

Proof. Let K be a compact subset of $\mathbf{R}$. Then using Lemma 3.1 we get

$$\xi_k(\phi \odot \tau_x \varphi) \le \sup_{x \in K}\left|\frac{d^{k+1}}{dx^{k+1}}\tau_x \varphi\right|. \tag{3.10}$$

The inequality (3.10) can be explicitly expressed as

$$\xi_k(\phi \odot \tau_x \varphi) \le \xi_k(\varphi), \tag{3.11}$$

where ξ_k is the norm in the topology equipped with $\mathbb{E}(\mathbf{R})$. Hence, the lemma follows from (3.11). This completes the proof. □

Lemma 3.3. *Let $f \in \mathbb{E}'(\mathbf{R})$ and $\phi \in \mathbb{D}(\mathbf{R})$, and then $f \bullet \phi \in \mathbb{E}'(\mathbf{R})$.*

Proof. In view of Lemma 3.2 we get

$$f \odot \tau_x \phi \in \mathbb{E}(\mathbf{R}). \tag{3.12}$$

Therefore, the righthand side of (3.1) is meaningful. To show that $f \bullet \phi \in \mathbb{E}'(\mathbf{R})$ we are requested to show that $f \bullet \phi$ is continuous and linear. To establish continuity, let $(\psi_n) \to 0$ in $\mathbb{E}(\mathbf{R})$, then from (3.11) we get

$$\xi_k(f \odot \tau_x \psi_n) \le \xi_k(\psi_n) \longrightarrow 0 \quad \text{as } n \longrightarrow \infty. \tag{3.13}$$

□

Hence we have

$$(f \bullet \phi)\psi_n(x) = f(\phi \odot \tau_x \psi_n) \longrightarrow 0 \tag{3.14}$$

as $n \to \infty$. Linearity condition is obvious. Hence the lemma is completely proved.

Lemma 3.4. *Let $\phi_1, \phi_2 \in \mathbb{D}(\mathbf{R})$ and $\psi \in \mathbb{E}(\mathbf{R})$ be given, and then*

$$(\phi_1 * \phi_2) \odot \tau_x \psi = \phi_1 \bullet (\phi_2 \odot \tau_x \psi) \tag{3.15}$$

Proof. It is a straightforward consequence of definitions and change of variables. □

Lemma 3.5. *Let $\phi_1, \phi_2 \in \mathbb{D}(\mathbf{R})$ and $f \in \mathbb{E}'(\mathbf{R})$, and then*

$$f \bullet (\phi_1 * \phi_2) = (f \bullet \phi_1) \bullet \phi_2. \tag{3.16}$$

Proof. Using (3.1) and Lemma 3.4. we get

$$\begin{aligned} (f \bullet (\phi_1 * \phi_2))\psi(x) &= f((\phi_1 * \phi_2) \odot \tau_x \psi) \\ &= f(\phi_1 \bullet (\phi_2 \odot \tau_x \psi)) \\ &= (f \bullet \phi_1) \bullet \phi_2. \end{aligned} \tag{3.17}$$

Hence the lemma is as follows. □

Lemma 3.6. *Let $f_1, f_2 \in \mathbb{E}'(\mathbf{R})$ and $\phi \in \mathbb{D}(\mathbf{R})$, and then one has*

(1) $\alpha f \bullet \phi = \alpha(f \bullet \phi)$, $\alpha \in \mathbb{C}$

(2) $(f_1 + f_2) \bullet \phi = f_1 \bullet \phi + f_2 \bullet \phi$.

Proof. It is a straightforward result of definitions. □

Lemma 3.7. *Let $f_n \to f$ in $\mathbb{E}'(\mathbf{R})$ and $\phi \in \mathbb{D}(\mathbf{R})$ be given then*

$$f_n \bullet \phi \longrightarrow f \bullet \phi \quad \text{in } \mathbb{E}'(\mathbf{R}) \tag{3.18}$$

as $n \to \infty$.

Proof. By virtue of Lemma 3.2, $\phi \odot \tau_x \psi \in \mathbb{E}(\mathbf{R})$. Hence, using (3.1) we get

$$\begin{aligned} (f_n \bullet \phi - f \bullet \phi)\psi(x) &= ((f_n - f) \bullet \phi)\psi(x) \\ &= (f_n - f)(\phi \odot \tau_x \psi). \end{aligned} \tag{3.19}$$

Allowing $n \to \infty$ completes the proof of the lemma. □

Lemma 3.8. *Let $f \in \mathbb{E}'(\mathbf{R})$ and $(\phi_n) \in \Delta$, and then $f \bullet \phi \to f \in \mathbb{E}'(\mathbf{R})$.*

Proof. Considering a compact subset K of $\mathbf{R}$ and a sequence $(\phi_n) \in \Delta$ such that $\operatorname{supp} \phi_n \subset (-\varepsilon_n, \varepsilon_n)$ for each $n \in \mathbb{N}$, we show that $\phi \odot \tau_x \psi \to \psi(x)$ as $n \to \infty$ in the sense of $\mathbb{E}(\mathbf{R})$. By Lemma 3.1 we have

$$\left| \frac{d^k}{dx^k} (\phi \odot \tau_x \psi - \psi(x)) \right| \leq \int_{-\varepsilon_n}^{\varepsilon_n} \left| \frac{d^k}{dx^k} (\psi(x+y) - \psi(x)) \right| |\phi_n(y)| dy, \tag{3.20}$$

and by applying (3.4) we get

$$\left|\frac{d^k}{dx^k}(\phi \odot \tau_x \psi - \psi(x))\right| \le \int_{-\varepsilon_n}^{\varepsilon_n} M \left|\frac{d^k}{dx^k}(\psi(x+y) - \psi(x))\right| dx. \tag{3.21}$$

Then the mean value theorem implies that

$$\left|\frac{d^k}{dx^k}(\phi \odot \tau_x \psi - \psi(x))\right| \le \int_{-\varepsilon_n}^{\varepsilon_n} M|y| \left|\frac{d^{k+1}}{dx^{k+1}}\psi(x+\xi)\right| dy \tag{3.22}$$

for some $\xi \in (0, y)$. Let $A = \sup_{s \in K} |(d^{k+1}/ds^k)\psi(s)|$ then considering supremum over all $x \in K$ with the fact that $|y| \le \varepsilon_n$ yields

$$\xi_k(\phi \odot \tau_x \psi - \psi(x)) \le AM\varepsilon_n. \tag{3.23}$$

Now allowing $n \to \infty$ in (3.23) yields $\xi_k(\phi \odot \tau_x \psi - \psi(x)) \to 0$. Hence we have established that

$$\phi \odot \tau_x \psi \longrightarrow \psi(x). \tag{3.24}$$

On using (3.24) can be observed as

$$(f \bullet \phi_n)\psi(x) = f(\phi \odot \tau_x \psi) \longrightarrow f(\psi)(x) \quad \text{as } n \longrightarrow \infty. \tag{3.25}$$

This implies that $f \bullet \phi_n \to f$ as $n \to \infty$. The proof is therefore completed. □

Finally, by virtue of the above sequence of results (Lemma 3.1–3.8), our desired Boehmian space $\mathbb{B}_1$ is well defined.

4. The Boehmian Space $\mathbb{B}_{\mathbb{F}_w}$

In this section we construct the space of all Fresnel-wavelet transforms of Boehmians from the space $\mathbb{B}_1$ as follows.

Let $\mathbb{F}_w(\mathbf{R})$ be the space of all analytic functions which are Fresnel-wavelet transforms of distributions in $\mathbb{E}'(\mathbf{R})$. Then, we define convergence as follows. We say $T_n \to T$ in $\mathbb{F}_w(\mathbf{R})$ if and only if there are $f_n, f \in \mathbb{E}'(\mathbf{R})$ such that $f_n \to f$ in $\mathbb{E}'(\mathbf{R})$, where $T_n = f_w f_n$ and $T = f_w f$. Let $T \in \mathbb{F}_w(\mathbf{R})$ and $\phi \in \mathbb{D}(\mathbf{R})$ be given, and then define

$$(T \star \phi)(x_2) = \phi \odot \tau_{x_2} T. \tag{4.1}$$

Theorem 4.1. *Let $f \in \mathbb{E}'(\mathbf{R})$ and $\phi \in \mathbb{D}(\mathbf{R})$, and then $f_w(f \bullet \phi) = T \star \phi$, where $T = f_w f$.*

Proof. By the aid of (2.3) we write

$$f_w(f \bullet \phi)(x_2) = \langle f \bullet \phi, K_{\lambda,\mu,x_2}(x_1)\rangle. \tag{4.2}$$

By using (3.1) we get

$$f_w(f \bullet \phi)(x_2) = f(\phi \odot \tau_{x_2} K_{\lambda,\mu,x_2}(x_1)) = \phi(f \odot \tau_{x_2} K_{\lambda,\mu,x_2}(x_1)). \tag{4.3}$$

That is $f_w(f \bullet \phi)(x_2) = \phi \odot \tau_{x_2} T$. Employing (4.1) yields $f_w(f \bullet \phi)(x_2) = (T \star \phi)(x_2)$, where $T = f_w f$. This proves the theorem. □

Lemma 4.2. *Let $T \in \mathbb{F}_w(\mathbf{R})$ and $\phi \in \mathbb{D}(\mathbf{R})$, and then $T \star \phi \in \mathbb{F}_w(\mathbf{R})$.*

Proof. Let $f \in \mathbb{E}'(\mathbf{R})$ be such that $T = f_w f$, and that then Theorem 4.1 implies

$$T \star \phi = f_w(f \bullet \phi). \tag{4.4}$$

Thus $T \star \phi \in \mathbb{F}_w(\mathbf{R})$ by Lemma 3.3. Hence the lemma. □

Lemma 4.3. *Let $T \in \mathbb{F}_w(\mathbf{R})$ and $\phi \in \mathbb{D}(\mathbf{R})$, and then $f_w^{-1}(T \star \phi) = f \bullet \phi$.*

Proof. Theorem 4.1 implies that $f_w^{-1}(T \star \phi) = f_w^{-1}(f_w(f \bullet \phi)) = f \bullet \phi$. This completes the proof of the lemma. □

Lemma 4.4. *Let $T_1, T_2 \in \mathbb{F}_w(\mathbf{R})$ and $\phi_1, \phi_2 \in \mathbb{D}(\mathbf{R})$, then*

(1) $(\alpha T_1 + \beta T_2) \star \phi = \alpha T_1 \star \phi + \beta T_2 \star \phi$,

(2) $T \star (\phi_1 \star \phi_2) = (T \star \phi_1) \star \phi_2$.

Proof. It is obvious. □

Lemma 4.5. (i) *Let $T_n \rightarrow T$ as $n \rightarrow \infty$ and $\phi \in \mathbb{D}(\mathbf{R})$, and then $T_n \star \phi \rightarrow T \star \phi$ as $n \rightarrow \infty$ in $\mathbb{F}_w(\mathbf{R})$.*

(ii) *Let $T_n \rightarrow T$ as $n \rightarrow \infty$ and $(\phi_n) \in \Delta$, and then $T_n \star \phi_n \rightarrow T$ as $n \rightarrow \infty$ in $\mathbb{F}_w(\mathbf{R})$.*

Proof. (i) Let $T_n, T \in \mathbb{F}_w(\mathbf{R})$ then $T = f_w f$ and $T_n = f_w f_n$ for some $f, f_n \in \mathbb{E}'(\mathbf{R})$. Hence, using Theorem 4.1, we have

$$T_n \star \phi = f_w f_n \star \phi = f_w(f_n \bullet \phi). \tag{4.5}$$

By Lemma 3.7 we get

$$T_n \star \phi \longrightarrow f_w(f \bullet \phi). \tag{4.6}$$

Once again Theorem 4.1 implies that

$$T_n \star \phi \longrightarrow f_w f \star \phi. \tag{4.7}$$

Thus we ahve

$$T_n \star \phi \longrightarrow T \star \phi. \tag{4.8}$$

This proves part (i) of the Lemma.

(ii) can be proved similarly by using Lemma 3.8 and Theorem 4.1. The space $\mathbb{B}_{\mathbb{F}_w}$ is therefore established. □

The sum of two Boehmians and multiplication by a scalar in $\mathbb{B}_{\mathbb{F}_w}$ is defined in a natural way as follows:

$$\begin{gathered}\left[\frac{f_n}{\phi_n}\right] + \left[\frac{g_n}{\psi_n}\right] = \left[\frac{(f_n \star \psi_n) + (g_n \star \phi_n)}{\phi_n \star \psi_n}\right], \\ \alpha\left[\frac{f_n}{\phi_n}\right] = \left[\alpha\frac{f_n}{\phi_n}\right], \quad \alpha \in \mathbb{C}.\end{gathered} \tag{4.9}$$

The operation $\star$ and the differentiation are defined by

$$\left[\frac{f_n}{\phi_n}\right] \star \left[\frac{g_n}{\psi_n}\right] = \left[\frac{f_n \star g_n}{\phi_n \star \psi_n}\right], \qquad D^\alpha\left[\frac{f_n}{\phi_n}\right] = \left[\frac{D^\alpha f_n}{\phi_n}\right]. \tag{4.10}$$

5. Optical Fresnel-Wavelet Transforms of Boehmians

In view of the analysis obtained in Sections 4 and 5 and Theorem 4.1 we are led to state the following definition.

Definition 5.1. Let $[f_n/\phi_n\ ] \in \mathbb{B}_1$, and then

$$\mathfrak{F}_w^{-1}\left[\frac{T_{f_n}}{\phi_n}\right] = \left[\frac{T_{f_n}^{-1}}{\phi_n}\right], \qquad \mathfrak{F}_w\left[\frac{f_n}{\phi_n}\right] = \left[\frac{T_{f_n}}{\phi_n}\right], \tag{5.1}$$

for each $(\phi_n) \in \Delta$, where $T_{f_n} = f_w f_n$.

Lemma 5.2. *The optical Fresnel-wavelet transform $\mathfrak{F}_w : \mathbb{B}_1 \to \mathbb{B}_{\mathbb{F}_w}$ is well defined.*

Proof. It is a straightforward. □

Lemma 5.3. *The optical Fresnel-wavelet transform $\mathfrak{F}_w : \mathbb{B}_1 \to \mathbb{B}_{\mathbb{F}_w}$ is linear.*

Proof. It is straightforward by using Definition 5.1. □

Lemma 5.4. *The optical Fresnel-wavelet transform $\mathfrak{F}_w : \mathbb{B}_1 \to \mathbb{B}_{\mathbb{F}_w}$ is an isomorphism.*

Proof. Assume that $\mathfrak{F}_w[f_n/\phi_n] = \mathfrak{F}_w[g_n/\psi_n]$, and then using (5.1) and the concept of quotients we get $T_{f_n} \star \psi_m = T_{g_m} \star \phi_n$, where $T_{f_n} = f_w f_n$ and $T_{g_m} = f_w g_m$. Therefore, Theorem 4.1 implies that $f_w(f_n \bullet \psi_m) = f_w(g_m \bullet \phi_n)$. Properties of f_w imply that $f_n \bullet \psi_m = g_m \bullet \phi_n$. Therefore,

$[f_n/\phi_n] = [g_n/\psi_n]$. To establish f_w is surjective, and let $[T_{f_n}/\phi_n] \in \mathbb{B}_{F_w}$. Then $T_{f_n} \star \phi_m = T_{f_m} \star \phi_n$ for every $m, n \in \mathbb{N}$. Hence $f_n, f_m \in \mathbb{E}'(\mathbf{R})$ are such that $T_{f_n} = f_w f_n$ and $T_{f_m} = f_w f_m$. Theorem 4.1 implies that $f_w(f_n \bullet \phi_m) = f_w(f_m \bullet \phi_n)$. Hence $[f_n/\phi_n] \in \mathbb{B}_1$ is such that $\mathfrak{F}_w[f_n/\phi_n] = [T_{f_n}/\phi_n\ ]$. This completes the proof of the lemma. □

Now, Let $[f_n/\phi_n] \in \mathbb{B}_1$, and then we define the inverse optical Fresnel-wavelet transform of $[f_n/\phi_n]$ as

$$\mathfrak{F}_w^{-1}\left[\frac{f_n}{\phi_n}\right] = \left[\frac{T_{f_n}^{-1}}{\phi_n}\right], \tag{5.2}$$

where $T_{f_n}^{-1} = f_w^{-1} f_{\mathrm{n}}$.

Lemma 5.5. *Let* $[T_{f_n}/\phi_n] \in \mathbb{B}_{\mathbb{F}_w}$, $T_{f_n} = f_w f_n$, *and* $\phi \in \mathbb{D}(\mathbb{R})$ *then*

$$\mathfrak{F}_w^{-1}\left(\left[\frac{T_{f_n}}{\phi_n}\right] \star \phi\right) = \left[\frac{T_{f_n}^{-1}}{\phi_n}\right] \bullet \phi, \qquad \mathfrak{F}_w\left(\left[\frac{f_n}{\phi_n}\right] \bullet \phi\right) = \left[\frac{T_{f_n}}{\phi_n}\right] \star \phi. \tag{5.3}$$

Proof. Applying Definition 5.1 yields

$$\mathfrak{F}_w^{-1}\left(\left[\frac{T_{f_n}}{\phi_n}\right] \star \phi\right) = \mathfrak{F}_w^{-1}\left(\left[\frac{T_{f_n} \star \phi}{\phi_n}\right]\right) = \left[\frac{f_w^{-1}(T_{f_n} \star \phi)}{\phi_n}\right]. \tag{5.4}$$

Using Lemma 4.3 we obtain

$$\mathfrak{F}_w^{-1}\left(\left[\frac{T_{f_n}}{\phi_n}\right] \star \phi\right) = \left[\frac{f_w^{-1} T_{f_n}}{\phi_n}\right] \bullet \phi = \left[\frac{T_{f_n}^{-1}}{\phi_n}\right] \bullet \phi. \tag{5.5}$$

This completes the proof of the Lemma. □

Theorem 5.6. $\mathfrak{F}_w : \mathbb{B}_1 \to \mathbb{B}_{\mathbb{F}_w}$ *and* $\mathfrak{F}_w^{-1} : \mathbb{B}_{\mathbb{F}_w} \to \mathbb{B}_1$ *are continuous with respect to* δ *and* Δ *convergences.*

Proof. First of all, we show that $\mathfrak{F}_w : \mathbb{B}_1 \to \mathbb{B}_{\mathbb{F}_w}$ and $\mathfrak{F}_w^{-1} : \mathbb{B}_{\mathbb{F}_w} \to \mathbb{B}_1$ are continuous with respect to δ convergence.

Let $\beta_n \xrightarrow{\delta} \beta$ in $\mathbb{B}_1$ as $n \to \infty$, and then we show that $\mathfrak{F}_w \beta_n \to \mathfrak{F}_w \beta$ as $n \to \infty$. By virtue of [25] we can find $f_{n,k}$ and f_k in $\mathbb{E}'(\mathbf{R})$ such that

$$\beta_n = \left[\frac{f_{n,k}}{\phi_k}\right], \qquad \beta = \left[\frac{f_k}{\phi_k}\right] \tag{5.6}$$

such that $f_{n,k} \to f_k$ as $n \to \infty$ for every $k \in \mathbb{N}$. Employing the continuity condition of the optical Fresnel-wavelet transform implies that $T_{f_{n,k}} \to T_{f_k}$ as $n \to \infty$ in the space $\mathbb{F}_w(\mathbf{R})$. Thus, $[T_{f_{n,k}}/\phi_k] \to [T_{f_k}/\phi_k]$ as $n \to \infty$ in $\mathbb{B}_{\mathbb{F}_w}$.

To prove the second part, let $g_n \xrightarrow{\delta} g$ in $\mathbb{B}_{\mathbb{F}_w}$ as $n \to \infty$. Then, once again, by [4], $g_n = [T_{f_{n,k}}/\phi_k]$ and $g = [T_{f_k}/\phi_k]$ for some $T_{f_{n,k}}, T_{f_k} \in \mathbb{F}_w(\mathbf{R})$ and $T_{f_{n,k}} \to T_{f_k}$ as $n \to \infty$. Hence $f_w^{-1}T_{f_{n,k}} \to f_w^{-1}T_{f_k}$ in $\mathbb{B}_1$ as $n \to \infty$. Or, $[T_{f_{n,k}}^{-1}/\phi_k] \to [T_{f_k}^{-1}/\phi_k]$ as $n \to \infty$. Using Definition 5.1 we get $\mathfrak{F}_w^{-1}[T_{f_{n,k}}/\phi_k] \to \mathfrak{F}_w^{-1}[T_{f_k}/\phi_k]$ as $n \to \infty$.

Now, we establish continuity of $\mathfrak{F}_w$ and $\mathfrak{F}_w^{-1}$ with respect to Δ convergence. Let $\beta_n \xrightarrow{\Delta} \beta$ in $\mathbb{B}_1$ as $n \to \infty$. Then, there exist $f_n \in \mathbb{E}'(\mathbf{R})$ and $\phi_n \in \Delta$ such that $(\beta_n - \beta) \bullet \phi_n = [(f_n \bullet \phi_k)/\phi_k]$ and $f_n \to 0$ as $n \to \infty$. Employing Definition 5.1 we get

$$\mathfrak{F}_w((\beta_n - \beta) \bullet \phi_n) = \left[\frac{f_w(f_n \bullet \phi_k)}{\phi_k}\right]. \tag{5.7}$$

Hence, from Lemma 4.2 we have $\mathfrak{F}_w((\beta_n - \beta) \bullet \phi_n) = [(T_{f_n} \star \phi_k)/\phi_k] = T_{f_n} \to 0$ as $n \to \infty$ in $\mathbb{F}_w$. Therefore consider

$$\mathfrak{F}_w((\beta_n - \beta) \bullet \phi_n) = (\mathfrak{F}_w\beta_n - \mathfrak{F}_w\beta) \star \phi_n \longrightarrow 0 \quad \text{as } n \longrightarrow \infty. \tag{5.8}$$

Hence, $\mathfrak{F}_w\beta_n \xrightarrow{\Delta} \mathfrak{F}_w\beta$ as $n \to \infty$. Finally, let $g_n \xrightarrow{\Delta} g$ in $\mathbb{B}_{\mathbb{F}_w}$ as $n \to \infty$, and then we find $T_{f_k} \in \mathbb{F}_w(\mathbf{R})$ such that $(g_n - g) \star \phi_n = [(T_{f_k} \star \phi_k)/\phi_k]$ and $T_{f_k} \to 0$ as $n \to \infty$ for some $(\phi_n) \in \Delta$ and $T_{f_k} = f_w f_n$. Now, using Definition 5.1, we obtain that

$$\mathfrak{F}_w^{-1}((g_n - g) \star \phi_n) = \left[\frac{f_w^{-1}(T_{f_k} \star \phi_k)}{\phi_k}\right]. \tag{5.9}$$

Lemma 5.5 implies that

$$\mathfrak{F}_w^{-1}((g_n - g) \star \phi_n) = \left[\frac{f_n \bullet \phi_k}{\phi_k}\right] = f_n \longrightarrow 0 \quad \text{as } n \longrightarrow \infty \text{ in } \mathbb{E}'(\mathbf{R}). \tag{5.10}$$

Thus we have

$$\mathfrak{F}_w^{-1}((g_n - g) \star \phi_n) = \left(\mathfrak{F}_w^{-1}g_n - \mathfrak{F}_w^{-1}g\right) \bullet \phi_n \longrightarrow 0 \quad \text{as } n \longrightarrow \infty. \tag{5.11}$$

From this we find that $\mathfrak{F}_{\mathrm{w}}^{-1}g_n \xrightarrow{\Delta} \mathfrak{F}_w^{-1}g$ as $n \to \infty$ in $\mathbb{B}_1$. This completes the proof of the theorem. □

Acknowledgment

The authors would like to express their sincere thanks and gratitude to the reviewer(s) for their valuable comments and suggestions for the improvement of this paper.

References

[1] P. K. Banerji, S. K. Al-Omari, and L. Debnath, "Tempered distributional Fourier sine (cosine) transform," *Integral Transforms and Special Functions*, vol. 17, no. 11, pp. 759–768, 2006.

[2] J. W. Goodman, *Introductionto Fourier Optics*, Mc Graw-Hill, New York, NY, USA, 1972.

[3] H.-Y. Fan and H. L. Lu, "Wave-function transformations by general SU(1, 1) single-mode squeezing and analogy to Fresnel transformations in wave optics," *Optics Communications*, vol. 258, no. 1, pp. 51–58, 2006.

[4] H.-Y. Fan and L. Y. Hu, "Optical Fresnel transformation and quantum tomography," *Optics Communications*, vol. 282, no. 18, pp. 3734–3736, 2009.

[5] H. Kogelink, "On the propagation of Gaussian beams of light through Lenslike media including those with a loss or gain variation," *Applied Optics*, vol. 4, pp. 121562–121569, 1965.

[6] A. W. Lohmann, "Image rotation, Wigner rotation, and the fractional Fourier transform," *Journal of the Optical Society of America A*, vol. 10, no. 10, pp. 2181–2186, 1993.

[7] A. C. McBride and F. H. Kerr, "On Namias's fractional Fourier transforms," *IMA Journal of Applied Mathematics*, vol. 39, no. 2, pp. 159–175, 1987.

[8] P. Mikusiński, "Fourier transform for integrable Boehmians," *The Rocky Mountain Journal of Mathematics*, vol. 17, no. 3, pp. 577–582, 1987.

[9] H. Ozaktas and D. Mendlovic, "Fractional Fourier transforms and their optical implementation. II," *Journal of the Optical Society of America A*, vol. 10, no. 12, pp. 2522–2531, 1993.

[10] M. Moshinsky and C. Quesne, "Linear canonical transformations and their unitary representations," *Journal of Mathematical Physics*, vol. 12, 9 pages, 1971.

[11] S. K. Q. Al-Omari and A. Kılıçman, "On diffraction Fresnel transforms for Boehmians," *Abstract and Applied Analysis*, vol. 2011, Article ID 712746, 11 pages, 2011.

[12] M. Holschneider, *Wavelets, an Analysis Tool*, Oxford Mathematical Monographs, The Clarendon Press, Oxford, UK, 1995.

[13] M. Holschneider, "Wavelet analysis on the circle," *Journal of Mathematical Physics*, vol. 31, no. 1, pp. 39–44, 1990.

[14] A. Kılıçman, "On the Fresnel sine integral and the convolution," *International Journal of Mathematics and Mathematical Sciences*, no. 37, pp. 2327–2333, 2003.

[15] A. Kılıçman and B. Fisher, "On the Fresnel integrals and the convolution," *International Journal of Mathematics and Mathematical Sciences*, no. 41, pp. 2635–2643, 2003.

[16] L. M. Bernardo and O. D. Soaares, "Fractional Fourier transform and optical systems," *Optics Communications*, vol. 110, pp. 517–522, 1994.

[17] L. Mertz, *Transformations in Optics*, Wiley, New York, NY, USA, 1965.

[18] A. Kılıçman, "A comparison on the commutative neutrix convolution of distributions and the exchange formula," *Czechoslovak Mathematical Journal*, vol. 51(126), no. 3, pp. 463–471, 2001.

[19] A. Kılıçman, "On the commutative neutrix product of distributions," *Indian Journal of Pure and Applied Mathematics*, vol. 30, no. 8, pp. 753–762, 1999.

[20] R. Roopkumar, "Mellin transform for Boehmians," *Bulletin of the Institute of Mathematics. Academia Sinica*, vol. 4, no. 1, pp. 75–96, 2009.

[21] H. Eltayeb, A. Kılıçman, and B. Fisher, "A new integral transform and associated distributions," *Integral Transforms and Special Functions*, vol. 21, no. 5-6, pp. 367–379, 2010.

[22] S. K. Q. Al-Omari, D. Loonker, P. K. Banerji, and S. L. Kalla, "Fourier sine (cosine) transform for ultradistributions and their extensions to tempered and ultraBoehmian spaces," *Integral Transforms and Special Functions*, vol. 19, no. 5-6, pp. 453–462, 2008.

[23] T. K. Boehme, "The support of Mikusiński operators," *Transactions of the American Mathematical Society*, vol. 176, pp. 319–334, 1973.

[24] D. Mendlovic and H. M. Ozaktas, "Fractional Fourier transforms and their optical implementation: I," *Journal of the Optical Society of America A*, vol. 10, no. 9, pp. 1875–1881, 1993.

[25] P. Mikusiński, "Tempered Boehmians and ultradistributions," *Proceedings of the American Mathematical Society*, vol. 123, no. 3, pp. 813–817, 1995.

[26] V. Namias, "The fractional order Fourier transform and its application to quantum mechanics," *Journal of the Institute of Mathematics and its Applications*, vol. 25, no. 3, pp. 241–265, 1980.

[27] R. S. Pathak, *Integral Transforms of Generalized Functions and Their Applications*, Gordon and Breach Science, Amsterdam, The Netherlands, 1997.

[28] B. Fisher and A. Kılıçman, "A commutative neutrix product of ultradistributions," *Integral Transforms and Special Functions*, vol. 4, no. 1-2, pp. 77–82, 1996.

[29] S. Al-Omari, “The generalized stieltjes and Fourier transforms of certain spaces of generalized functions,” *The Jordanian Journal of Mathematics and Statistics*, vol. 2, no. 2, pp. 55–66, 2009.

[30] S. K. Q. Al-Omari, “On the distributional Mellin transformation and its extension to Boehmian spaces,” *International Journal of Contemporary Mathematical Sciences*, vol. 6, no. 17-20, pp. 801–810, 2011.

[31] S. K. Q. Al-Omari, “A Mellin transform for a space of Lebesgue integrable Boehmians,” *International Journal of Contemporary Mathematical Sciences*, vol. 6, no. 29-32, pp. 1597–1606, 2011.

Hindawi Publishing Corporation
Journal of Function Spaces and Applications
Volume 2012, Article ID 945467, 15 pages
doi:10.1155/2012/945467

Research Article

Positive Periodic Solutions for Second-Order Ordinary Differential Equations with Derivative Terms and Singularity in Nonlinearities

Yongxiang Li and Xiaoyu Jiang

Department of Mathematics, Northwest Normal University, Lanzhou 730070, China

Correspondence should be addressed to Yongxiang Li, liyxnwnu@163.com

Received 17 July 2012; Accepted 26 August 2012

Academic Editor: Gabriel N. Gatica

The existence results of positive ω-periodic solutions are obtained for the second-order ordinary differential equation $u''(t) = f(t, u(t), u'(t)), t \in \mathbb{R}$ where, $f : \mathbb{R} \times (0, \infty) \times \mathbb{R} \to \mathbb{R}$ is a continuous function, which is ω-periodic in t and $f(t, u, v)$ may be singular at $u = 0$. The discussion is based on the fixed point index theory in cones.

1. Introduction

In this paper, we discuss the existence of positive ω-periodic solutions of the second-order ordinary differential equation with first-order derivative term in the nonlinearity

$$u''(t) = f\big(t, u(t), u'(t)\big), \quad t \in \mathbb{R}, \tag{1.1}$$

where the nonlinearity $f : \mathbb{R} \times (0, \infty) \times \mathbb{R} \to \mathbb{R}$ is a continuous function, which is ω-periodic in t and $f(t, u, v)$ may be singular at $u = 0$.

The existence problems of periodic solutions for nonlinear second-order ordinary differential equations have attracted many authors' attention and concern, and most works are on the special equation

$$u''(t) = f(t, u(t)), \quad t \in \mathbb{R}, \tag{1.2}$$

that does not contain explicitly first-order derivative term in nonlinearity. Many theorems and methods of nonlinear functional analysis have been applied to the periodic problems of

(1.2). These theorems and methods are mainly the upper and lower solutions method and monotone iterative technique [1–4], the continuation method of topological degree [5–7], variational method and critical point theory, [8–10] and so forth.

In recent years, the fixed point theorems of cone mapping, especially the fixed point theorem of Krasnoselskii's cone expansion or compression type, have been extensively applied to two-point boundary value problems of second-order ordinary differential equations, and some results of existence and multiplicity of positive solutions have been obtained, see [11–15]. Lately, the authors of [16–18] have also applied the Krasnoselskii's fixed point theorem to periodic problems of second-order nonlinear ordinary differential equations, and obtained existence results of positive periodic solutions. In these works, the new discovered positivity of Green function of the corresponding linear second-order periodic boundary value problems plays an important role. The positivity guarantees that the integral operators of the second-order periodic problems are cone-preserving in the cone

$$K_0 = \{u \in C[0,\omega] \mid u(t) \geq \sigma\|u\|, t \in [0,\omega]\} \tag{1.3}$$

in the Banach space $C[0,\omega]$, where $\sigma > 0$ is a constant. Hence the fixed point theorems of cone mapping can be applied to the second-order periodic problems. For more precise results using the theory of the fixed point index in cones to discuss the existence of positive periodic solutions of second-order ordinary differential equation, see [19–22]. However, all of these works are on the special second-order equation (1.2), and few people consider the existence of the positive periodic solutions for the general second-order equation (1.1) that explicitly contains the first order derivative term.

The purpose of this paper is to extend the results of [16–22] to the general second-order equation (1.1). We will use the theory of the fixed point index in cones to discuss the existence of positive periodic solutions of (1.1). For the periodic problem of (1.1), since the corresponding integral operator has no definition on the cone K_0 in $C[0,\omega]$, the argument methods used in [16–22] are not applicable. We will use a completely different method to treat (1.1). Our main results will be given in Section 3. Some preliminaries to discuss (1.1) are presented in Section 2.

2. Preliminaries

Let $C_\omega(\mathbb{R})$ denote the Banach space of all continuous ω-periodic function $u(t)$ with norm $\|u\|_C = \max_{0\leq t\leq\omega}|u(t)|$. Let $C^1_\omega(\mathbb{R})$ be the Banach space of all continuous differentiable ω-periodic function $u(t)$ with the norm

$$\|u\|_{C^1} = \|u\|_C + \|u'\|_C. \tag{2.1}$$

Generally, $C^n_\omega(\mathbb{R})$ denotes the nth-order continuous differentiable ω-periodic function space for $n \in \mathbb{N}$. Let $C^+_\omega(\mathbb{R})$ be the cone of all nonnegative functions in $C_\omega(\mathbb{R})$.

Let $M \in (0,\ \pi^2/\omega^2)$ be a constant. For $h \in C_\omega(\mathbb{R})$, we consider the linear second-order differential equation

$$u''(t) + Mu(t) = h(t), \quad t \in \mathbb{R}. \tag{2.2}$$

The ω-periodic solutions of (2.2) are closely related with the linear second-order boundary value problem

$$\begin{gathered} u''(t) + Mu(t) = 0, \qquad 0 \le t \le \omega, \\ u(0) - u(\omega) = 0, \qquad u'(0) - u'(\omega) = 1, \end{gathered} \tag{2.3}$$

see [19]. It is easy to see that Problem (2.3) has a unique solution, which is explicitly given by

$$U(t) = \frac{\cos\beta(t - \omega/2)}{2\beta\sin(\beta\omega/2)}, \qquad 0 \le t \le \omega, \tag{2.4}$$

where $\beta = \sqrt{M}$. We have the following Lemma.

Lemma 2.1. *Let $M \in (0, \pi^2/\omega^2)$. Then for every $h \in C_\omega(\mathbb{R})$, the linear equation* (2.2) *has a unique ω-periodic solution $u(t)$, which is given by*

$$u(t) = \int_{t-\omega}^{t} U(t-s)h(s)ds := Sh(t), \quad t \in \mathbb{R}. \tag{2.5}$$

Moreover, $S : C_\omega(\mathbb{R}) \to C^1_\omega(\mathbb{R})$ is a completely continuous linear operator.

Proof. Taking the derivative in (2.5) and using the boundary condition of $U(t)$, we obtain that

$$\begin{aligned} u''(t) &= \left(U'(0) - U'(\omega)\right)h(t) + \int_{t-\omega}^{t} U''(t-s)h(s)ds \\ &= h(t) - M\int_{t-\omega}^{t} U(t-s)h(s)ds \\ &= h(t) - Mu(t). \end{aligned} \tag{2.6}$$

Therefore, $u(t)$ satisfies (2.2). Let $\tau = s + \omega$; it follows from (2.5) that

$$\begin{aligned} u(t) &= \int_{t}^{t+\omega} U(t+\omega-\tau)h(\tau-\omega)d\tau \\ &= \int_{t}^{t+\omega} U(t+\omega-\tau)h(\tau)d\tau = u(t+\omega). \end{aligned} \tag{2.7}$$

Hence, $u(t)$ is an ω-periodic solution of (2.2). From the maximum principle for second-order periodic boundary value problems [4], it is easy to see that $u(t)$ is the unique ω-periodic solution of (2.2).

From (2.5) and (2.6), we easily see that $S : C_\omega(\mathbb{R}) \to C^2_\omega(\mathbb{R})$ is a linear bounded operator. By the compactness of the embedding $C^2_\omega(\mathbb{R}) \hookrightarrow C^1_\omega(\mathbb{R})$, $S : C_\omega(\mathbb{R}) \to C^1_\omega(\mathbb{R})$ is a completely continuous operator. □

Since $U(t) > 0$ for every $t \in [0,\omega]$, by (2.5), if $h \in C_\omega^+(\mathbb{R})$ and $h(t) \not\equiv 0$, then the ω-periodic solution of (2.2) $u(t) > 0$ for every $t \in \mathbb{R}$, and we term it the positive ω-periodic solution. Let

$$\overline{U} = \max_{0\le t\le\omega} U(t) = \frac{1}{2\beta\sin(\beta\omega/2)}, \qquad \underline{U} = \min_{0\le t\le\omega} U(t) = \frac{\cos(\beta\omega/2)}{2\beta\sin(\beta\omega/2)},$$
$$\overline{U}_1 = \max_{0\le t\le\omega}\left|U'(t)\right| = \max_{0\le t\le\omega}\frac{\left|\sin\beta(t-\omega/2)\right|}{2\sin(\beta\omega/2)} = \frac{1}{2}, \tag{2.8}$$
$$\sigma = \frac{\underline{U}}{\overline{U}} = \cos\frac{\beta\omega}{2}, \qquad C_0 = \frac{\overline{U}_1}{\underline{U}} = \beta\tan\frac{\beta\omega}{2}.$$

Define the cone K in $C_\omega^1(\mathbb{R})$ by

$$K = \left\{u \in C_\omega^1(\mathbb{R}) \mid u(t) \ge \sigma\|u\|_C, \left|u'(t)\right| \le C_0|u(t)|, t \in \mathbb{R}\right\}. \tag{2.9}$$

We have the following Lemma.

Lemma 2.2. *Let $M \in (0, \pi^2/\omega^2)$. Then for every $h \in C_\omega^+(\mathbb{R})$, the positive ω-periodic solution of* (2.2) *$u = Sh \in K$. Namely, $S(C_\omega^+(\mathbb{R})) \subset K$.*

Proof. Let $h \in C_\omega^+(\mathbb{R})$, $u = Sh$. For every $t \in \mathbb{R}$, from (2.5) it follows that

$$u(t) = \int_{t-\omega}^{t} U(t-s)h(s)ds \le \overline{U}\int_{t-\omega}^{t} h(s)ds = \overline{U}\int_0^\omega h(s)ds, \tag{2.10}$$

and therefore,

$$\|u\|_C \le \overline{U}\int_0^\omega h(s)ds. \tag{2.11}$$

Using (2.5), we obtain that

$$u(t) = \int_{t-\omega}^{t} U(t-s)h(s)ds \ge \underline{U}\int_{t-\omega}^{t} h(s)ds = \underline{U}\int_0^\omega h(s)ds \ge \sigma\|u\|_C. \tag{2.12}$$

For every $t \in \mathbb{R}$, since

$$u'(t) = \int_{t-\omega}^{t} U'(t-s)h(s)ds, \tag{2.13}$$

we have

$$\begin{aligned}|u'(t)| &\leq \int_{t-\omega}^{t} |U'(t-s)| h(s)ds \leq \overline{U}_1 \int_{t-\omega}^{t} h(s)ds \\ &= \overline{U}_1 \int_{0}^{\omega} h(s)ds = C_0 \, \underline{U} \int_{0}^{\omega} h(s)ds \leq C_0 u(t).\end{aligned} \tag{2.14}$$

Hence, $u \in K$. □

Now we consider the nonlinear equation (1.1). Hereafter, we assume that the nonlinearity f satisfies the following condition.

(F0) There exists $M \in (0, \pi^2/\omega^2)$ such that

$$f(t, x, y) + Mx \geq 0, \quad x > 0, \ t, y \in \mathbb{R}. \tag{2.15}$$

Let $f_1(t, x, y) = f(t, x, y) + Mx$, then $f_1(t, x, y) \geq 0$ for $x > 0$, $t, y \in \mathbb{R}$, and (1.1) is rewritten to

$$u''(t) + Mu(t) = f_1(t, u(t), u'(t)), \quad t \in \mathbb{R}. \tag{2.16}$$

For $u \in K$, if $u \neq 0$, then $\|u\|_C > 0$ and by the definition of K, $u(t) \geq \sigma \|u\|_C > 0$ for every $t \in \mathbb{R}$. Hence

$$F(u)(t) := f_1(t, u(t), u'(t)), \quad t \in \mathbb{R} \tag{2.17}$$

is well defined, and we can define the integral operator $A : K \setminus \{0\} \to C^1_\omega(\mathbb{R})$ by

$$Au(t) = \int_{t-\omega}^{t} U(t-s) f_1(s, u(s), u'(s)) ds = (S \circ F)(t). \tag{2.18}$$

By the definition of operator S, the positive ω-periodic solution of (1.1) is equivalent to the nontrivial fixed point of A. From Assumption (F0), Lemmas 2.1 and 2.2, we easily see the following Lemma.

Lemma 2.3. *$A(K \setminus \{0\}) \subset K$, and $A : K \setminus \{0\} \to K$ is completely continuous.*

We will find the nonzero fixed point of A by using the fixed point index theory in cones. Since the singularity of f at $x = 0$ implies that A has no definition at $u = 0$, the fixed point index theory in the cone K cannot be directly applied to A. We need to make some Preliminaries.

We recall some concepts and conclusions on the fixed point index in [23, 24]. Let E be a Banach space and $K \subset E$ a closed convex cone in E. Assume Ω is a bounded open subset of E with boundary $\partial\Omega$, and $K \cap \Omega \neq \emptyset$. Let $A : K \cap \overline{\Omega} \to K$ be a completely continuous mapping. If $Au \neq u$ for any $u \in K \cap \partial\Omega$, then the fixed point index $i(A, K \cap \Omega, K)$ has a definition. One important fact is that if $i(A, K \cap \Omega, K) \neq 0$, then A has a fixed point in $K \cap \Omega$. The following two lemmas are needed in our argument.

Lemma 2.4 (see [24]). *Let Ω be a bounded open subset of E with $\theta \in \Omega$ and $A : K \cap \overline{\Omega} \to K$ a completely continuous mapping. If $\lambda Au \neq u$ for every $u \in K \cap \partial\Omega$ and $0 < \lambda \leq 1$, then $i(A, K \cap \Omega, K) = 1$.*

Lemma 2.5 (see [24]). *Let Ω be a bounded open subset of E and $A : K \cap \overline{\Omega} \to K$ a completely continuous mapping. If there exists an $e \in K \setminus \{\theta\}$ such that $u - Au \neq \tau e$ for every $u \in K \cap \partial\Omega$ and $\tau \geq 0$, then $i(A, K \cap \Omega, K) = 0$.*

We use Lemmas 2.4 and 2.5 to show the following fixed-point theorem in cones which is applicable to the operator A defined by (2.18).

Theorem 2.6. *Let E be a Banach space and $K \subset E$ a closed convex cone. Assume Ω_1 and Ω_2 are bounded open subsets of E with $\theta \in \Omega_1$, $\overline{\Omega}_1 \subset \Omega_2$. Let $A : K \cap (\overline{\Omega}_2 \setminus \Omega_1) \to K$ be a completely continuous mapping. If A satisfies the following conditions:*

(1) *$\lambda Au \neq u$ for $u \in K \cap \partial\Omega_1$, $0 < \lambda \leq 1$;*

(2) *there exists $e \in K \setminus \{\theta\}$ such that $u - Au \neq \tau e$ for $u \in K \cap \partial\Omega_2$, $\tau \geq 0$, or the following conditions:*

(3) *there exists $e \in K \setminus \{\theta\}$ such that $u - Au \neq \tau e$ for $u \in K \cap \partial\Omega_1$, $\tau \geq 0$;*

(4) *$\lambda Au \neq u$ for $u \in K \cap \partial\Omega_2$, $0 < \lambda \leq 1$,*

then A has a fixed-point in $K \cap (\Omega_2 \setminus \overline{\Omega}_1)$.

Proof. By Dugundji's extension theorem, the operator $A : K \cap (\overline{\Omega}_2 \setminus \Omega_1) \to K$ can be extended into a completely continuous operator from $K \cap \overline{\Omega}_2$ to K, says $\widetilde{A} : K \cap \overline{\Omega}_2 \to K$.

If A satisfies conditions (1) and (2) of Theorem 2.6, then $\widetilde{A}$ also satisfies them. By Lemmas 2.4 and 2.5, respectively, we have

$$i\left(\widetilde{A}, K \cap \Omega_1, K\right) = 1, \qquad i\left(\widetilde{A}, K \cap \Omega_2, K\right) = 0. \tag{2.19}$$

By the additivity of the fixed point index, we have

$$i\left(\widetilde{A}, K \cap \left(\Omega_2 \setminus \overline{\Omega}_1\right), K\right) = i\left(\widetilde{A}, K \cap \Omega_2, K\right) - i\left(\widetilde{A}, K \cap \Omega_1, K\right) = -1. \tag{2.20}$$

Hence $\widetilde{A}$ has a fixed-point in $K \cap (\Omega_2 \setminus \overline{\Omega}_1)$. Since $\widetilde{A}$ is an extension of A, it follows that A has a fixed-point in $K \cap (\Omega_2 \setminus \overline{\Omega}_1)$.

If A satisfies conditions (3) and (4) of Theorem 2.6, with a similar count, we obtain that

$$i\left(\widetilde{A}, K \cap \left(\Omega_2 \setminus \overline{\Omega}_1\right), K\right) = 1. \tag{2.21}$$

This means that $\widetilde{A}$ has a fixed-point in $K \cap (\Omega_2 \setminus \overline{\Omega}_1)$. Hence, A has a fixed-point in $K \cap (\Omega_2 \setminus \overline{\Omega}_1)$. □

Theorem 2.6 is an improvement of the fixed point theorem of Krasnoselskii's cone expansion or compression. We will use it to discuss the existence of positive ω-periodic solutions of (1.1) in the next section.

3. Main Results

We consider the the existence of positive ω-periodic solutions of (1.1). Let $f \in C(\mathbb{R}\times(0,\infty)\times\mathbb{R})$ satisfy Assumption (F0) and $f(t,x,y)$ be ω-periodic in t. Let C_0 be the constant defined by (2.8) and $I = [0,\omega]$. To be convenient, we introduce the notations

$$\begin{aligned} f_0 &= \liminf_{x\to 0^+} \min_{|y|\le C_0|x|,t\in I} \left(\frac{f(t,x,y)}{x}\right), \\ f^0 &= \limsup_{x\to 0^+} \max_{|y|\le C_0|x|,t\in I} \left(\frac{f(t,x,y)}{x}\right), \\ f_\infty &= \liminf_{x\to +\infty} \min_{|y|\le C_0|x|,t\in I} \left(\frac{f(t,x,y)}{x}\right), \\ f^\infty &= \limsup_{x\to +\infty} \max_{|y|\le C_0|x|,t\in I} \left(\frac{f(t,x,y)}{x}\right). \end{aligned} \tag{3.1}$$

Our main results are as follows.

Theorem 3.1. *Let $f : \mathbb{R}\times(0,\infty)\times\mathbb{R} \to \mathbb{R}$ be continuous and $f(t,x,y)$ be ω-periodic in t. If f satisfies Assumption* (F0) *and the condition*

(F1) $f^0 < 0, f_\infty > 0$,

then (1.1) *has at least one positive ω-periodic solution.*

Theorem 3.2. *Let $f : \mathbb{R}\times(0,\infty)\times\mathbb{R} \to \mathbb{R}$ be continuous and $f(t,x,y)$ be ω-periodic in t. If f satisfies Assumption* (F0) *and the conditions*

(F2) $f_0 > 0, f^\infty < 0$,

then (1.1) *has at least one positive ω-periodic solution.*

Noting that 0 is an eigenvalue of the associated linear eigenvalue problems of (1.1) with periodic boundary condition, if one inequality concerning comparison with 0 in (F1) or (F2) of Theorem 3.1 or Theorem 3.2 is not true, the existence of periodic solution to (1.1) cannot be guaranteed. Hence, the 0 is the optimal value in condition (F1) and (F2).

In Theorem 3.1, the condition (F1) allows $f(t,x,y)$ to have superlinear growth on x and y. For example,

$$f(t,x,y) = x^2 + y^2 - \frac{1}{4}\frac{\pi^2}{\omega^2}\left(2+\sin\frac{\pi t}{\omega}\right)x \tag{3.2}$$

satisfies (F0) with $M = (3/4)(\pi^2/\omega^2)$ and (F1) with $f^0 = -(1/4)(\pi^2/\omega^2)$ and $f_\infty = +\infty$.

In Theorem 3.2, the condition (F2) allows that $f(t,x,y)$ has singularity at $x = 0$. For example,

$$f(t,x,y) = \frac{xy^2 + 2 + \sin(\pi t/\omega)}{x^3} - \frac{\pi^2}{2\omega^2}\, x \tag{3.3}$$

satisfies (F0) with $M = \pi^2/2\omega^2$, and (F2) with $f_0 = +\infty$ and $f^\infty = -\pi^2/2\omega^2$. The existence of periodic solutions for singular ordinary differential equations has been studied by several authors, see [20, 25, 26]. But the equations considered by these authors do not contain derivative term $u'(t)$.

Proof of Theorem 3.1. Choose the working space $E = C^1_\omega(\mathbb{R})$. Let $K \subset C^1_\omega(\mathbb{R})$ be the closed convex cone in $C^1_\omega(\mathbb{R})$ defined by (2.9) and $A : K \setminus \{0\} \to K$ the operator defined by (2.18). Then the positive ω-periodic solution of (1.1) is equivalent to the nontrivial fixed point of A. Let $0 < r < R < +\infty$ and set

$$\Omega_1 = \left\{u \in C^1_\omega(\mathbb{R}) \mid \|u\|_{C^1} < r\right\}, \qquad \Omega_2 = \left\{u \in C^1_\omega(\mathbb{R}) \mid \|u\|_{C^1} < R\right\}. \tag{3.4}$$

We show that the operator A has a fixed point in $K \cap (\Omega_2 \setminus \overline{\Omega}_1)$ by Theorem 2.6 when r is small enough and R large enough.

By $f^0 < 0$ and the definition of f^0, there exist $\varepsilon \in (0, M)$ and $\delta > 0$, such that

$$f(t,x,y) \le -\varepsilon x, \quad t \in [0,\omega], |y| \le C_0, 0 < x \le \delta. \tag{3.5}$$

Let $r \in (0,\delta)$. We now prove that A satisfies the Condition (1) of Theorem 2.6, namely, $\lambda\, Au \neq u$ for every $u \in K \cap \partial\Omega_1$ and $0 < \lambda \le 1$. In fact, if there exist $u_0 \in K \cap \partial\Omega_1$ and $0 < \lambda_0 \le 1$ such that $\lambda_0\, Au_0 = u_0$, then by definition of A and Lemma 2.1, $u_0 \in C^2_\omega(\mathbb{R})$ satisfies the differential equation

$$u_0''(t) + Mu_0(t) = \lambda_0 f_1(t, u_0(t), u_0'(t)), \quad t \in \mathbb{R}. \tag{3.6}$$

Since $u_0 \in K \cap \partial\Omega_1$, by the definitions of K and Ω_1, we have

$$|u_0'(t)| \le C_0 u_0(t), \quad 0 < \sigma\|u_0\|_C \le u_0(t) \le \|u_0\|_{C^1} = r < \delta, \quad t \in \mathbb{R}. \tag{3.7}$$

Hence from (3.5) it follows that

$$f(t, u_0(t), u_0'(t)) \le -\varepsilon u_0(t), \quad t \in \mathbb{R}. \tag{3.8}$$

By this, (3.6), and the definition of f_1 we have

$$u_0''(t) + Mu_0(t) \le \lambda_0(Mu_0(t) - \varepsilon u_0(t)) \le (M - \varepsilon)u_0(t), \quad t \in \mathbb{R}. \tag{3.9}$$

Integrating both sides of this inequality from 0 to ω and using the periodicity of u_0, we obtain that

$$M\int_0^{\omega} u_0(t)dt \le (M-\varepsilon)\int_0^{\omega} u_0(t)dt. \tag{3.10}$$

Since $\int_0^{\omega} u_0(t)dt \ge \omega\,\sigma\|u_0\|_C > 0$, it follows that $M \le M-\varepsilon$, which is a contradiction. Hence the Condition (1) of Theorem 2.6 holds.

On the other hand, since $f_\infty > 0$, by the definition of f_∞, there exist $\varepsilon_1 > 0$ and $H > 0$ such that

$$f(t,x,y) \ge \varepsilon_1 x, \quad t \in [0,\omega], |y| \le C_0 x, x \ge H. \tag{3.11}$$

Define a function $g : (0,\infty) \to \mathbb{R}^+$ by

$$g(x) = \max\left\{\frac{f(t,x,y)+Mx}{x} \mid t \in [0,\omega], |y| \le x\right\}. \tag{3.12}$$

Then $g : (0,\infty) \to \mathbb{R}^+$ is continuous. By (3.5) and Assumption (F0),

$$0 \le g(x) \le \varepsilon + M, \quad 0 < x \le \delta. \tag{3.13}$$

This implies that

$$C_1 := \sup\{xg(x) \mid 0 < x \le H\} < +\infty. \tag{3.14}$$

Hence for every $t \in [0,\omega]$, $0 < x \le H$, and $|y| \le C_0 x$, we have

$$\begin{aligned} |f(t,x,y)-\varepsilon_1 x| &\le |f(t,x,y)+Mx| + |(M+\varepsilon_1)x| \\ &= (f(t,x,y)+Mx) + (M+\varepsilon_1)x \\ &\le xg(x) + (M+\varepsilon_1)x \\ &\le C_1 + (M+\varepsilon_1)H := C_2. \end{aligned} \tag{3.15}$$

Combining this with (3.11), it follows that

$$f(t,x,y) \ge \varepsilon_1 x - C_2, \quad t \in [0,\omega], |y| \le C_0 x, x > 0. \tag{3.16}$$

Choose $e(t) \equiv 1$. Clearly, $e \in K \setminus \{\theta\}$. We show that A satisfies the Condition (2) of Theorem 2.6 if R is large enough, namely, $u - Au \ne \tau e$ for every $u \in K \cap \partial\Omega_2$ and $\tau \ge 0$. In fact, if there exist $u_1 \in K \cap \partial\Omega_2$ and $\tau_1 \ge 0$ such that $u_1 - Au_1 = \tau_1 e$, since $u_1 - \tau_1 e = Au_1$, by definition of A and Lemma 2.1, $u_1 \in C^2_{\omega}(\mathbb{R})$ satisfies the differential equation

$$u_1''(t) + M(u_1(t)-\tau_1) = f_1(t,u_1(t),u_1'(t)), \quad t \in \mathbb{R}. \tag{3.17}$$

From (3.17) and (3.16), it follows that

$$\begin{aligned} u_1''(t) &= f\left(t, u_1(t), u_1'(t)\right) + M\tau_1 \\ &\geq f\left(t, u_1(t), u_1'(t)\right) \geq \varepsilon_1 u_1(t) - C_2, \quad t \in \mathbb{R}. \end{aligned} \tag{3.18}$$

Integrating this inequality on $[0, \omega]$ and using the periodicity of u_1, we get that

$$\int_0^\omega u_1(t)dt \leq \frac{C_2}{\varepsilon_1}. \tag{3.19}$$

Since $u_1 \in K \cap \partial\Omega_2$, by the definition of K, we have

$$u_1(t) \geq \sigma\|u_1\|_C, \quad \left|u_1'(t)\right| \leq C_0 u_1(t), \quad t \in \mathbb{R}. \tag{3.20}$$

By the first inequality of (3.20), we have

$$\int_0^\omega u_1(t)dt \geq \omega\sigma\|u_1\|_C. \tag{3.21}$$

From this and (3.19), it follows that

$$\|u_1\|_C \leq \frac{1}{\omega\sigma}\int_0^\omega u_1(t)dt \leq \frac{C_2}{\omega\sigma\varepsilon_1}. \tag{3.22}$$

By this and the second inequality of (3.20), we have

$$\|u_1\|_{C^1} = \|u_1\|_C + \left\|u_1'\right\|_C \leq \|u_1\|_C + C_0\|u_1\|_C \leq \frac{(1 + C_0)C_2}{\omega\sigma\varepsilon_1} := \overline{R}. \tag{3.23}$$

Therefore, choose $R > \max\{\overline{R}, \delta\}$, then A satisfies the Condition (2) of Theorem 2.6.

Now by the first part of Theorem 2.6, A has a fixed point in $K \cap (\Omega_2 \setminus \overline{\Omega}_1)$, which is a positive ω-periodic solution of (1.1). □

Proof of Theorem 3.2. Let $\Omega_1, \Omega_2 \subset C^1_\omega(\mathbb{R})$ be defined by (3.4). We use Theorem 2.6 to prove that the operator A has a fixed point in $K \cap (\Omega_2 \setminus \overline{\Omega}_1)$ if r is small enough and R large enough.

By $f_0 > 0$ and the definition of f_0, there exist $\varepsilon > 0$ and $\delta > 0$, such that

$$f\left(t, x, y\right) \geq \varepsilon x, \quad t \in [0, \omega], \left|y\right| \leq C_0 x, 0 < x \leq \delta. \tag{3.24}$$

Let $r \in (0, \delta)$ and $e(t) \equiv 1$. We prove that A satisfies the Condition (3) of Theorem 2.6, namely, $u - Au \neq \tau e$ for every $u \in K \cap \partial\Omega_1$ and $\tau \geq 0$. In fact, if there exist $u_0 \in K \cap \partial\Omega_1$ and $\tau_0 \geq 0$ such that $u_0 - Au_0 = \tau_0 e$, since $u_0 - \tau_0 e = Au_0$, by definition of A and Lemma 2.1, $u_0 \in C^2_\omega(\mathbb{R})$ satisfies the differential equation

$$u_0''(t) + M(u_0(t) - \tau_0) = f_1\left(t, u_0(t), u_0'(t)\right), \quad t \in \mathbb{R}. \tag{3.25}$$

Since $u_0 \in K \cap \partial\Omega_1$, by the definitions of K and Ω_1, u_0 satisfies (3.7). From (3.7), and (3.24) it follows that

$$f\left(t, u_0(t), u_0'(t)\right) \geq \varepsilon u_0(t), \quad t \in \mathbb{R}. \tag{3.26}$$

By this, (3.25), and the definition of f_1, we have

$$u_0''(t) + Mu_0(t) = f_1\left(t, u_0(t), u_0''(t)\right) + M\tau_0 \geq (M+\varepsilon)u_0(t), \quad t \in \mathbb{R}. \tag{3.27}$$

Integrating this inequality on $[0, \omega]$ and using the periodicity of $u_0(t)$, we obtain that

$$M\int_0^\omega u_0(t)dt \geq (M+\varepsilon)\int_0^\omega u_0(t)dt. \tag{3.28}$$

Since $\int_0^\omega u_0(t)dt \geq \omega\sigma\|u_0\|_C > 0$, from this inequality it follows that $M \geq M+\varepsilon$, which is a contradiction. Hence A satisfies the Condition (3) of Theorem 2.6.

Since $f^\infty < 0$, by the definition of f^∞, there exist $\varepsilon_1 \in (0, M)$ and $H > 0$ such that

$$f(t, x, y) \leq -\varepsilon_1 x, \quad t \in [0, \omega], |y| \leq C_0 x, x \geq H. \tag{3.29}$$

Choosing $R > \max\{(1+C_0)H/\sigma, \delta\}$, we show that A satisfies the Condition (4) of Theorem 2.6, namely, $\lambda Au \neq u$ for every $u \in K \cap \partial\Omega_2$ and $0 < \lambda \leq 1$. In fact, if there exist $u_1 \in K \cap \partial\Omega_2$ and $0 < \lambda_1 \leq 1$ such that $\lambda_1 Au_1 = u_1$, then by the definition of A and Lemma 2.1, $u_1 \in C_\omega^2(\Omega)$ satisfies the differential equation

$$u_1''(t) + Mu_1(t) = \lambda_1 f_1\left(t, u_1(t), u_1'(t)\right), \quad t \in \mathbb{R}. \tag{3.30}$$

Since $u_1 \in K \cap \partial\Omega_2$, by the definition of K, u_1 satisfies (3.20). By the second inequality of (3.20), we have

$$\|u_1\|_{C^1} = \|u_1\|_C + \left\|u_1'\right\|_C \leq \|u_1\|_C + C_0\|u_1\|_C = (1+C_0)\|u_1\|_C. \tag{3.31}$$

Consequently,

$$\|u_1\|_C \geq \frac{1}{(1+C_0)}\ \|u_1\|_{C^1}. \tag{3.32}$$

By (3.32) and the first inequality of (3.20), we have

$$u_1(t) \geq \sigma\|u_1\|_C \geq \frac{\sigma}{(1+C_0)}\ \|u_1\|_{C^1} = \frac{\sigma}{(1+C_0)}\ R > H, \quad t \in \mathbb{R}. \tag{3.33}$$

From this, the second inequality of (3.20) and (3.29), it follows that

$$f\left(t, u_1(t), u_1'(t)\right) \leq -\varepsilon_1 u_1(t), \quad t \in \mathbb{R}. \tag{3.34}$$

By this and (3.30), we have

$$u_1''(t) + Mu_1(t) \leq \lambda_1(M\ u_1(t) - \varepsilon_1 u_1(t)) \leq (M - \varepsilon_1)u_1(t), \quad t \in \mathbb{R}. \tag{3.35}$$

Integrating this inequality on $[0, \omega]$ and using the periodicity of $u_1(t)$, we obtain that

$$M \int_0^{\omega} u_1(t)dt \leq (M - \varepsilon_1) \int_0^{\omega} u_1(t)dt. \tag{3.36}$$

Since $\int_0^{\omega} u_1(t)\ dt \geq \omega\sigma\|u_1\|_C > 0$, from this inequality it follows that $M \leq M - \varepsilon_1$, which is a contradiction. This means that A satisfies the Condition (4) of Theorem 2.6.

By the second part of Theorem 2.6, A has a fixed point in $K \cap (\Omega_2 \setminus \overline{\Omega}_1)$, which is a positive ω-periodic solution of (1.1). □

Example 3.3. Consider the second-order differential equation

$$u'' = a_1(t)u + a_2(t)u^2 + a_3(t)(u')^2 u, \quad t \in \mathbb{R}, \tag{3.37}$$

where $a_i(t) \in C_{\omega}(\mathbb{R}),\ i = 1, 2, 3$. If $-\pi^2/\ \omega^2 < a_1(t) < 0$ and $a_2(t), a_3(t) > 0$ for $t \in [0, \omega]$, then $f(t, x, y) = a_1(t)x + a_2(t)x^2 + a_3 xy^2$ satisfies the conditions (F0) and (F1). By Theorem 3.1, (3.37) has at least one positive ω-periodic solution.

Example 3.4. Consider the singular differential equation:

$$u'' = a(t)u + \frac{b(t)u + c(t)(u')^2}{u^2}, \quad t \in \mathbb{R}, \tag{3.38}$$

where $a(t), b(t), c(t) \in C_{\omega}(\mathbb{R})$. If $-\pi^2/\omega^2 < a(t) < 0$ and $b(t), c(t) > 0$ for $t \in [0, \omega]$, then $f(t, x, y) = a(t)x + (b(t)x + c(t)y^2)/x^2$ satisfies the conditions (F0) and (F2). By Theorem 3.2, the (3.38) has a positive ω-periodic solution.

4. Remarks

Our discussion on the existence of the positive ω-periodic solutions to (1.1) is applicable to the following ordinary differential equation:

$$-u''(t) = f(t, u(t), u'(t)), \quad t \in \mathbb{R}, \tag{4.1}$$

where the nonlinearity $f : \mathbb{R} \times (0, \infty) \times \mathbb{R} \to \mathbb{R}$ is continuous and $f(t, x, y)$ is ω-periodic in t. For (4.1), we need the following assumption.

(F0)* There exists $M > 0$ such that

$$f(t, x, y) + Mx \geq 0, \quad x > 0,\ t, y \in \mathbb{R}. \tag{4.2}$$

Similarly to Lemma 2.1, we have the following conclusion.

Lemma 4.1. *Let $M > 0$ be a constant. Then for every $h \in C_\omega(\mathbb{R})$, the linear second order differential equation*

$$-u''(t) + Mu(t) = h(t), \quad t \in \mathbb{R}, \tag{4.3}$$

has a unique ω-periodic solution $u(t)$, which is given by

$$u(t) = \int_{t-\omega}^{t} V(t-s)h(s)ds \quad t \in \mathbb{R}, \tag{4.4}$$

where $V(t)$ is the unique solution of the linear second-order boundary value problem

$$\begin{aligned} -u''(t) + Mu(t) = 0, &\quad 0 \le t \le \omega, \\ u(0) - u(\omega) = 0, &\qquad u'(0) - u'(\omega) = -1, \end{aligned} \tag{4.5}$$

which is explicitly given by

$$V(t) = \frac{\cosh\beta(t-\omega/2)}{2\beta\sinh(\beta\omega/2)}, \quad 0 \le t \le \omega, \tag{4.6}$$

with $\beta = \sqrt{M}$.

Since

$$\begin{gathered} \overline{V} := \max_{0\le t\le\omega} V(t) = \frac{\cosh(\beta\omega/2)}{2\beta\sinh(\beta\omega/2)}, \qquad \underline{V} := \min_{0\le t\le\omega} V(t) = \frac{1}{2\beta\sinh(\beta\omega/2)}, \\ \overline{V}_1 := \max_{0\le t\le\omega}\left|V'(t)\right| = \max_{0\le t\le\omega}\frac{\left|\sinh\beta(t-\omega/2)\right|}{2\sinh(\beta\omega/2)} = \frac{1}{2}, \end{gathered} \tag{4.7}$$

we renew to define σ and C_0 by

$$\sigma = \frac{\underline{V}}{\overline{V}} = \frac{1}{\cosh(\beta\omega/2)}, \qquad C_0 = \frac{\overline{V}_1}{\underline{V}} = \beta\sinh\frac{\beta\omega}{2}. \tag{4.8}$$

Now, using the similar arguments to Theorems 3.1 and 3.2, we can obtain the following results.

Theorem 4.2. *Let $f : \mathbb{R} \times (0,\infty) \times \mathbb{R} \to \mathbb{R}$ be continuous and $f(t,x,y)$ be ω-periodic in t. If f satisfies Assumption* (F0)* *and the condition*

(F1) $f^0 < 0,\ f_\infty > 0,$

then (4.1) *has at least one positive ω-periodic solution.*

Theorem 4.3. *Let $f : \mathbb{R} \times (0, \infty) \times \mathbb{R} \to \mathbb{R}$ be continuous and $f(t, x, y)$ be ω-periodic in t. If f satisfies Assumption* (F0)* *and the conditions*

(F2) $f_0 > 0$, $f^\infty < 0$,

then (4.1) *has at least one positive ω-periodic solution.*

Theorems 4.2 and 4.3 improve and extend some results in References [18, 19, 22].

Acknowledgment

This paper is supported by NNSFs of China (11261053 and 11061031).

References

[1] S. Leela, “Monotone method for second order periodic boundary value problems,” *Nonlinear Analysis*, vol. 7, no. 4, pp. 349–355, 1983.
[2] J. J. Nieto, “Nonlinear second-order periodic boundary value problems,” *Journal of Mathematical Analysis and Applications*, vol. 130, no. 1, pp. 22–29, 1988.
[3] A. Cabada and J. J. Nieto, “A generalization of the monotone iterative technique for nonlinear second order periodic boundary value problems,” *Journal of Mathematical Analysis and Applications*, vol. 151, no. 1, pp. 181–189, 1990.
[4] A. Cabada, “The method of lower and upper solutions for second, third, fourth, and higher order boundary value problems,” *Journal of Mathematical Analysis and Applications*, vol. 185, no. 2, pp. 302–320, 1994.
[5] J. P. Gossez and P. Omari, “Periodic solutions of a second order ordinary differential equation: a necessary and sufficient condition for nonresonance,” *Journal of Differential Equations*, vol. 94, no. 1, pp. 67–82, 1991.
[6] P. Omari, G. Villari, and F. Zanolin, “Periodic solutions of the Liénard equation with one-sided growth restrictions,” *Journal of Differential Equations*, vol. 67, no. 2, pp. 278–293, 1987.
[7] W. G. Ge, “On the existence of harmonic solutions of Liénard systems,” *Nonlinear Analysis*, vol. 16, no. 2, pp. 183–190, 1991.
[8] J. Mawhin and M. Willem, “Multiple solutions of the periodic boundary value problem for some forced pendulum-type equations,” *Journal of Differential Equations*, vol. 52, no. 2, pp. 264–287, 1984.
[9] V. C. Zelati, “Periodic solutions of dynamical systems with bounded potential,” *Journal of Differential Equations*, vol. 67, no. 3, pp. 400–413, 1987.
[10] L. Lassoued, “Periodic solutions of a second order superquadratic system with a change of sign in the potential,” *Journal of Differential Equations*, vol. 93, no. 1, pp. 1–18, 1991.
[11] H. Wang, “On the existence of positive solutions for semilinear elliptic equations in the annulus,” *Journal of Differential Equations*, vol. 109, no. 1, pp. 1–7, 1994.
[12] L. H. Erbe and H. Wang, “On the existence of positive solutions of ordinary differential equations,” *Proceedings of the American Mathematical Society*, vol. 120, no. 3, pp. 743–748, 1994.
[13] Z. Liu and F. Li, “Multiple positive solutions of nonlinear two-point boundary value problems,” *Journal of Mathematical Analysis and Applications*, vol. 203, no. 3, pp. 610–625, 1996.
[14] J. Henderson and H. Wang, “Positive solutions for nonlinear eigenvalue problems,” *Journal of Mathematical Analysis and Applications*, vol. 208, no. 1, pp. 252–259, 1997.
[15] Y. Li, “Positive solutions of second-order boundary value problems with sign-changing nonlinear terms,” *Journal of Mathematical Analysis and Applications*, vol. 282, no. 1, pp. 232–240, 2003.
[16] Y. X. Li, “Positive periodic solutions of nonlinear second order ordinary differential equations,” *Acta Mathematica Sinica*, vol. 45, no. 3, pp. 481–488, 2002 (Chinese).
[17] F. M. Atici and G. Sh. Guseinov, “On the existence of positive solutions for nonlinear differential equations with periodic boundary conditions,” *Journal of Computational and Applied Mathematics*, vol. 132, no. 2, pp. 341–356, 2001.
[18] P. J. Torres, “Existence of one-signed periodic solutions of some second-order differential equations via a Krasnoselskii fixed point theorem,” *Journal of Differential Equations*, vol. 190, no. 2, pp. 643–662, 2003.

[19] Y. Li, "Positive periodic solutions of first and second order ordinary differential equations," *Chinese Annals of Mathematics B*, vol. 25, no. 3, pp. 413–420, 2004.
[20] Y. X. Li, "Oscillatory periodic solutions of nonlinear second order ordinary differential equations," *Acta Mathematica Sinica*, vol. 21, no. 3, pp. 491–496, 2005.
[21] F. Li and Z. Liang, "Existence of positive periodic solutions to nonlinear second order differential equations," *Applied Mathematics Letters*, vol. 18, no. 11, pp. 1256–1264, 2005.
[22] J. R. Graef, L. Kong, and H. Wang, "Existence, multiplicity, and dependence on a parameter for a periodic boundary value problem," *Journal of Differential Equations*, vol. 245, no. 5, pp. 1185–1197, 2008.
[23] K. Deimling, *Nonlinear Functional Analysis*, Springer, New York, NY, USA, 1985.
[24] D. J. Guo and V. Lakshmikantham, *Nonlinear Problems in Abstract Cones*, Academic Press, New York, NY, USA, 1988.
[25] I. Rachůnková, M. Tvrdý, and I. Vrkoč, "Existence of nonnegative and nonpositive solutions for second order periodic boundary value problems," *Journal of Differential Equations*, vol. 176, no. 2, pp. 445–469, 2001.
[26] L. Kong, S. Wang, and J. Wang, "Positive solution of a singular nonlinear third-order periodic boundary value problem," *Journal of Computational and Applied Mathematics*, vol. 132, no. 2, pp. 247–253, 2001.

Hindawi Publishing Corporation
Journal of Function Spaces and Applications
Volume 2012, Article ID 184186, 12 pages
doi:10.1155/2012/184186

Research Article

On the Frame Properties of Degenerate System of Sines

Bilal Bilalov and Fatima Guliyeva

Institute of Mathematics and Mechanics of NAS of Azerbaijan, B. Vahabzade 9, 1141 Baku, Azerbaijan

Correspondence should be addressed to Bilal Bilalov, bilalov.bilal@gmail.com

Received 27 June 2012; Accepted 17 August 2012

Academic Editor: Maria Isabel Berenguer

Systems of sines with degenerate coefficients are considered in this paper. Frame properties of these systems in Lebesgue spaces are studied.

1. Introduction

Basis properties of classical system of exponents $\{e^{\mathrm{int}}\}_{n\in\mathbb{Z}}$ ($\mathbb{Z}$ is the set of all integers) in Lebesgue spaces $L_p(-\pi,\pi)$, $1 \le p < +\infty$, are well studied in the literature (see [1–4]). Bari in her fundamental work [5] raised the issue of the existence of normalized basis in L_2 which is not Riesz basis. The first example of this was given by Babenko [6]. He proved that the degenerate system of exponents $\{|t|^{\alpha} e^{\mathrm{int}}\}_{n\in\mathbb{Z}}$ with $|\alpha| < (1/2)$ forms a basis for $L_2(-\pi,\pi)$ but is not Riesz basis when $\alpha \neq 0$. This result has been extended by Gaposhkin [7]. In [8], the condition on the weight ρ was found which make the system $\{e^{\mathrm{int}}\}_{n\in\mathbb{Z}}$ forms a basis for the weight space $L_{p,\rho}(-\pi,\pi)$ with a norm $\|f\|_{p,\rho} = (\int_{-\pi}^{\pi} |f(t)|^p \rho(t)dt)^{(1/p)}$. Basis properties of a degenerate system of exponents are closely related to the similar properties of an ordinary system of exponents in corresponding weight space. In all the mentioned works, the authors consider the cases when the weight or the degenerate coefficient satisfies the Muckenhoupt condition (see, e.g., [9]). It should be noted that the above stated is true for the systems of sines and cosines, too.

Basis properties of the system of exponents and sines with the linear phase in weighted Lebesgue spaces have been studied in [10–12]. Those of the systems of exponents with degenerate coefficients have been studied in [13, 14]. Similar questions have previously been considered in papers [15–18].

In this work, we study the frame properties of the system of sines with degenerate coefficient in Lebesgue spaces, when the degenerate coefficient, generally speaking, does not satisfy the Muckenhoupt condition.

2. Needful Information

To obtain our main results, we will use some concepts and facts from the theory of bases.

We will use the standard notation. $\mathbb{N}$ will be the set of all positive integers; $\exists$ will mean "there exist(s)"; $\Rightarrow$ will mean "it follows"; $\Leftrightarrow$ will mean "if and only if"; $\exists!$ will mean "there exists unique"; $K \equiv \mathbb{R}$ or $K \equiv \mathbb{C}$ will stand for the set of real or complex numbers, respectively; δ_{nk} is Kronecker symbol, $\delta_k = \{\delta_{kn}\}_{k\in\mathbb{N}}$.

Let X be some Banach space with a norm $\|\cdot\|_X$. Then X^* will denote its dual with a norm $\|\cdot\|_{X^*}$. By $L[M]$, we denote the linear span of the set $M \subset X$, and $\overline{M}$ will stand for the closure of M.

System $\{x_n\}_{n\in\mathbb{N}} \subset X$ is said to be uniformly minimal in X if $\exists\delta > 0$

$$\inf_{\forall u\in L\left[\{x_n\}_{n\neq k}\right]} \|x_k - u\|_X \geq \delta\|x_k\|_X, \quad \forall k \in \mathbb{N}. \tag{2.1}$$

System $\{x_n\}_{n\in\mathbb{N}} \subset X$ is said to be complete in X if $\overline{L[\{x_n\}_{n\in\mathbb{N}}]} = X$. It is called minimal in X if $x_k \notin \overline{L[\{x_n\}_{n\neq k}]}$, for all $k \in \mathbb{N}$.

The following criteria of completeness and minimality are available.

Criterion 1 (Hahn-Banach theorem). System $\{x_n\}_{n\in\mathbb{N}} \subset X$ is complete in X if $f(x_n) = 0$, for all $n \in \mathbb{N}, f \in X^* \Rightarrow f = 0$.

Criterion 2 (see [19]). System $\{x_n\}_{n\in\mathbb{N}} \subset X$ is minimal in $X \Leftrightarrow$ it has a biorthogonal system $\{f_n\}_{n\in\mathbb{N}} \subset X^*$, that is, $f_n(x_k) = \delta_{nk}$, for all $n, k \in \mathbb{N}$.

Criterion 3. Complete system $\{x_n\}_{n\in\mathbb{N}} \subset X$ is uniformly minimal in $X \Leftrightarrow \sup_n \|x_n\|_X \|y_n\|_{X^*} < +\infty$, where $\{y_n\}_{n\in\mathbb{N}} \subset X^*$ is a system biorthogonal to it.

System $\{x_n\}_{n\in\mathbb{N}} \subset X$ is said to be a basis for X if for all $x \in X$, $\exists!\{\lambda_n\}_{n\in\mathbb{N}} \subset K : x = \sum_{n=1}^{\infty} \lambda_n x_n$.

If system $\{x_n\}_{n\in\mathbb{N}} \subset X$ forms a basis for X, then it is uniformly minimal.

Definition 2.1 (see [20, 21]). Let X be a Banach space and $\mathcal{K}$ a Banach sequence space indexed by $\mathbb{N}$. Let $\{f_k\}_{k\in\mathbb{N}} \subset X$, $\{g_k\}_{k\in\mathbb{N}} \subset X^*$. Then $(\{g_k\}_{k\in\mathbb{N}}, \{f_k\}_{k\in\mathbb{N}})$ is an atomic decomposition of X with respect to $\mathcal{K}$ if

(i) $\{g_k(f)\}_{k\in\mathbb{N}} \in \mathcal{K}$, for all $f \in X$;

(ii) $\exists A, B > 0$:

$$A\|f\|_X \leq \left\|\{g_k(f)\}_{k\in\mathbb{N}}\right\|_{\mathcal{K}} \leq B\|f\|_X, \quad \forall f \in X; \tag{2.2}$$

(iii) $f = \sum_{k=1}^{\infty} g_k(f) f_k$, for all $f \in X$.

Definition 2.2 (see [20, 21]). Let X be a Banach space and $\mathcal{K}$ a Banach sequence space indexed by $\mathbb{N}$. Let $\{g_k\}_{k\in\mathbb{N}} \subset X^*$ and $S : \mathcal{K} \to X$ be a bounded operator. Then $(\{g_k\}_{k\in\mathbb{N}}, S)$ is a Banach frame for X with respect to $\mathcal{K}$ if

(i) $\{g_k(f)\}_{k\in\mathbb{N}} \in \mathcal{K}$, for all $f \in X$;

(ii) $\exists A, B > 0$:

$$A\|f\|_X \leq \|\{g_k(f)\}_{k\in\mathbb{N}}\|_{\mathcal{K}} \leq B\|f\|_X, \quad \forall f \in X; \tag{2.3}$$

(iii) $S[\{g_k(f)\}_{k\in\mathbb{N}}] = f$, for all $f \in X$.

It is true the following.

Proposition 2.3 (see [20, 21]). *Let X be a Banach space and $\mathcal{K}$ a Banach sequence space indexed by $\mathbb{N}$. Assume that the canonical unit vectors $\{\delta_k\}_{k\in\mathbb{N}}$ constitute a basis for $\mathcal{K}$ and let $\{g_k\}_{k\in\mathbb{N}} \subset X^*$ and $S : \mathcal{K} \to X$ be a bounded operator. Then the following statements are equivalent:*

(i) *$(\{g_k\}_{k\in\mathbb{N}}, S)$ is a Banach frame for X with respect to $\mathcal{K}$.*

(ii) *$(\{g_k\}_{k\in\mathbb{N}}, \{S(\delta_k)\}_{k\in\mathbb{N}})$ is an atomic decomposition of X with respect to $\mathcal{K}$.*

More details about these facts can be found in [20–23].

3. Completeness and Minimality

We consider a system of sines

$$\{S_n^{\nu}\}_{n\in\mathbb{N}} \equiv \{\nu(t)\sin nt\}_{n\in\mathbb{N}}, \tag{3.1}$$

with a degenerate coefficient ν

$$\nu(t) = \prod_{k=0}^{r} |t - t_k|^{\alpha_k}, \tag{3.2}$$

where $0 = t_0 < t_1 < \cdots < t_r = \pi$ are points of degeneration and $\{\alpha_k\}_0^r \subset R$.

The notation $f \sim g$, $t \to a$, means that the inequality $0 < \delta \leq |f(t)/g(t)| \leq \delta^{-1} < +\infty$ holds in sufficiently small neighborhood of the point $t = a$ with respect to the functions f and g. Thus, it is clear that $\sin nt \sim t$, $t \to 0$ and $\sin nt \sim \pi - t$, $t \to \pi$ for all $n \in \mathbb{N}$. Proceeding from these relations, we immediately obtain that the inclusion $\{S_n^{\nu}\}_{n\in\mathbb{N}} \subset L_p(0, \pi)$, $1 \leq p < +\infty$, is true if and only if the following relations hold

$$\alpha_0;\ \alpha_r \in \left(-\frac{1}{p} - 1, +\infty\right), \qquad \{\alpha_k\}_1^{r-1} \subset \left(-\frac{1}{p}, +\infty\right). \tag{3.3}$$

In what follows, we will always suppose that this condition is satisfied. Assume that the function $f \in L_q(0,\pi)((1/p)+(1/q)=1)$ is otrhogonal to the system $\{S_n^{\nu}\}_{n\in\mathbb{N}}$, that is

$$\int_0^{\pi} \nu(t)\sin nt\ \overline{f}(t)dt = 0, \quad \forall n \in \mathbb{N}, \tag{3.4}$$

where $(\overline{\cdot})$ is a complex conjugate. By $C_0[0,\pi]$, we denote the Banach space of functions which are continuous on $[0,\pi]$ with a sup-norm and vanish at the ends of the interval $[0,\pi]$. It is absolutely clear that $\nu f \in L_1(0,\pi) \subset C_0^*[0,\pi]$. As the system of sines $\{\sin nt\}_{n\in\mathbb{N}}$ is complete in $C_0[0,\pi]$, we obtain from the relations (3.4) that $\nu(t)f(t)=0$ a.e. on $(0,\pi)$, and, consequently, $f(t)=0$ a.e. on $(0,\pi)$. This proves the completeness of system (3.3) in $L_p(0,\pi)$.

Now consider the minimality of system (3.3) in $L_p(0,\pi)$. It is clear that $\{S_n^{\nu^{-1}}\}_{n\in\mathbb{N}} \subset L_q(0,\pi)$ if and only if

$$\alpha_0;\alpha_r \in \left(-\infty, \frac{1}{q}+1\right), \qquad \{\alpha_k\}_1^{r-1} \subset \left(-\infty, \frac{1}{q}\right). \tag{3.5}$$

It is easily seen that the system $\{\sqrt{(2/\pi)}S_n^{\nu^{-1}}\}_{n\in\mathbb{N}}$ is biorthogonal to $\{S_n^{\nu}\}_{n\in\mathbb{N}}$. So the following theorem is true.

Theorem 3.1. *System $\{S_n^{\nu}\}_{n\in\mathbb{N}}$ is complete in $L_p(0,\pi)$, $1 \le p < +\infty$, if the relations* (3.3) *hold. Besides, it is minimal in $L_p(0,\pi)$ if both* (3.3) *and* (3.5) *hold. Consequently, system $\{S_n^{\nu}\}_{n\in\mathbb{N}}$ is complete and minimal in $L_p(0,\pi)$ if the following relations hold:*

$$\alpha_0;\alpha_r \in \left(-\frac{1}{p}-1, \frac{1}{q}+1\right), \qquad \{\alpha_k\}_1^{r-1} \subset \left(-\frac{1}{p}, \frac{1}{q}\right). \tag{3.6}$$

It is known that (see, e.g., [10, 11]) if $\{\alpha_k\}_0^r \subset (-(1/p),(1/q))$, then system $\{S_n(\nu)\}_{n\in\mathbb{N}}$ forms a basis for $L_p(0,\pi)$, $1<p<+\infty$. Let $\beta \in [(1/q),(1/q)+1)$, where either $\beta=\alpha_0$ or $\beta=\alpha_r$. In the sequel, we will suppose that the condition (3.6) is satisfied for $\{\alpha_k\}_1^{r-1}$. We have

$$\|S_n^{\nu}\|_p^p = \int_0^{\pi} |\nu(t)|^p |\sin nt|^p dt \le \int_0^{\pi} |\nu(t)|^p dt < +\infty, \quad \forall n \in \mathbb{N}. \tag{3.7}$$

On the other hand

$$\|S_n^{\nu}\|_p^p \ge \int_0^{\delta} |\nu(t)|^p |\sin nt|^p dt \ge c\int_0^{\delta} t^{\alpha_0 p}|\sin nt|^p dt = \frac{c}{n^{1+\alpha_0 p}} \int_0^{n\delta} t^{\alpha_0 p}|\sin t|^p dt, \tag{3.8}$$

where $c>0$ is some constant (in what follows c will denote constants that may be different from each other), $\delta>0$ is such that $[0,\delta]$ does not contain the points $\{\alpha_k\}_1^{r-1}$. Let us show that $\inf_{n\in\mathbb{N}}\|S_n^{\nu}\|_p > 0$. We have $(\alpha=\alpha_0 p+1)$

$$\|S_n^{\nu}\|_p^p \ge \frac{c}{n^{\alpha}} \sum_{k\in M_n} \int_{k\pi+(\pi/4)}^{(k+1)\pi-(\pi/4)} t^{\alpha-1}|\sin t|^p dt \ge \frac{c}{n^{\alpha}} \sum_{k\in M_n} \int_{k\pi+(\pi/4)}^{(k+1)\pi-(\pi/4)} t^{\alpha-1} dt, \tag{3.9}$$

where $M_n \equiv \{k \geq 0 : (k+1)\pi - (\pi/4) \leq n\delta\}$. Thus

$$\|S_n^\nu\|_p^p \geq \frac{c}{n^\alpha} \sum_{k \in M_n} \int_{4k+1}^{4k+3} t^{\alpha-1} dt. \tag{3.10}$$

It is absolutely clear that

$$\int_{4k-1}^{4k+1} t^{\alpha-1} dt \leq \int_{4k+1}^{4k+3} t^{\alpha-1} dt, \quad \forall k \in M_n. \tag{3.11}$$

Taking into account this relation, we obtain

$$\|S_n^\nu\|_p^p \geq \frac{c}{n^\alpha} \sum_{k \in M_n} \left[\int_{4k+1}^{4k+3} t^{\alpha-1} dt + \int_{4k-1}^{4k+1} t^{\alpha-1} dt \right] \geq \frac{c}{n^\alpha} \int_0^{\lambda_n} t^{\alpha-1} dt = c \left(\frac{\lambda_n}{n} \right)^\alpha, \tag{3.12}$$

where $\lambda_n \geq (n\delta/\pi) - 2$. Consequently

$$\|S_n^\nu\|_p^p \geq c \left(\frac{\delta}{\pi} - \frac{2}{n} \right)^\alpha \longrightarrow c \left(\frac{\delta}{\pi} \right)^\alpha > 0, \quad n \longrightarrow \infty. \tag{3.13}$$

It follows immediately that $\inf_n \|S_n^\nu\|_p > 0$.

Regarding biorthogonal system we get

$$\left\| S_n^{-\nu} \right\|_q^q = \int_0^\pi \nu^{-q}(t) |\sin nt|^q dt. \tag{3.14}$$

Choose $\varepsilon > 0$ as small as the interval $[0, \varepsilon]$ does not contain the points $\{\alpha_k\}_1^{r-1}$. Consequently

$$\left\| S_n^{-\nu} \right\|_q^q = m \int_0^\varepsilon t^{-\alpha_0 q} |\sin nt|^q dt, \tag{3.15}$$

where $m > 0$ is some constant. We have

$$\left\| S_n^{-\nu} \right\|_q^q \geq m n^{\alpha_0 q - 1} \int_0^{n\varepsilon} \frac{|\sin t|^q}{t^{\alpha_0 q}} dt. \tag{3.16}$$

First we consider the case $\alpha_0 \in ((1/q), (1/q)+1)$. In this case, for sufficiently great n, we have

$$\left\| S_n^{-\nu} \right\|_q^q \geq m n^{\alpha_0 q - 1} \int_0^1 \frac{|\sin t|^q}{t^{\alpha_0 q}} dt \longrightarrow \infty, \quad n \longrightarrow \infty. \tag{3.17}$$

Let $\alpha_0 = (1/q)$. Consequently

$$\left\| S_n^{-\nu} \right\|_q^q \geq m \int_0^{n\varepsilon} \frac{|\sin t|^q}{t} dt, \tag{3.18}$$

and, as a result

$$\sup_n \left\| S_n^{-\nu} \right\|_q^q \geq m \int_1^{+\infty} \frac{|\sin t|^q}{t} dt \geq m \sum_{k=1}^{\infty} \int_{k\pi+(\pi/4)}^{(k+1)\pi-(\pi/4)} \frac{|\sin t|^q}{t} dt$$
$$\geq mc_1 \sum_{k=1}^{\infty} \frac{1}{(k+1)\pi - (\pi/4)} \int_{k\pi+(\pi/4)}^{(k+1)\pi-(\pi/4)} 1\, dt = c_2 \sum_{k=1}^{\infty} \frac{1}{(k+1)\pi - (\pi/4)} = +\infty, \tag{3.19}$$

where c_i are some constants. So we obtain that for $\beta \in [(1/q), (1/q) + 1)$, $\sup_n \|S_n^{-\nu}\|_q = +\infty$. Consequently, in this case we have

$$\sup_n \|S_n^{\nu}\|_p \left\| S_n^{-\nu} \right\|_q = +\infty. \tag{3.20}$$

Then it is known that (see, e.g., [22]) the system $\{S_n(\nu)\}_{n\in\mathbb{N}}$ is not uniformly minimal and, besides, does not form a basis for L_p.

Consider the case $\beta \in (-(1/p) - 1, -(1/p)]$. Without limiting the generality, we will suppose that $\beta = \alpha_0$. In this case, with regard to the biorthogonal system we have

$$\left\| S_n^{-\nu} \right\|_q^q = \int_0^{\pi} \nu^{-q}(t) |\sin nt|^q dt \leq \int_0^{\pi} \nu^{-q}(t) dt < +\infty, \quad \forall n \in \mathbb{N}. \tag{3.21}$$

Taking sufficiently small $\delta > 0$, we obtain

$$\left\| S_n^{-\nu} \right\|_q^q \geq \int_0^{\delta} \nu^{-q}(t) |\sin nt|^q dt \geq c \int_0^{\delta} t^{-\alpha_0 q} |\sin nt|^q dt. \tag{3.22}$$

As $\alpha_0 q < 0$, then, in the absolutely same way as in the previous case, we get

$$\inf_n \left\| S_n^{-\nu} \right\|_q > 0. \tag{3.23}$$

On the other hand,

$$\|S_n^{\nu}\|_p^p = \int_0^{\pi} \nu^p(t) |\sin nt|^p dt \geq c \int_0^{\delta} \frac{|\sin nt|^p}{t^{-\alpha_0 p}} dt, \tag{3.24}$$

where $\alpha_0 p \leq 1$. Similarly to the previous case again, we get

$$\int_0^{\delta} t^{\alpha_0 p} |\sin nt|^p dt \longrightarrow +\infty, \quad n \longrightarrow \infty. \tag{3.25}$$

As a result we obtain

$$\sup_n \|S_n^{\nu}\|_p \left\| S_n^{-\nu} \right\|_q = +\infty, \quad \text{for } \beta \in \left(-\frac{1}{p} - 1, -\frac{1}{p} \right]. \tag{3.26}$$

Thus, the following theorem is true.

Theorem 3.2. *Let* $\{\alpha_0;\ \alpha_r\} \subset (-(1/p)-1, -(1/p)+2)$*;* $\{\alpha_0;\ \alpha_r\} \bigcap M_p^{(0)} \neq \emptyset$*, and* $A_r \subset (-(1/p), (1/q))$*, where* $M_p^{(0)} \equiv (-(1/p)-1, -(1/p)] \bigcup [-(1/p)+1, -(1/p)+2)$*,* $A_r \equiv \{\alpha_k\}_1^{r-1}$*. Then the system* $\{S_n^{\nu}\}_{n\in\mathbb{N}}$ *is complete and minimal in* $L_p(0,\pi)$*,* $1 \le p < +\infty$*, but does not form a basis for it.*

4. Defective Case

Here, we consider the defective system of sines $\{S_n^{\nu}\}_{n\in\mathbb{N}_{(k_0)}}$, where $\mathbb{N}_{(k_0)} \equiv \mathbb{N} \setminus \{k_0\}$, $k_0 \in \mathbb{N}$ is some number. It follows directly from Theorem 3.2 that if the condition

$$\{\alpha_0;\ \alpha_r\} \bigcap M_p^{(0)} \neq \emptyset; \qquad A_r \subset \left(-\frac{1}{p}, \frac{1}{q}\right), \tag{4.1}$$

holds, then the system $\{S_n^{\nu}\}_{n\in\mathbb{N}_{(k_0)}}$ is minimal but not complete in $L_p(0,\pi)$, $1 \le p < +\infty$. Assume $M_p^{(1)} \equiv [(1/q)+1, (1/q)+3)$. Let $\alpha_0 \in M_p^{(1)}$. Consider the completeness of system $\{S_n^{\nu}\}_{n\in\mathbb{N}_{(k_0)}}$ in $L_p(0,\pi)$. Suppose that $f \in L_q(0,\pi)$ is orthogonal to the system, that is,

$$\int_0^{\pi} \nu(t) \sin nt \overline{f(t)} dt = 0, \quad \forall n \in \mathbb{N}_{(k_0)}. \tag{4.2}$$

As $\nu f \in L_1 \subset C_0^*[0,\pi]$ and system $\{\sin nt\}_{n\in\mathbb{N}}$ is complete and minimal in $C_0[0,\pi]$, from (4.2) we get

$$\nu(t) f(t) = c \sin k_0 t \Longrightarrow f(t) = c \frac{\sin k_0 t}{\nu(t)}. \tag{4.3}$$

It is clear that $\nu^{-1}(t) \sim t^{-\alpha_0}$, $\sin k_0 t \sim t$ as $t \to 0$. Consequently, $f \sim t^{-\alpha_0+1}$, $t \to 0$. As $q(-\alpha_0+1) \le -1$, then $f \in L_q(0,\pi)$ if and only if $c = 0$, and, consequently, $f = 0$. The similar result is true for $\alpha_r \in M_p^{(1)}$. Thus, if $\alpha_0; \alpha_r > -(1/p)-1$, and $\max\{\alpha_0; \alpha_r\} \in M_p^{(1)}$, then the system $\{S_n^{\nu}\}_{n\in\mathbb{N}_{(k_0)}}$ is complete in $L_p(0,\pi)$. Now we consider the minimality of this system. Let

$$\vartheta_n(t) = \nu^{-1}(t) \left[\frac{\sin nx}{n} - \frac{\sin k_0 x}{k_0}\right], \quad n \in \mathbb{N}_{(k_0)}. \tag{4.4}$$

We have

$$\langle S_k^{\nu}, \vartheta_n \rangle = \int_0^{\pi} S_k^{\nu}(t) \overline{\vartheta_n(t)} dt = \frac{\pi}{2n} \delta_{kn}, \quad \forall k, n \in \mathbb{N}_{(k_0)}. \tag{4.5}$$

Let us show that $\{\vartheta_n\}_{n\in\mathbb{N}_{(k_0)}} \subset L_q(0,\pi)$. In fact

$$\frac{\sin nt}{n} = t - \frac{n^2t^3}{6} + o\left(t^3\right), \quad t \longrightarrow 0,$$
$$\frac{\sin k_0 t}{k_0} = t - \frac{k_0^2t^3}{6} + o\left(t^3\right), \quad t \longrightarrow 0, \tag{4.6}$$

and, consequently

$$\frac{\sin nt}{n} - \frac{\sin k_0 t}{k_0} = \frac{1}{6}\left(k_0^2 - n^2\right)t^3 + o\left(t^3\right), \quad t \longrightarrow 0. \tag{4.7}$$

From these relations, we immediately find that $\vartheta_n(t) \sim t^{3-\alpha_0}$, $t \to 0$. As a result, $\{\vartheta_n\}_{n\in\mathbb{N}_{(k_0)}} \subset L_q(0,\pi)$. Then the relations (4.5) imply the minimality of system $\{S_n^\nu\}_{n\in\mathbb{N}_{(k_0)}}$ in $L_p(0,\pi)$. Similar result is true for $\alpha_r \in M_p^{(1)}$. In the end, we obtain that if $\max\{\alpha_0;\alpha_r\} \in M_p^{(1)}$, then the system $\{S_n^\nu\}_{n\in\mathbb{N}}$ has a defect equal to 1.

Consider the case when $\max\{\alpha_0;\alpha_r\} = \alpha_0 \in M_p^{(2)}$, where $M_p^{(2)} \equiv [(1/q)+3,(1/q)+5)$. We look at the system $\{S_n^\nu\}_{n\in\mathbb{N}_{(k_1;k_2)}}$, where $\mathbb{N}_{(k_1;k_2)} \equiv \mathbb{N}\setminus\{k_1;k_2\}$, $k_1;k_2 \in \mathbb{N}, k_1 \neq k_2$, are some numbers. Let $f \in L_q(0,\pi)$ cancel this system out, that is,

$$\left\langle S_n^\nu, f\right\rangle = 0, \quad \forall n \in \mathbb{N}_{(k_1;k_2)}. \tag{4.8}$$

Using the previous reasoning, we find that for some constants c_1, c_2, the following is true:

$$f(t) = c_1\nu^{-1}(t)\sin k_1 t + c_2\nu^{-1}(t)\sin k_2 t. \tag{4.9}$$

Using representations

$$\sin k_i t = k_i t - \frac{k_i^3}{6}t^3 + o\left(t^4\right), \quad t \longrightarrow 0,\ i = 1,2, \tag{4.10}$$

we obtain

$$f(t) \sim ct^{-\alpha_0}g_1(t) + g_2(t), \quad t \longrightarrow 0, \tag{4.11}$$

($c \neq 0$ is some constant), where it can be easily seen that $g_2 \in L_q$ and

$$g_1(t) = (c_1k_1 + c_2k_2)t - \frac{1}{6}\left(c_1k_1^3 + c_2k_2^3\right)t^3. \tag{4.12}$$

Thus, $f \in L_q$ if and only if $t^{-\alpha_0}g_1(t) \in L_q$. Assume $b_1 = c_1k_1 + c_2k_2$; $b_2 = -(1/6)(c_1k_1^3 + c_2k_2^3)$. As $(1-\alpha_0)q \leq -1(3-\alpha_0)q \leq -1$, it is clear that $t^{1-\alpha_0} \notin L_q$ and $t^{3-\alpha_0} \notin L_q$. Suppose $b_1 \neq 0$. We have

$$\left|t^{-\alpha_0}g_1(t)\right| = |b_1|t^{1-\alpha_0}\left|1 + b_1^{-1}b_2t^2\right|. \tag{4.13}$$

It follows directly that for sufficiently small $\delta > 0$, we have

$$\left|t^{-\alpha_0} g_1(t)\right| \geq c_\delta |b_1| t^{1-\alpha_0}, \quad \forall t \in (0, \delta), \tag{4.14}$$

where $c_\delta > 0$ is some constant depending only on δ and b_2. As a result, $f \notin L_q$.

Consequently, $b_1 = 0$. Moreover, it is not difficult to derive that $b_2 = 0$. Thus, we obtain the following system for c_1 and c_2:

$$\begin{aligned} c_1 k_1 + c_2 k_2 &= 0, \\ c_1 k_1^3 + c_2 k_2^3 &= 0. \end{aligned} \tag{4.15}$$

It is clear that $\det\begin{vmatrix} k_1 & k_2 \\ k_1^3 & k_2^3 \end{vmatrix} \neq 0$. And, consequently, $c_1 = c_2 = 0$. As a result, $f = 0$, which, in turn, implies that the system $\{S_n^\nu\}_{n \in \mathbb{N}_{(k_1;k_2)}}$ is complete in L_p. Let us show that it is also minimal in L_p. Assume $\gamma_n^{(k)} = (1/6)(k^2 - n^2)$. Consider the system $\vartheta_n^{(k_1;k_2)}(t) \equiv [a_n^{(k_1;k_2)} \sin nt - (1/k_1 \gamma_n^{(k_1)}) \sin k_1 t + (1/k_2 \gamma_n^{(k_2)}) \sin k_2 t] \nu^{-1}(t)$, for all $n \in \mathbb{N}_{(k_1;k_2)}$, where

$$a_n^{(k_1;k_2)} = \frac{1}{n}\left(\frac{1}{\gamma_n^{(k_1)}} - \frac{1}{\gamma_n^{(k_2)}}\right) \neq 0. \tag{4.16}$$

Simple calculations give the following representation:

$$\vartheta_n^{(k_1;k_2)}(t) \sim c_n t^5, \quad t \longrightarrow 0, \tag{4.17}$$

where $c_n \neq 0$, for all $n \in \mathbb{N}_{(k_1;k_2)}$ are some constants. We obtain directly from this representation that $\{\vartheta_n^{(k_1;k_2)}\}_{n \in \mathbb{N}_{(k_1;k_2)}} \subset L_q$. On the other hand,

$$\left\langle S_n^\nu, \vartheta_n^{(k_1;k_2)} \right\rangle = a_n^{(k_1;k_2)} \delta_{nk} = \begin{cases} \neq 0, & n \neq k, \\ = 0, & n = k, \end{cases} \quad \forall n, k \in \mathbb{N}_{(k_1;k_2)}. \tag{4.18}$$

Thus, if $\alpha_0 \in M_p^{(2)}$, then the system $\{S_n^\nu\}_{n \in \mathbb{N}_{(k_1;k_2)}}$ is complete and minimal in L_p, and, as a result, the system $\{S_n^\nu\}_{n \in \mathbb{N}}$ has a defect equal to 2. It is easy to see that the similar result is true if $\alpha_r \in M_p^{(2)}$ with $\alpha_0 \leq \alpha_r$. Continuing this way, we obtain that if $\beta = \max\{\alpha_0; \alpha_r\} = \alpha_0 \in M_p^{(k)}$, where $M_p^{(k)} \equiv [-(1/p) + 2k, -(1/p) + 2(k+1))$, then the system $\{S_n^\nu\}_{n \in \mathbb{N}_{\{\overline{n}_k\}}}$ is complete and minimal in L_p, where $\{\overline{n}_k\} = \{n_1; \ldots; n_k\} \subset \mathbb{N}$, $n_i \neq n_j$ with $i \neq j$.

Consider the basicity of system $\{S_n^\nu\}_{n \in \mathbb{N}_{\{\overline{n}_1\}}}$ (i.e., the case of $k = 1$) in L_p. Similar to the case of $M_p^{(0)}$, it can be proved that

$$0 < \inf_{n \in \mathbb{N}_{\{\overline{n}_1\}}} \|S_n^\nu\|_p \leq \sup_{n \in \mathbb{N}_{\{\overline{n}_1\}}} \|S_n^\nu\|_p < +\infty. \tag{4.19}$$

Concerning biorthogonal system, we have

$$\int_0^{\pi} v^{-q}(x)\left|\frac{\sin nx}{n}-\frac{\sin k_1 x}{k_1}\right|^q dx \geq c\int_0^{\varepsilon} x^{-q\alpha_0}\left|\frac{\sin nx}{n}-\frac{\sin n_1 x}{n_1}\right|^q dx, \tag{4.20}$$

where the interval $[0,\varepsilon]$ $(\varepsilon>0)$ does not contain the points $\{t_k\}_1^{r-1}$. As $(\sin n_1 x/n_1)-x\sim x^3$, for $x\to 0$, it is clear that $(-q\alpha_0+3>-1)$

$$\int_0^{\varepsilon} x^{-q\alpha_0}\left|\frac{\sin n_1 x}{n_1}-x\right|^q dx<+\infty. \tag{4.21}$$

Taking this circumstance into account, we have

$$\left\|S_n^{-\nu}\right\|_q^q \geq c\left[\int_0^{\varepsilon} x^{-q\alpha_0}\left|\frac{\sin nx}{n}-x\right|^q dx-\int_0^{\varepsilon} x^{-q\alpha_0}\left|\frac{\sin n_1 x}{n_1}-x\right|^q dx\right]. \tag{4.22}$$

Consider the case of $\alpha_0\in((1/q)+1,(1/q)+3)$:

$$\begin{aligned}\int_0^{\varepsilon} x^{-q\alpha_0}\left|\frac{\sin nx}{n}-x\right|^q dx &= n^{-q}\int_0^{\varepsilon} x^{-q\alpha_0}|\sin nx-nx|^q dx\\ &= n^{-\alpha}\int_0^{n\varepsilon} t^{-q\alpha_0}|\sin nt-t|^q dt\\ &\geq cn^{-\alpha}\int_0^{n\varepsilon} t^{-q\alpha_0+q}dt=\frac{c}{\alpha}\left(\varepsilon^{\alpha}-n^{-\alpha}\right),\end{aligned} \tag{4.23}$$

where $\alpha=-\alpha_0 q+q+1<0$. Consequently, $\sup_n\|S_n^{-\nu}\|_q=+\infty$. Let $\alpha_0=(1/q)+1$. In this case we have

$$\int_0^{\varepsilon} x^{-q\alpha_0}\left|\frac{\sin nx}{n}-x\right|^q dx \geq c\int_1^{n\varepsilon} t^{-1}dt=c\ln n\varepsilon, \tag{4.24}$$

and, consequently $\sup_n\|S_n^{-\nu}\|_q=+\infty$. As a result, we get that for $\alpha_0\in M_p^{(1)}$, the system $\{S_n^{\nu}\}_{n\in\mathbb{N}_{\{\bar{n}_1\}}}$ does not form a basis for L_p. Assume that in this case, the system $\{S_n^{\nu}\}_{n\in\mathbb{N}}$ is a frame in L_p, that is any function from L_p can be expanded with respect to this system. As it does not form a basis for L_p, zero has a non trivial decomposition, that is,

$$0=\sum_{n=1}^{\infty}a_n S_n^{\nu}, \tag{4.25}$$

where $\exists n_0\in\mathbb{N}: a_{n_0}\neq 0$. As the system $\{S_n^{\nu}\}_{n\in\mathbb{N}_{\{\bar{n}_1\}}}$ is complete and minimal in L_p, it is clear that $a_{n_1}\neq 0$. Consequently, $S_{n_1}^{\nu}=\sum_{n\neq n_1}(a_n/a_{n_1})S_n^{\nu}$. It follows directly that the arbitrary element can be expanded with respect to the system $\{S_n^{\nu}\}_{n\in\mathbb{N}_{\{\bar{n}_1\}}}$. But this is impossible. Similar result is true for $\max\{\alpha_0;\alpha_r\}\in M_p^{(1)}$.

Proceeding in an absolutely similar way as we did in the previous case, we can prove that for $\max\{\alpha_0; \alpha_r\} \in M_p^{(k)}$, the system $\{S_n^{\nu}\}_{n\in\mathbb{N}_{\{\overline{n}_k\}}}$ is complete and minimal in L_p, but does not form a basis for it. Consequently, system $\{S_n^{\nu}\}_{n\in\mathbb{N}}$ has a defect equal to (k). The fact that it is not a frame in L_p in this case too is proved as follows. Let $k = 2 : \{\overline{n}_k\} \equiv \{n_1; n_2\}$. Assume that the system $\{S_n\}_{n\in\mathbb{N}}$ is a frame in L_p. Then zero has a non trivial decomposition: $0 = \sum_{n=1}^{\infty} a_n S_n^{\nu}$. It is clear that $|a_{n_1}| + |a_{n_2}| > 0$, and let $a_{n_1} \neq 0$. It follows directly that the system $\{S_n\}_{n\neq n_1}$ is a frame in L_p. The further reasoning is absolutely similar to the case of $k = 1$. This scheme is applicable for for all $k \in \mathbb{N}$. Thus, we have proved the following main theorem.

Theorem 4.1. *Let the following necessary condition be satisfied*

$$\alpha_0; \alpha_r \in \left(-\frac{1}{p} - 1, +\infty\right), \qquad \{\alpha_k\}_1^{r-1} \subset \left(-\frac{1}{p}; \frac{1}{q}\right). \tag{4.26}$$

Then the system $\{S_n^{\nu}\}_{n\in\mathbb{N}}$ is a frame (basis) in L_p if and only if $\alpha_0; \alpha_r \in (-(1/p), (1/q))$. Moreover, for $\max\{\alpha_0; \alpha_r\} \in M_p^{(k)}$, $k \in \mathbb{N}$, it has a defect equal to (k), where $M_p^{(k)} \equiv [(1/q) + 2k, (1/q) + 2(k+1))$.

Acknowledgment

The authors are thankful to the referees for their valuable comments.

References

[1] R. Edwards, *Fourier Series in A Modern Exposition*, vol. 1, Mir, Moscow, Russia, 1985.
[2] R. Edwards, *Fourier Series in A Modern Exposition*, vol. 2, Mir, Moscow, Russia, 1985.
[3] A. Zigmund, *Trigonometric Series*, vol. 1, Mir, Moscow, Russia, 1965.
[4] A. Zigmund, *Trigonometric Series*, vol. 2, Mir, Moscow, Russia, 1965.
[5] N. K. Bari, *Trigonometric Series*, Fizmatgiz, Moscow, Russia, 1961.
[6] K. I. Babenko, "On conjugate functions," *Doklady Akademii Nauk SSSR*, vol. 62, no. 2, pp. 157–160, 1948.
[7] V. F. Gaposhkin, "One generalization of M.Riesz theorem on conjugated functions," *Matematicheskii Sbornik*, vol. 46(88), no. 3, pp. 359–372, 1958.
[8] K. S. Kazaryan and P. I. Lizorkin, "Multipliers, bases and unconditional bases of the weighted spaces *B* and *SB*," *Proceedings of the Steklov Institute of Mathematics*, vol. 187, pp. 111–130, 1989.
[9] J. Garnett, *Bounded Analytic Functions*, Mir, Moscow, Russia, 1984.
[10] E. I. Moiseev, "On basicity of systems of cosines and sines in weight space," *Differentsial'nye Uravneniya*, vol. 34, no. 1, pp. 40–44, 1998.
[11] E. I. Moiseev, "The basicity in the weight space of a system of eigen functions of a differential operator," *Differentsial'nye Uravneniya*, vol. 35, no. 2, pp. 200–205, 1999.
[12] S. S. Pukhov and A. M. Sedletskiĭ, "Bases of exponentials, sines, and cosines in weighted spaces on a finite interval," *Rossiĭskaya Akademiya Nauk. Doklady Akademii Nauk*, vol. 425, no. 4, pp. 452–455, 2009.
[13] B. T. Bilalov and S. G. Veliyev, "On completeness of exponent system with complex coefficients in weight spaces," *Transactions of NAS of Azerbaijan*, vol. 25, no. 7, pp. 9–14, 2005.
[14] B. T. Bilalov and S. G. Veliev, "Bases of the eigenfunctions of two discontinuous differential operators," *Differentsial'nye Uravneniya*, vol. 42, no. 10, pp. 1503–1506, 2006.
[15] B. T. Bilalov, "Bases of exponentials, cosines, and sines that are eigenfunctions of differential operators," *Differentsial'nye Uravneniya*, vol. 39, no. 5, pp. 652–657, 2003.
[16] B. T. Bilalov, "On basicity of some systems of exponents, cosines and sines," *Rossiĭskaya Akademiya Nauk. Doklady Akademii Nauk*, vol. 379, no. 2, pp. 7–9, 2001.

[17] B. T. Bilalov, “Basis properties of some systems of exponentials, cosines, and sines,” *Sibirskiĭ Matematicheskiĭ Zhurnal*, vol. 45, no. 2, pp. 264–273, 2004.

[18] E. S. Golubeva, “The System of weighted exponentials with power weights. Herald of Samara State University,” *Natural Sciences*, vol. 83, no. 2, pp. 15–25, 2011.

[19] J. Lindenstrauss and L. Tzafriri, *Classical Banach Spaces*, Springer, 1996.

[20] O. Christensen, *An Introduction to Frames and Riesz Bases*, Springer, 2003.

[21] A. Rahimi, *Frames and Their Generalizations in Hilbert and Banach Spaces*, Lambert Academic Publishing, 2011.

[22] C. Heil, *A Basis Theory Primer*, Springer, 2011.

[23] M. G. Krein, *Functional Analysis*, Nauka, Moscow, Russia, 1972.